



Pacific Northwest
NATIONAL LABORATORY

Proudly Operated by Battelle Since 1965

Contaminant Attenuation and Transport Characterization of 200- DV-1 Operable Unit Sediment Samples from Boreholes C9497, C9498, C9603, C9488, and C9513

August 2018

DI Demirkanli
MJ Truex
JE Szecsody
MM Snyder

JJ Moran
MK Nims
AR Lawter
CT Resch

DL Saunders
NP Qafoku
SR Baum
BD Williams

DISCLAIMER

This report was prepared as an account of work sponsored by an agency of the United States Government. Neither the United States Government nor any agency thereof, nor Battelle Memorial Institute, nor any of their employees, makes **any warranty, express or implied, or assumes any legal liability or responsibility for the accuracy, completeness, or usefulness of any information, apparatus, product, or process disclosed, or represents that its use would not infringe privately owned rights.** Reference herein to any specific commercial product, process, or service by trade name, trademark, manufacturer, or otherwise does not necessarily constitute or imply its endorsement, recommendation, or favoring by the United States Government or any agency thereof, or Battelle Memorial Institute. The views and opinions of authors expressed herein do not necessarily state or reflect those of the United States Government or any agency thereof.

PACIFIC NORTHWEST NATIONAL LABORATORY

operated by

BATTELLE

for the

UNITED STATES DEPARTMENT OF ENERGY

under Contract DE-AC05-76RL01830

Printed in the United States of America

Available to DOE and DOE contractors from the

Office of Scientific and Technical Information,

P.O. Box 62, Oak Ridge, TN 37831-0062;

ph: (865) 576-8401

fax: (865) 576-5728

email: reports@adonis.osti.gov

Available to the public from the National Technical Information Service

5301 Shawnee Rd., Alexandria, VA 22312

ph: (800) 553-NTIS (6847)

email: orders@ntis.gov <<http://www.ntis.gov/about/form.aspx>>

Online ordering: <http://www.ntis.gov>



This document was printed on recycled paper.

(8/2010)

Contaminant Attenuation and Transport Characterization of 200- DV-1 Operable Unit Sediment Samples from Boreholes C9497, C9498, C9603, C9488, and C9513

DI Demirkanli
MJ Truex
JE Szecsody
MM Snyder

JJ Moran
MK Nims
AR Lawter
CT Resch

DL Saunders
NP Qafoku
SR Baum
BD Williams

August 2018

Prepared for
the U.S. Department of Energy
under Contract DE-AC05-76RL01830

Pacific Northwest National Laboratory
Richland, Washington 99352

Executive Summary

The 200-DV-1 Operable Unit (OU), located in the inner cleanup area of the Hanford's Central Plateau, was delineated to include forty-three waste sites selected based on (1) the remediation challenges associated with mobile contaminants in the vadose zone; (2) the complex technical and regulatory challenges, such as co-mingled plumes or determining the nature and extent of contamination; and (3) the geographic proximity to waste management areas associated with vadose zone contamination in the Central Plateau from within the B-, S-, and T-Complexes (DOE 2016). The final remedy selection for the 200-DV-1 OU will be supported by a combined *Comprehensive Environmental Response, Compensation, and Liability Act of 1980* (CERCLA) remedial investigation (RI) and feasibility study (FS) and *Resource Conservation and Recovery Act of 1976* (RCRA) facility investigation (RFI) and corrective measures study (CMS). Because deep vadose zone contaminants at the 200-DV-1 OU waste sites present a significant issue as a potential source for continued release of contaminants to the groundwater, both RI/FS and RFI focus on determining the nature and extent of the contamination within this OU to assess ongoing and potential future contaminant impacts to groundwater and select appropriate remedies and remedial treatment technologies. These remedial investigation activities also provide information and approaches relevant to designing and implementing characterization at other vadose zone operable units in the Central Plateau.

As recognized in the 'Characterization Sampling and Analysis Plan for the 200-DV-1 Operable Unit Addendum 1: Attenuation Process Characterization' (Attenuation SAP Addendum, DOE 2017), information about contaminant attenuation and transport processes is important to meet the needs of the remedial investigation and feasibility study objectives. In particular, this type of information is foundational for conducting the fate and transport modeling efforts whereby ongoing and future contaminant flux to groundwater are estimated to support risk assessment and remedy evaluation. The report herein, in conjunction with the previous two 200-DV-1 OU attenuation characterization reports (Truex et al. 2017; Szecsody et al. 2017), provide information on the nature and extent of contaminants, observation of attenuation processes, and quantification of attenuation and transport parameters through an effort of detailed laboratory studies for the selected vadose zone samples from various 200-DV-1 waste sites. Waste sites selected and associated contaminants identified and evaluated by these laboratory studies are listed in Table ES.1. The laboratory analyses were conducted using approaches defined in national guidance for quantifying attenuation processes.

The results presented in this report and the previous two reports provide important findings for the 200-DV-1 OU RI/FS efforts. One of the major outcomes presented is that only a small fraction of the total uranium and iodine contamination was observed in mobile forms in the vadose zone. These contaminants have been attenuated and uranium- and iodate-carbonate precipitation was identified as an important attenuation mechanism that will have to be accounted for in transport assessments. In contrast, Tc-99 was present only in aqueous and adsorbed phases and is therefore only attenuated by hydraulic processes in the vadose zone. Cr(VI) concentrations were low in almost all samples. Some historical chromate reduction may have occurred, but the observed total chromium concentrations were interpreted to be primarily from naturally occurring mineral phases. Overall geochemical evaluations presented varying effects of waste chemistry at different waste sites. While the majority of the samples from S- and T-complexes showed a limited influence of waste chemistry, B-complex samples showed more significant effects with varying characteristics between boreholes and with depth. However, some S- and T-complex

boreholes also showed high nitrate concentrations with very minimal attenuation potential. These results demonstrate that attenuation of contaminants has occurred and will continue to occur for major contaminants in the vadose zone, such as uranium and iodine rendering these contaminants relatively less mobile, whereas contaminants like Tc-99 and nitrate are more mobile. These results support the quantification of the attenuation processes and transport parameters for each of the targeted mobile contaminants selected for analysis, as identified in the Attenuation SAP Addendum (DOE 2017).

Table ES.1. Waste sites selected for contaminant characterization and attenuation assessment for the 200-DV-1 OU.

Waste Site	COCs	Report
B-42 Trench (C9497)	Technetium-99, Uranium, Chromium, Total Iodine, Cr(VI), Nitrate	Current Report
T-3 Reverse Well (C9555)	Uranium, Chromium, Cr(VI), Nitrate	Current Report
T-7 Tile Field (C9503)	Uranium, Chromium, Cr(VI), Nitrate	Current Report
S-13 Crib (C9513)	Uranium, Chromium, Cr(VI), Nitrate	Current Report
B-8 Crib and Tile Field (C9488) ^a	--	Current Report
T-19 (C9507)	Technetium-99, Uranium, U(VI), Chromium, Total Iodine, Iodate, Iodide, Cr(VI), Cyanide, Nitrate	Truex et al. 2017
T-25 (C9510)	Technetium-99, Uranium, U(VI), Chromium, Total Iodine, Cr(VI), Cyanide, Nitrate	Truex et al. 2017
S-9 (C9512)	Technetium-99, Uranium, U(VI), Chromium, Total Iodine, Iodate, Iodide, Cr(VI), Cyanide, Nitrate	Truex et al. 2017
BY Cribs (C9552)	Technetium-99, Uranium, Chromium, Iodine, Cr(VI), Cyanide, Nitrate	Szecsody et al. 2017
B7-AB (C9487)	Technetium-99, Uranium, Chromium, Iodine, Cr(VI), Cyanide, Nitrate	Szecsody et al. 2017
B-8 Crib and Tile Field (C9488)	Technetium-99, Uranium, Chromium, Iodine, Cr(VI), Cyanide, Nitrate	Szecsody et al. 2017

(a) These perched zone samples were selected only for sediment total carbon, total organic carbon, and x-ray diffraction analyses for the current report.

Summary

Contaminants disposed of at the land surface must migrate through the vadose zone before entering groundwater. Processes that occur in the vadose zone can attenuate contaminant concentrations during transport through the vadose zone. Thus, quantifying contaminant attenuation and contaminant transport processes in the vadose zone, in support of the conceptual site model (CSM) and fate and transport assessments, is important for evaluating the need for, and type of, remediation in the vadose zone and groundwater. The framework to characterize attenuation and transport processes provided in U.S. Environmental Protection Agency (EPA)¹ guidance documents was used to guide the laboratory characterization effort reported herein.

The 200-DV-1 Operable Unit (OU) is in the process of characterizing the vadose zone to support a remedial investigation and feasibility study. Through a data quality objectives process, specific 200-DV-1 waste sites were selected for evaluation of attenuation and transport processes for mobile uranium (U), technetium-99 (Tc-99), iodine-129 (I-129), chromium (Cr), and nitrate (NO₃⁻) contaminants. Not all of these constituents are present at every waste site, so a site-specific set of these contaminants was assessed based on the waste disposal inventory information for each site. The specific elements of the laboratory characterization effort were selected to provide data and associated interpretation to support the following three objectives:

- Define the contaminant distribution and the hydrologic and geochemical setting
- Identify attenuation processes and describe the associated attenuation mechanisms
- Quantify the mobility of contaminants and transport parameters for use in evaluating remedies

These objectives are elements of the framework identified in EPA guidance for evaluating Monitored Natural Attenuation (MNA) of inorganic contaminants, and they directly support updating the CSM for these waste sites (and generally for the Hanford Central Plateau). Importantly, the information supports defining suitable parameters for evaluating transport of contaminants through the vadose zone and to the groundwater. This type of transport assessment supports a coupled analysis of groundwater and vadose zone contamination. The laboratory study information, in conjunction with transport analyses, can be used as input to evaluate the feasibility of remedies for the 200-DV-1 OU. This remedy evaluation will be enhanced by considering these study results that improve the understanding of controlling features and processes for transport of contaminants through the vadose zone to the groundwater.

The laboratory study described in this report was conducted using the samples shown in Table ES-1 for the following selected waste sites in the 200-DV-1 OU: B-42 Trench (borehole C9497), T-3 Reverse Well (borehole C9555), T-7 Tile Field (borehole C9503), S-13 Crib (borehole C9513), and B-8 Crib and Tile Field (borehole C9488). The laboratory study included categories of individual analysis and experiments derived from EPA guidance for MNA of inorganic contaminants. Sediment characterization included determining contaminant concentrations, concentrations of important geochemical constituents, physical properties, and pore-water oxygen and hydrogen isotopes. The character of iron and manganese

¹ EPA. 2015. *Use of Monitored Natural Attenuation for Inorganic Contaminants in Groundwater at Superfund Sites*. OSWER Directive 9283.1-36, U.S. Environmental Protection Agency, Office of Solid Waste and Emergency Response, Washington, D.C.

phases in the sediments was also determined in relation to their role in redox reactions. For the majority of these baseline analyses an initial set of core samples was used. For more detailed analyses, a combination of both core and grab samples (i.e., samples, other than those originally targeted for attenuation testing, collected and analyzed by CH2M Hill Plateau Remediation Company (CHPRC)) were selected during collective discussions between PNNL and CHPRC. These detailed analyses provided additional information to help assess attenuation processes through sequentially applying increasingly harsh extraction solutions to the sediment and measuring contaminants in the extractions (sequential-extraction analysis). This technique helps interpret the distribution of contaminants among mobile, partially mobile, and functionally immobile phases in the sediments. Several types of methods were applied to evaluate transport characteristics and to develop transport parameters for contaminants. Where existing contaminant concentrations were high enough to enable testing, soil-column leaching experiments were conducted that are used to evaluate and quantify contaminant release rates.

Table ES.2. Samples included in this laboratory study.

Waste Site	Borehole ID	Core	Nominal Geologic Unit	Depth Interval (ft bgs)
B-42	C9497	39C	CCUg	237-238
S-13	C9513	18E	H2/CCUz	115.6-116.6
S-13	C9513	25D	CCUc	151.7-152.7
S-13	C9513	39D	Rwei	221.5-222.5
T-3	C9555	57B	H2/CCUz	106-107
T-3	C9555	31D	Rwie	181.3-182.3
T-7	C9503	5C	H2/CCUz	87-88
T-7	C9503	6B	CCUz/CCUc	91-92
T-7	C9503	18C	Rwei	152-153
B-8	C9488	37D	CCU Perched Interval	223.5-224.5
B-8	C9488	37E	CCU Perched Interval	224.5-225.5
B-42	C9497	23 (Grab)	H2	161-163.5
B-42	C9497	44 (Grab)	CCUg	260-261.2
S-13	C9513	13 (Grab)	H2	90.5-92
S-13	C9513	21 (Grab)	CCUc	131.5-133.5
S-13	C9513	24 (Grab)	CCUc	146.1-148.8
S-13	C9513	29 (Grab)	Below CCUc	171-172

CCU is Cold Creek Unit; CCUc is Cold Creek unit – carbonate; CCUg is Cold Creek unit – gravel-dominated; CCUz is Cold Creek unit – silt-dominated; H2 is Hanford formation unit 2 – sand-dominated; Rwei is Ringold Formation member Wooded Island unit E.

Interpretation of this laboratory study can be considered from several perspectives relevant to supporting 200-DV-1 OU activities. Results for each contaminant were evaluated across all of the samples to identify contaminant-specific conclusions and to enable consideration of how results from this study may be relevant to other waste sites. Results were also evaluated with respect to conclusions relevant to the specific waste sites included in the study. Lastly, study results were evaluated with respect

to updating CSMS and future evaluation of remedies, including the associated fate and transport assessment needed as a basis for remedy evaluation.

The data and information from this laboratory study were interpreted to support the following conclusions for each contaminant included in the study.

- Uranium

- Uranium concentrations were low in most samples analyzed for this study, which indicates that a significant fraction of uranium may be associated with natural background. However, moderate levels of uranium were observed in two of the core samples (B39X10 and B39X55) from borehole S-13 (C9513) and one of the core samples (B39VY1) from borehole T-7 (C9503). The total uranium found in B39VY1 was still significantly lower than the S-13 (C9513) samples, and mostly in mineral precipitate forms. Sample B39X55 was from the CCU caliche unit with a high carbonate concentration. Consistently, the results for this sample indicated high total inorganic carbon which suggests formation of uranium carbonate compounds potentially attenuating uranium in this formation. Sequential extraction results for the same unit as discussed below confirmed this behavior. Sample B39X10 was from a transition zone between H2 and CCUz formations. Sequential extractions conducted for a grab sample in H2 formation for this borehole also indicated moderate levels of uranium with about 20% being in the aqueous and adsorbed phases. Thus, some portion of uranium in this borehole (S-13, C9513) may be migrating from H2 sediments into CCUc and where it may then complex with carbonate. Uranium-carbonate precipitation was identified as an important attenuation mechanism that reduce uranium mobility. This attenuation mechanism will have to be accounted for in transport assessments.
- Uranium surface phases showed significant differences for different boreholes. Aqueous and adsorbed uranium, that would be transported under equilibrium conditions, ranged from 0.5% to 20% among the samples from the S-13 (C9513), T-3 (C9555), and T-7 (C9503) boreholes, with the highest fraction observed in sample B3DCJ2 (grab sample, S-13, C9513). The mobile fraction of uranium that also includes part of the acetate-extractable uranium in addition to the aqueous and adsorbed phases ranged from 10% to 55%, with the highest mobility observed in the samples from borehole S-13 (C9513). While the T-3 (C9555) sample yielded the highest amount of total contamination (29.44 $\mu\text{g/g}$), most of the uranium in borehole T-3 (C9555) was associated with precipitates where transport of uranium would be controlled by slow dissolution processes.
- Slow-release uranium transport behavior that is potentially due to slow carbonate dissolution was observed in soil-column leaching experiments for the samples from borehole S-13 (C9513). However, core sample B3DB67 (T-3, C9555) showed an unusual transport behavior with initially decreasing concentrations followed by slight increase, indicating a slowly released uranium-complex that is unidentified.
- Uranium distribution coefficient (K_d) values varied across the different samples tested. The highest K_d value was associated with the sample (B3DB67) from borehole T-3 (C9555), which also had the highest amount of uranium contamination. Thus, in transport assessments, selection of a K_d value for uranium should consider spatial variation of the K_d value.

- Iodine

- Total iodine concentrations in the vadose zone were only measured for the sample from borehole B-42 (C9497), which showed a very low level.

- Tc-99
 - Tc-99 was only measured for the sample from borehole B-42 (C9497) and was a non-detect.
 - A grab sample (i.e., samples other than those originally targeted for attenuation testing) from borehole B-42 (C9497) with a Tc-99 concentration of 11.1 pCi/g was selected collectively by PNNL and CHPRC for sequential extractions. A sample adjacent to this grab sample was analyzed for Tc-99. The result indicated a very small amount of total extractable Tc-99 in this sediment (about four orders of magnitude lower than the grab sample targeted), indicating heterogeneity in Tc-99 distribution. No further soil-column leaching tests were conducted for this sample due to the low value observed for this sample. However, sequential extraction results indicate that Tc-99 is in the mobile phase in this sediment.
- Chromium
 - Cr(VI) was not detected in most core samples and, when detected, was present at a low concentration. Total chromium measured in acid extractions was likely from natural background.
 - Sequential extraction results (conducted with a set of grab samples) showed a wide range of total Cr concentrations (8.9 to 68 µg/g) among the selected samples. However, the mobile chromium ranged only from 0.95 to 1.6 µg/g. Some of the elevated K_d values determined in sequential extractions for Cr indicated more sorption than expected for the sediment from borehole S-13 (C9513), attenuating its mobility in this borehole.
- Nitrate
 - Nitrate concentrations were low in all of the samples, except the samples from borehole T-7 (C9503), which indicated an increasing trend with depth, indicating very little attenuation potential.

The following conclusions were developed for the specific boreholes/waste sites analyzed in this study.

- B-42
 - One core sample selected for the laboratory study from the B-42 waste site (borehole C9497) was comprised of CCU gravel material. This sample did not show any signs of altered geochemistry induced by the waste discharge. Contaminant levels were also observed to be very low or non-detect.
 - Six samples analyzed for isotopic signature, with varying depths from this borehole, showed two distinct patterns over the depth profile correlated to the historic water table depth for this location (256 ft below surface). Results suggested mixing of a distinct upper water (above 256 ft) with a distinct lower water near the location of the historical water table. Furthermore, upper data (above 256 ft) also showed isotopic shifts that are consistent with a flux of industrial process water near the surface that is propagating downward.
- S-13
 - Core samples for the contaminant concentration and geochemical evaluation from the S-13 waste site (borehole C9513) included materials from the transition of Hanford formation to CCU silt, CCU caliche (CCUc), and Ringold (silty, sandy gravel). The samples from the transition zone and CCUc showed moderate levels of uranium and total chromium with very small amounts of

Cr(VI). The sample from the Ringold Formation only had very small amounts of contaminants present. None of these samples showed any significant nitrate levels. The sediment from the CCUc formation also showed high levels of total carbon and total inorganic carbon, as well as higher calcium and magnesium, indicating the presence of carbonate in this sample. Slightly elevated levels of uranium found in this sample are likely due to formation of uranium carbonate compounds.

- A total of four grab samples were selected for sequential extractions for this borehole for uranium and chromium analyses. For the two samples analyzed for uranium, it was observed that some uranium was in mobile phase (aqueous, adsorbed, and acetate extractable), which may transport in aqueous phase under equilibrium-partitioning conditions. The sample from the CCUc formation showed uranium associated with the acetate-extractable portion, indicating complexation with carbonate. All four samples were analyzed for chromium and showed total chromium concentrations ranging from 30.28 to 67.60 $\mu\text{g/g}$ with a very small fraction of mobile chromium. Slightly elevated K_d values for Cr (0.382-7.64 mL/g) indicated more sorption behavior than expected. Soil-column leaching experiments confirmed a decreasing release rate over time for uranium consistent with dissolution of a solid phase. For chromium, these experiments indicated a small release during the early stages of the experiment and a very slow kinetic dissolution of a Cr-containing precipitate.
 - Isotope analysis for this borehole showed an anthropogenic influence similar to borehole B-42. It is likely that the isotopic signature indicates a high flux of Columbia River water (e.g., as process water) into the system.
 - Based on the data collected in this laboratory study, the following attenuation processes are important at this waste site. Sorption processes are important for uranium. Formation of uranium-carbonate precipitates also appears to be an attenuation mechanism in S-13 borehole samples. The potential for reduction through abiotic (e.g., ferrous iron) mechanisms is very limited, and would not affect the future contaminant migration.
- T-7
 - Core samples from the T-7 waste site (borehole C9503), analyzed for contaminant distribution and geochemistry, were materials from the transition of Hanford formation to CCU silt, transition of CCU silt to caliche, and Ringold (silty, sandy gravel). Only one sample (B39VY1) showed a slightly elevated uranium concentration where the other two samples yielded very low concentrations. All sampled showed low levels of chromium. However, nitrate levels were noticeably elevated, showing an increasing trend with depth.
 - Sequential extractions yielded a very small amount of total uranium, with a large fraction in functionally immobile form associated with solid phases in the sediment. The K_d value was calculated as 3.17 ml/g.
 - Isotope analysis for this borehole yielded patterns largely consistent with expected natural patterns, indicating very little anthropogenic influence in this area.
 - Based on the data collected in this laboratory study, the following attenuation processes are important at this waste site. Sorption processes are important for uranium. No indications of reduction were observed in these samples and the potential for reduction through abiotic (e.g., ferrous iron) processes is limited.

- T-3
 - Core samples from the T-3 reverse well waste site (borehole C9555), analyzed for contaminant distribution and geochemistry, were from the transition of Hanford formation to CCU silt and Ringold (silty, sandy gravel). The sample from the transition zone showed slightly elevated nitrate levels accompanied by a high uranium concentration in acid extractions. No Cr(VI) was detected in water extractions and acid extractions yielded a very small amount of total chromium for this sample. The sample from the Ringold unit didn't show any significant contaminant levels.
 - The sample from the transition unit was further evaluated through sequential extractions. The total uranium contamination was observed to be the highest among the selected samples from all boreholes. However, the majority of this uranium was found to be associated with functionally immobile solid phases, requiring dissolution processes for contaminant release. The total uranium leached from this sediment was less than predicted from the sequential extractions, with an unusual leaching behavior of initially decreasing, but later slowly increasing, concentrations. This behavior may indicate the presence of a slowly released uranium-complex that is unidentified. The K_d value for uranium was calculated to be 14.23 mL/g. A very small concentration of Cr was also observed in the leaching experiments with the initial few leach samples. Stop-flow events indicated a very slow dissolution of a Cr-containing precipitate.
 - Isotope analysis for this borehole indicates a strong influence of an industrial process that correlates with a reverse well and its screen depth.
 - Based on the data collected in this laboratory study, the following attenuation processes are important at this waste site. Sorption processes are important for uranium and chromium. No indications of reduction were observed in these samples and the potential for reduction through abiotic (e.g., ferrous iron) processes is limited.

The study provided a set of data that addressed the study objectives and can support future evaluation of remedies, including MNA and the associated fate and transport assessment that is needed as a basis for remedy evaluations. The first objective was to jointly evaluate contaminant concentrations and the biogeochemical and hydrologic setting for these data. This information provides a baseline for interpreting attenuation and transport studies. As noted, there were significant variations in transport parameter values and some attenuation mechanisms linked to specific sediment characteristics (e.g., carbonate content). For scaling and use of this information in fate and transport assessments, these variations should be considered in light of the sample properties. For this study, the sample properties were linked to the sediment units sampled. However, geochemical indicators did not show any significant difference or effect of contamination. Scaling and use in future efforts can translate the attenuation and transport information from this laboratory study to other waste sites based on the distribution of similar sediment units (e.g., the CCU silt and CCU caliche).

Another objective of the study was to identify attenuation processes that appear to be active in these samples and that will affect contaminant transport through the vadose zone. Sorption processes were found important for uranium, and to a lesser extent for chromate. Carbonate content appeared to be important for uranium and its release behavior. Accumulation in carbonate precipitates was identified as an attenuation mechanism for uranium. Slow release of uranium was evident in leaching experiments. Geochemical signatures of reducing conditions were minimal or non-existent in the samples. Attenuation

mechanisms relevant to Tc-99 could not be fully assessed because of the low/non-detect concentrations of this contaminant. Chromium release from the sediment occurred only during the initial phases of the leaching experiments and chromium was found to be strongly associated with mineral precipitates, which were most likely naturally occurring.

A key objective of the study was to quantify attenuation and transport parameters to support parameterization of fate and transport assessments. This type of assessment will be needed to evaluate transport of contaminants through the vadose zone, to evaluate the coupled vadose zone-groundwater system, and to assess the need for, magnitude of, and/or design of remediation. The contaminant- and sample-specific values from stop-flow portions of soil-column experiments and sequential extractions provide a set of information that can be directly used to develop transport parameters. Soil-column effluent concentration data can also be compared to one-dimensional simulations to assess fate and transport model configurations for K_d or for surface complexation models.

Collectively, the information from this laboratory study can be considered in terms of updating the CSM for contaminants in the vadose zone. It can also provide input to describing the coupled vadose zone-groundwater system that needs to be considered for remedy determinations. CSM elements from this laboratory study are listed below. These elements will need to be incorporated with other data collected during the 200-DV-1 OU remedial investigation as part of updating the CSMs for the 200-DV-1 OU component waste sites.

- Sequential extraction experiments (and more coarsely indicated by comparison of water- and acid-extraction contaminant data) show that only a small fraction of the uranium mass in samples is in a mobile form that would transport under equilibrium-partitioning conditions. Leaching experiment results confirmed that slow-release processes affect the transport behavior of uranium. The relative amount of uranium mass in the mobile versus functionally immobile phases affects the potential for future mass discharge from the vadose zone to the groundwater.
- Laboratory data suggest that formation and dissolution of uranium-carbonate precipitates is a potential attenuation mechanism affecting the relative mobile and immobile mass fractions and the transport characteristics of uranium.
- Attenuation and sorption are not uniform in the vadose zone, especially for uranium. Lithology (e.g., the presence and extent of layers such as the CCU) and carbonate content affected the transport parameter values for these contaminants.
- For the waste sites included in this study, the effects of waste chemistry, other than contaminant concentrations, did not penetrate deep into the vadose zone. The geochemical signature of samples shows that transport evaluations at these waste sites will not need to include properties modified by waste chemistry for the deep portion of the vadose zone.
- While the CSM should acknowledge the potential for transformation processes (e.g., abiotic reduction), minimal evidence was observed that these processes are active. However, such transformations may have occurred in the past and contributed to the currently observed contaminant distribution within the sediment and pore water.
- Oxygen and hydrogen isotope data were collected and primarily show correlation to regional precipitation with some variations from evaporative and condensation processes. They also indicate anthropogenic effects (e.g., industrial processes) for some of the waste sites.

- It will be important to incorporate variations in physical property data into the CSM to augment existing data and correlate to indirect measures of lithology (e.g., geophysical logging). Additional detailed hydraulic property data were collected for this laboratory study and will be documented in a separate report.

This laboratory study extended the characterization of the 200-DV-1 OU to include identification and quantification of contaminant attenuation processes and parameters that will be needed to evaluate transport of contaminants through the vadose zone into the groundwater. The data generated in this laboratory study enable the site CSMs and transport analyses to be updated to reflect the observed contaminant behavior. In addition, the laboratory study was structured to address the information requirements for considering MNA as all or part of a remedy (i.e., EPA's guidance document *Use of Monitored Natural Attenuation for Inorganic Contaminants in Groundwater at Superfund Sites*¹) and can be used as part of the technical defensibility for identifying attenuated transport through the vadose zone within the remedial investigation and feasibility study for the 200-DV-1 OU.

¹ EPA. 2015. *Use of Monitored Natural Attenuation for Inorganic Contaminants in Groundwater at Superfund Sites*. OSWER Directive 9283.1-36, U.S. Environmental Protection Agency, Office of Solid Waste and Emergency Response, Washington, D.C.

Acknowledgments

This work was funded by the CH2M Hill Plateau Remediation Company as part of the 200-DV-1 Operable Unit activities at the Hanford Site. The Pacific Northwest National Laboratory is operated by Battelle Memorial Institute for the DOE under Contract DE-AC05-76RL01830.

Acronyms and Abbreviations

CAWSRP	<i>Conducting Analytical Work in Support of Regulatory Programs</i>
CCU	Cold Creek Unit
CCUc	Cold Creek unit – carbonate
CCUg	Cold Creek unit – gravel-dominated
CCUz	Cold Creek unit – silt-dominated
CHPRC	CH2M Hill Plateau Remediation Company
COC	contaminant of concern
CSM	conceptual site model
DI	deionized
EPA	U.S. Environmental Protection Agency
ESL	Environmental Sciences Laboratory
H1	Hanford formation unit 1 – gravel-dominated
H2	Hanford formation unit 2 – sand-dominated
HASQARD	<i>Hanford Analytical Services Quality Assurance Requirements Document</i>
ICP	inductively coupled plasma
MS	mass spectrometry
MNA	Monitored Natural Attenuation
OES	optical emission spectrometry
OU	operable unit
PNNL	Pacific Northwest National Laboratory
QA	quality assurance
Rwie	Ringold Formation member Wooded Island unit E
TC	total carbon
TIC	total inorganic carbo
TOC	total organic carbon
WE	water extraction
XRD	X-ray diffraction

Contents

Executive Summary	iii
Summary	iii
Acknowledgments.....	xi
Acronyms and Abbreviations	xiii
1.0 Introduction	1.1
2.0 Objectives	2.1
3.0 Approach	3.1
3.1 Sample Handling, and Selection of Sample Intervals and Associated Analyses	3.1
3.2 Laboratory Methods	3.4
3.2.1 Analysis Objective 1: Physical Characterization	3.4
3.2.2 Analysis Objective 2: Contaminant Concentration, Distribution, and Oxidation- Reduction State	3.5
3.2.3 Analysis Objective 3: Geochemical Conditions.....	3.6
3.2.4 Analysis Objective 4: Contaminant Release Rate from Sediment and Mobility	3.7
3.2.5 Analysis Objective 5: Oxygen and Hydrogen Isotopic Signature of the Pore Water	3.8
3.2.6 Chemical Analysis Methods.....	3.9
4.0 Results	4.1
4.1 Contaminant Distribution.....	4.1
4.1.1 Contaminants and Geochemical Constituents.....	4.2
4.1.2 Iron and Manganese Characterization.....	4.7
4.1.3 Oxygen and Hydrogen Isotopes	4.10
4.1.4 Sediment Physical Characterization.....	4.16
4.1.5 B-Complex Perched Zone XRD Analysis.....	4.21
4.2 Contaminant Attenuation Processes.....	4.22
4.3 Contaminant Mobility	4.26
4.3.1 S-13 Waste Site (C9513) Samples	4.27
4.3.2 T-3 Reverse Well Waste Site (C9555) Sample	4.32
4.3.3 Uranium and Chromium Release Rate from Sediments.....	4.34
5.0 Quality Assurance.....	5.1
6.0 Conclusions	6.1
7.0 References	7.1
Appendix A Geologist Descriptions of Samples	A.1

Figures

Figure 1. Attenuation mechanisms (green font) for inorganic contaminants in the vadose zone and factors that can impact attenuation (black font) (Truex et al. 2015a).	1.1
Figure 2. Location of waste sites and boreholes where samples were obtained for this laboratory study (adapted from DOE 2012).	1.3
Figure 3. Nominal schematic of analysis on specific core intervals.	3.3
Figure 4. Water extraction line system used for quantitative collection of sorbed and pore waters from vadose zone samples. The insert shows a single cell on the line where a sample is placed in the large tube on the right and water is cryogenically trapped in the smaller tube on the left. The backdrop shows the larger system setup, whereby a series of these cells are connected and share access to a common vacuum manifold (the stainless steel line behind the extraction cells). The larger system contains a total of six extraction ports, which can be used in parallel to extract multiple samples simultaneously.	3.9
Figure 5. Iron (a) and manganese (b) surface phase distributions in sediments, based on liquid extractions.	4.9
Figure 6. Isotopic results from the analysis of vadose zone waters extracted.	4.12
Figure 7. Results for each set of samples showing dual isotope plots and isotopic variability of water isotopes ($\delta^{18}\text{O}$ and $\delta^2\text{H}$) over core depth.	4.14
Figure 8. Core images of borehole B-42 (C9497) for sample B39M00 (Liner 39C, CCUg sample).	4.17
Figure 9. Core images of borehole T-3 (C9555) for sample B39DB67 (Liner 57B, H2/CCUz sample).	4.17
Figure 10. Core images of borehole T-3 (C9555) for sample B39BL58 (Liner 31D, Rwie sample).	4.18
Figure 11. Core images of borehole T-7 (C9503) for sample B39VR9 (Liner 5C, H2/CCUz sample).	4.18
Figure 12. Core images of borehole T-7 (C9503) for sample B39VT4 (Liner 6B, CCUz/CCUc sample).	4.19
Figure 13. Core images of borehole T-7 (C9503) for sample B39VY1 (Liner 18C, Rwie sample).	4.19
Figure 14. Core images of borehole S-13 (C9513) for sample B39X10 (Liner 18E, H2/CCUz sample).	4.20
Figure 15. Core images of borehole S-13 (C9513) for sample B39X55 (Liner 25D, CCUc sample).	4.20
Figure 16. Core images of borehole S-13 (C9513) for sample B39XC3 (Liner 39D, Rwie sample).	4.21
Figure 17. Comparison of the XRD results from the perched zone sample analysis to the reference patterns. (For QA purposes, data presented in this figure are for information only.)	4.22
Figure 18. Sequential liquid extractions with analysis of uranium shown as: a) total uranium concentration in each phases, and b) fraction of uranium in each phases.	4.25
Figure 19. Sequential liquid extractions with analysis of chromium shown as a) total Cr concentration in each phases, and b) fraction of Cr in each phases.	4.26
Figure 20. Contaminant leaching behavior in sample B39DCJ2 (S-13, C9513) as shown by a) U sequential extraction, b) U leaching (0 to 10 pore volumes), c) U leaching (to 110 pore volumes), d) Cr sequential extraction, and e) Cr leaching (to 110 pore volumes).	4.29

Figure 21. Contaminant leaching behavior in sample B3DCJ7 (S-13, C9513) as shown by a) U sequential extraction, b) U leaching (to 125 pore volumes), c) Cr sequential extraction, and d) Cr leaching (to 125 pore volumes). 4.31

Figure 22. Contaminant leaching behavior in sample B3DB67 (T-3, C9555) as shown by a) U sequential extraction, b) U leaching (to 120 pore volumes), c) U leaching (to 120 pore volumes) in a duplicate experiment, d) Cr leaching (to 125 pore volumes), and e) Cr leaching (to 125 pore volumes) in a duplicate experiment. 4.33

Figure 23. Uranium release rate calculated from sediment leach studies at stop-flow events showing release rate as a function of: a) pore volume, b) uranium leached mass. 4.36

Figure 24. Chromium release rate calculated from sediment leach studies at stop-flow events showing release rate as a function of a) pore volume, b) chromium leached mass. 4.37

Figure 25. Correlation between the uranium and chromium release from sediments during stop-flow events in leach studies. 4.38

Tables

Table 1. Sediment samples selected for contaminant concentration and geochemical characterization.....	3.1
Table 2. Sediment samples selected for isotope analysis (Section 3.2.5).....	3.2
Table 3. Sediment samples selected for detailed hydraulic characterization (separate report, methods described in Section 3.2.1).....	3.2
Table 4. Physical sediment analysis methods.....	3.5
Table 5. Extraction methods for contaminant analysis.....	3.5
Table 6. Extraction methods for geochemical analysis.....	3.7
Table 7. Contaminant mobility tests.....	3.8
Table 8. Isotopic analysis tests.....	3.8
Table 9. Chemical analyses.....	3.10
Table 10. Water and acid extractable concentration of contaminants in sediments.....	4.3
Table 11. Geochemical characterization of sediment pore water by water/sediment (1:1) extraction.....	4.4
Table 12. Samples selected for sequential extractions.....	4.7
Table 13. Ferrous and ferric iron phases in sediments based on liquid extractions.....	4.8
Table 14. Manganese phases in sediments based on liquid extractions.....	4.8
Table 15. Summary of Hanford mineralogy (after Xue et al. 2003).....	4.10
Table 16. Sediment samples selected for isotope analyses and data values.....	4.11
Table 17. XRD analysis results of the perched zone samples from borehole B-8 (C9488). ^(a)	4.21
Table 18. Sequential extraction of contaminants from sediment samples.....	4.23
Table 19. Contaminant distribution in sequential liquid extracted sediments for U-238, Cr, and Tc-99.....	4.24
Table 20. Selected sediment samples for 1-D soil-column leaching experiments.....	4.27
Table 21. Contaminant release rates calculated for stop-flow events during soil-column leaching experiments.....	4.35

1.0 Introduction

Contaminants disposed of at the land surface and present in aqueous phase migrate through the vadose zone prior to entering groundwater. Such discharge creates a source for a contaminant plume in the underlying groundwater. Therefore, identification and quantification of attenuation processes and other factors that affect migration of contaminants of concern (COCs) in vadose zone are critical for assessing the need for, and type of, remediation in the vadose and groundwater. This type of information will enhance the existing conceptual site models (CSMs) for the 200-DV-1 Operable Unit (OU) (Serne et al. 2010; CHPRC 2015a,b) in support of fate and transport analysis and remedy evaluation.

Contaminant transport through the vadose zone beneath waste disposal sites is affected by two types of attenuation processes: (1) attenuation caused by advective and dispersive factors related to unsaturated water flow and (2) attenuation caused by biogeochemical reactions and/or physical/chemical interaction with sediments (e.g., phenomena such as sorption, solubility control, and decay/degradation that slow contaminant movement relative to water movement). Figure 1 summarizes the types of attenuation mechanisms that may affect contaminant transport in the vadose zone. Note that Figure 1 includes waste fluid properties and chemistry because wastes at Hanford were typically released directly to the vadose zone and attenuation may be affected by the nature of the waste material (e.g., Szecsody et al. 2013; Truex et al. 2014).

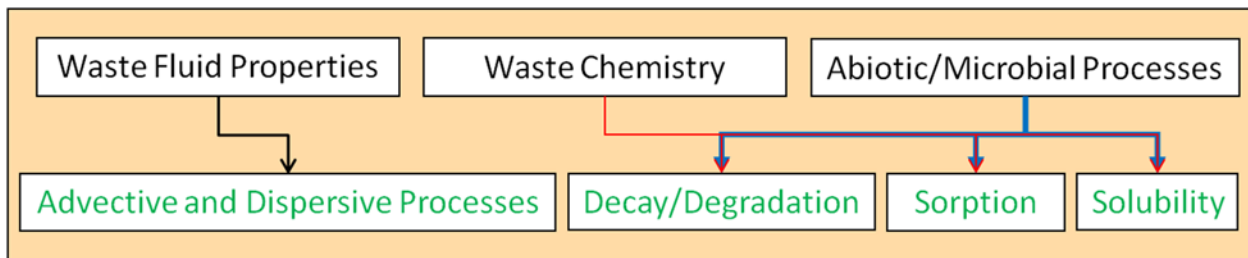


Figure 1. Attenuation mechanisms (green font) for inorganic contaminants in the vadose zone and factors that can impact attenuation (black font) (Truex et al. 2015a).

A framework to characterize these attenuation and transport processes is provided by U.S. Environmental Protection Agency (EPA) guidance document *Use of Monitored Natural Attenuation for Inorganic Contaminants in Groundwater at Superfund Sites* (EPA 2015). Additional information about vadose zone attenuation processes reported by Truex and Carroll (2013) and Truex et al. (2015a) is also relevant for characterization of the vadose zone. These documents point to approaches that can be applied to identify and describe transport parameters for a vadose zone site.

Deep vadose zone contamination is an important issue at the Central Plateau of the Hanford Site since it presents a potential source (due to past disposal practices) for continued release and discharge of contaminants into the underlying groundwater. The 200-DV-1 OU encompasses 43 waste sites and is currently being characterized to support understanding the nature and extent of contamination and the selection of appropriate remedies and remedial treatment technologies (DOE 2012, 2016). The purpose of the analysis conducted and described in this report is to provide the necessary contamination and attenuation characterization data and its interpretation for the selected waste sites for the 200-DV-1 OU characterization project. Through a data quality objectives process, specific 200-DV-1 waste sites were selected for evaluation of attenuation and transport processes for mobile uranium, technetium-99 (Tc-99),

iodine-129 (I-129), chromium, and nitrate contaminants. These waste sites were selected based on the following factors:

- Waste stream inventory (radiological and/or chemical component)
- Waste stream differentiation (acid/base, volume, unique characteristics)
- Disposal type (crib, trench, french drain, reverse well, etc.)
- Potential to obtain parameters from significant (site-specific) geologic units to fill data gaps in transport parameters

The data quality objectives process also identified that the characterization of attenuation and transport processes needed to include the following activities:

- Evaluate contaminant and geochemical constituents in the samples
- Identify interactions of contaminants with sediments
- Quantify contaminant mobility
- Evaluate factors controlling contaminant mobility

The waste sites covered in this report include B-42 Trench, T-3 Reverse Well, T-7 Tile Field, S-13 Crib, and B-8 Crib and Tile Field. The locations of the boreholes where the sediment samples were collected are shown in Figure 2. Detailed description of these waste sites and boreholes is contained in the 200-DV-1 OU characterization planning documents (DOE 2012, 2016) and will be compiled in future 200-DV-1 characterization reports. This report focuses only on description of the analyses conducted on the samples selected to assess attenuation and transport processes.

This characterization information will be used to refine CSMs by enhancing the understanding of controlling features and processes for transport of contaminants through the vadose zone to the groundwater. The characterization approach was developed based on EPA (2015) guidance, identifying specific objectives (Section 2.0) and types of laboratory analyses (Section 3.0) to conduct on sediment samples. This report provides results and interpretation of these laboratory analyses from analysis of samples collected in fiscal year 2018 (Section 4.0), and conclusions with respect to how these results are important for the remedial investigation/feasibility study for the 200-DV-1 OU and associated contaminant fate and transport assessment (Section 6.0). Quality assurance (QA) applied for this work is described in Section 5.0.

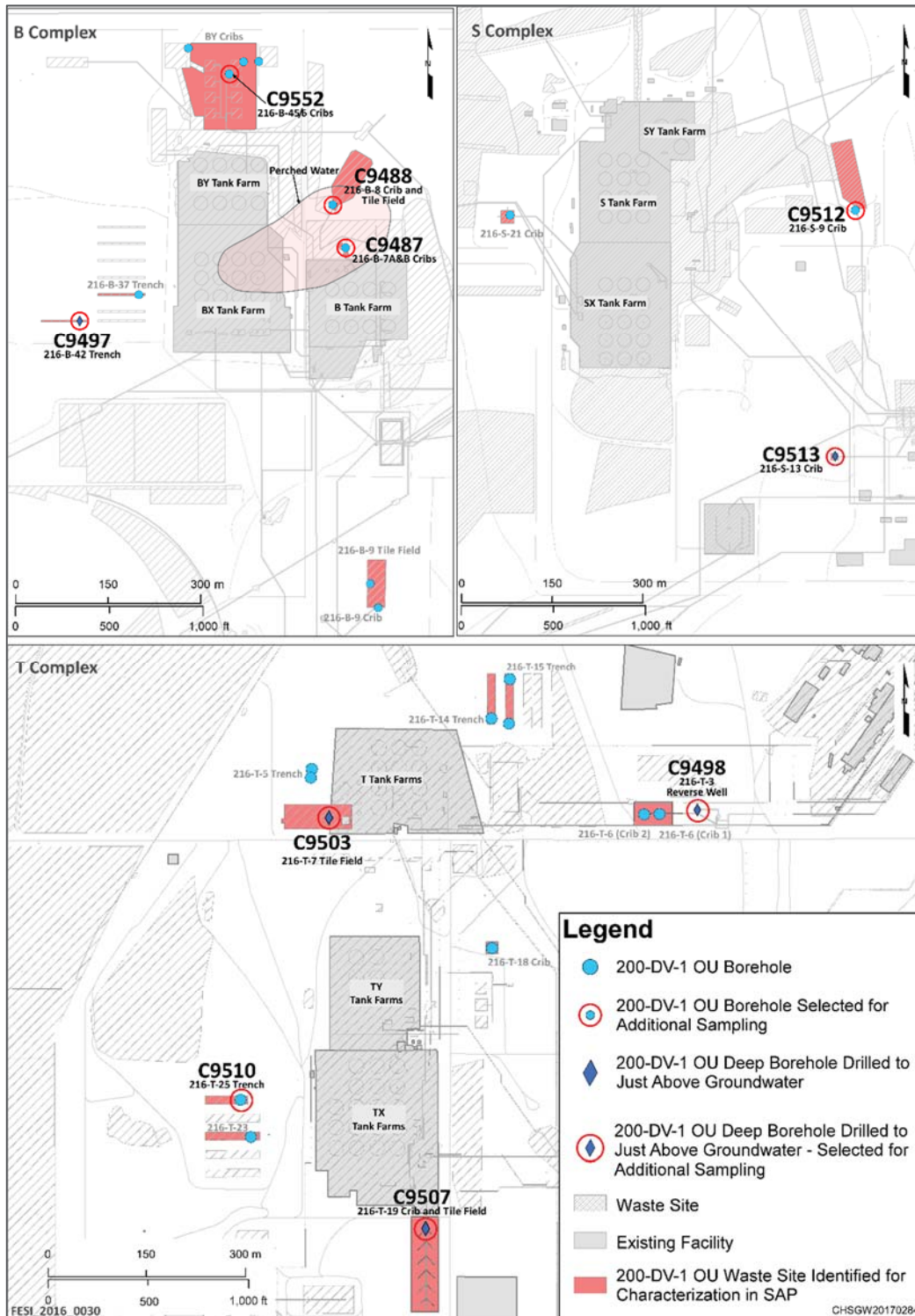


Figure 2. Location of waste sites and boreholes where samples were obtained for this laboratory study (adapted from DOE 2012).

2.0 Objectives

The specific types of data identified for inclusion in the laboratory study reported herein will provide data and associated interpretation to support the following three objectives. These objectives are elements of the framework identified in the EPA guidance (EPA 2015) for evaluating Monitored Natural Attenuation (MNA) of inorganic contaminants, which directly supports development of suitable contaminant transport parameters.

- Define the contaminant distribution and the hydrologic and biogeochemical setting
- Identify attenuation processes and describe the associated attenuation mechanisms
- Quantify attenuation and transport parameters for use in evaluating remedies

These overall objectives led to a series of laboratory analyses designed to provide suitable data and information. A phased approach was used for this effort to progressively gather more detailed information based on initial results. This progressive/tiered approach is consistent with EPA MNA guidance.

The information from these analyses will be used as input to evaluate the feasibility of MNA and other remedies for the 200-DV-1 OU. The information from these analyses will also be used as input to refine the CSM for the targeted vadose zone sites.

The objectives listed above are accomplished through the following:

- Measuring concentration and mass of contaminants associated with aqueous, adsorbed, and various solid phases by batch extractions
- Measuring concentration and mass of contaminants that leach from sediments over time in high sediment-water ratio 1-D column studies
- Characterizing Fe- and Mn-oxide surface phases, including reduced phases that can potentially cause abiotic reduction of some contaminants and oxic phases that are available for microbial reduction
- Characterizing the potential for uranium and chromate leaching in high sediment-water ratio stop-flow columns
- Determining the oxygen and hydrogen isotopic signature of the pore water

3.0 Approach

Samples for the laboratory analyses were collected by CH2M Hill Plateau Remediation Company (CHPRC) as part of the drilling campaign for the 200-DV-1 OU remedial investigation. Sets of samples for each borehole included multiple sample intervals as potential targets for the analyses. The sample handling procedures used upon sample delivery to the laboratory are described in Section 3.1. This section also describes the selection of the specific sample intervals and the analyses selected for these sample intervals. Laboratory and experimental methods were derived from the approaches described in *Use of Monitored Natural Attenuation for Inorganic Contaminants in Groundwater at Superfund Sites* (EPA 2015). The laboratory analysis methods are presented in Section 3.2.

3.1 Samples Sample Handling, and Selection of Sample Intervals and Associated Analyses

Pacific Northwest National Laboratory (PNNL) and CHPRC jointly selected samples for testing through meetings that were held after all of the samples for a borehole were collected. The selected samples from boreholes C9497, C9555, C9503, C9513, and C9488 for the analyses discussed in this report are listed in Table 1, 2, and 3. The samples selected for intact hydraulic property assessment will be described in a separate report.

Table 1. Sediment samples selected for contaminant concentration and geochemical characterization.

Borehole Designation	Borehole ID	Core	Sample ID	Nominal Geologic Unit	Depth Interval (ft bgs)	Analysis (Report Section)
B-42	C9497	39C	B39M00	CCUg	237-238	3.2.1 ^b , 3.2.2.1, 3.2.3, 3.2.6
S-13	C9513	18E	B39X10	H2/CCUz	115.6-116.6	3.2.1 ^b , 3.2.2.1, 3.2.3, 3.2.6
S-13	C9513	25D	B39X55	CCUc	151.7-152.7	3.2.1 ^b , 3.2.2.1, 3.2.3, 3.2.6
S-13	C9513	39D	B39XC3	Rwei	221.5-222.5	3.2.1 ^b , 3.2.2.1, 3.2.3, 3.2.6
T-3	C9555	57B	B3DB67	H2/CCUz	106-107	3.2.1 ^b , 3.2.2.1, 3.2.2.2, 3.2.3, 3.2.4, 3.2.6
T-3	C9555	31D	B3BL58	Rwie	181.3-182.3	3.2.1 ^b , 3.2.2.1, 3.2.3, 3.2.6
T-7	C9503	5C	B39VR9	H2/CCUz	87-88	3.2.1 ^b , 3.2.2.1, 3.2.3, 3.2.6
T-7	C9503	6B	B39VT4	CCUz/CCUc	91-92	3.2.1 ^b , 3.2.2.1, 3.2.3, 3.2.6
T-7	C9503	18C	B39VY1	Rwei	152-153	3.2.1 ^b , 3.2.2.1, 3.2.2.2, 3.2.3, 3.2.6
B-8 ^a	C9488	37D	B355M0	CCU Perched Interval	223.5-224.5	3.2.1, 3.2.6
B-8 ^a	C9488	37E	B355M1	CCU Perched Interval	224.5-225.5	3.2.1, 3.2.6
B-42	C9497	23 (Grab)	B3BMT1	H2	161-163.5	3.2.2.2
B-42	C9497	44 (Grab)	B3BMW9	CCUg	260-261.2	3.2.2.2
S-13	C9513	13 (Grab)	B3DCJ2	H2	90.5-92	3.2.2.2, 3.2.4
S-13	C9513	21 (Grab)	B3DCJ7	CCUc	131.5-133.5	3.2.2.2, 3.2.4
S-13	C9513	24 (Grab)	B3DCK2	CCUc	146.1-148.8	3.2.2.2
S-13	C9513	29 (Grab)	B3DCK7	Below CCUc	171-172	3.2.2.2

CCU is Cold Creek Unit; CCUc is Cold Creek unit – carbonate; CCUg is Cold Creek unit – gravel-dominated; CCUz Cold Creek unit – silt-dominated; H2 is Hanford formation unit 2 – sand-dominated; Rwie is Ringold Formation member Wooded Island unit E.

- (a) These perched zone samples were selected only for sediment total carbon, total organic carbon, and x-ray diffraction analyses.
- (b) These samples were analyzed for lithology, texture, petrologic composition (sand, gravel, basalt, quartz) and photos, and moisture content. Another set of samples was selected for more detailed hydraulic characterization (see Table 3).

Table 2. Sediment samples selected for isotope analysis (Section 3.2.5).

Borehole Designation	Borehole ID	Core	Sample ID	Nominal Geologic Unit	Depth Interval (ft bgs)
B-42	C9497	11	B3BMP8	H1	65.3-68.8
B-42	C9497	4	B3BMN2	H2	102.0-104.0
B-42	C9497	23	B3BMT0	H2	161.0-163.5
B-42	C9497	37	B3BMW2	CCUg	231.0-233.0
B-42	C9497	39	B3BM02	CCUg	235.0-236.0
B-42	C9497	44	B3BMW8	CCUg	260.0-261.2
T-7	C9503	6	B39VT5	CCUz	90.0-91.0
T-7	C9503	41	B3D1D9	CCUc	98.0-99.0
T-7	C9503	13	B3D1H2	Rwie	126.0-128.0
T-7	C9503	16	B3D1H8	Rwie	140.0-145.0
T-7	C9503	22	B3D1K0	Rwie	171.3-174.1
T-7	C9503	25	B3D1K7	Rwie	186.2-189.2
T-7	C9503	29	B3D1L4	Rwie	206.1-209.1
T-7	C9503	32	B3D1M0	Rwie	220.5-221.5
T-3	C9555	17-18	B3FCL5	CCUz	110.4-111.2
T-3	C9555	24	B3FCM1	CCUc	135.0-136.4
T-3	C9555	28	B3FCM8	Rtf	156.7-158.2
T-3	C9555	50	B3FLP9	Rwie	170.3-171.8
T-3	C9555	35	B3FLR3	Rwie	200.3-202.8
T-3	C9555	37	B3FLR7	Rwie	210.4-212.4
T-3	C9555	41	B3FLT1	Rwie	230.2-232.2
T-3	C9555	44	B3FLT5	Rwie	245.0-247.6
S-13	C9513	10	B3DCH7	H2	76.0-79.0
S-13	C9513	13	C3DCJ2	H2	90.5-92.0
S-13	C9513	18	B3F940	H2	115.6-116.6
S-13	C9513	21	B3DCJ7	H2	131.5-133.5
S-13	C9513	24	B3DCK2	CCUz	146.1-148.8
S-13	C9513	29	B3DCK7	Rtf	171.5-174.3
S-13	C9513	33	B3DCL2	Rtf	191.7-194.1
S-13	C9513	40	B3DCL7	Rwie	225.0-227.0
S-13	C9513	41	B3DCM2	Rwie	231.4-234.0

CCU is Cold Creek Unit; CCUc is Cold Creek unit – carbonate; CCUg is Cold Creek unit – gravel-dominated; CCUz is Cold Creek unit – silt-dominated; H2 is Hanford formation unit 2 – sand-dominated; Rwie is Ringold Formation member Wooded Island unit E

Table 3. Sediment samples selected for detailed hydraulic characterization (separate report, methods described in Section 3.2.1).

Borehole Designation	Borehole ID	Core	Sample ID	Nominal Geologic Unit	Depth Interval (ft bgs)
B-42	C9497	41B	B39M11	CCUg	248-249
S-13	C9513	25B	B39X53	CCUc	153.7-154.7
S-13	C9513	27C	B39X68	Rtf	162.7-163.7
T-7	C9503	8C	B39VV7	CCUc	102-103
T-7	C9503	19E	B39VY9	Rwie	155-156
B-8 ^a	C9488	37D	B355M0	CCU Perched Interval	223.5-224.5
B-8 ^a	C9488	37E	B355M1	CCU Perched Interval	224.5-225.5

(a) These perched zone samples were selected only for a limited hydraulic characterization.

Consistent with the recommendations given in Truex et al. (2017), two types of samples (i.e., core and grab samples) were used in a two-tiered approach in this study. Grab samples are the additional samples collected as a vertical profile in the borehole at selected vertical locations where contaminant of concern analyses are conducted by CHPRC. In the two-tiered approach used here, the baseline analyses (i.e., sediment geochemistry and contaminant distribution) used an initial set of core samples. The results from these samples were used to evaluate the value of conducting more detailed attenuation analyses, and where the contaminant concentrations were found insufficient, grab samples were used to augment the number of samples available for assessing leaching characteristics. Therefore, in this study, a combination of both core and grab samples were selected for more detailed attenuation evaluation (i.e., sequential extractions, 1-D soil-column experiments).

The samples were in 12-inch-long liners within a 5-ft-long sonic core. The liner samples were shipped from the drilling site to the PNNL 331 Building, where they were inspected, the chain of custodies were completed, and the samples were placed in a refrigerator (4°C). Once selected, the sample liner for use in isotopic analyses was frozen, except as noted in Table 1 where a subsample of liquid from a liner containing saturated sediment and free liquid was collected and frozen as the sample for isotopic analysis. The nominal liner sample disposition plan within a 5-ft core sample is shown in Figure 3. Target 5-ft cores selected for testing generally divide liners for specific types of tests according to this plan. However, the plan was modified in some cases depending on the observed sample recovery and initial inspection of material type within the liners by the PNNL-CHPRC technical team.

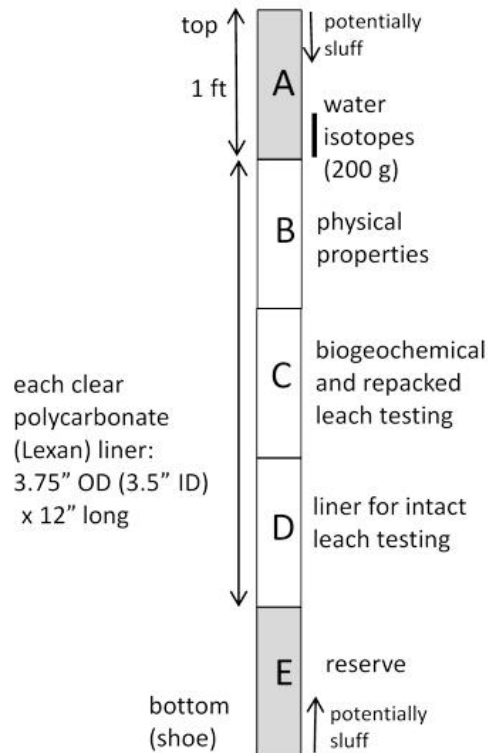


Figure 3. Nominal schematic of analysis on specific core intervals.

3.2 Laboratory Methods

Laboratory analyses were selected to evaluate attenuation processes and other factors affecting fate and transport of contaminants in the vadose zone. These analyses were based on the characterization approaches described for evaluating MNA of inorganic contaminants (EPA 2007a,b, 2010, 2015). The analyses were selected to provide data to support interpretation of contaminant behavior in the vadose zone, and will be used in conjunction with additional information produced by CHPRC as part of their related characterization efforts at these and other vadose zone boreholes.

The selected laboratory analyses for the overall characterization effort were applied in a two-step process: (1) basic analysis (Tier 1), and (2) advanced analysis (Tier 2). The purpose of this stepwise approach was to utilize the information generated during the basic analysis to inform decision making for the second stage, resulting in more targeted selection of samples for sequential extractions and column studies, as well as intact hydraulic property measurements.

The laboratory experimental effort was organized using the following specific analysis objectives, which are related to the overall objectives described in Section 2.0. The subsequent sections describe the laboratory methods applied for each of the analysis objectives.

Analysis Objectives

1. Characterize the physical aspects of the sample that are used to evaluate pore water flow and provide the sediment information needed to interpret and scale biogeochemical analysis results.
2. Characterize the contaminant concentration, distribution, and, where appropriate, the oxidation-reduction state and chemical form in the pore water and on sediment surfaces. This information allows interpretation of contaminant mobility in the context of the biogeochemical system data.
3. Characterize the geochemical conditions in the pore water and on sediment surfaces to facilitate interpretation of attenuation and transport processes. Information about elements and compounds in the samples enables evaluation of biogeochemical processes related to the contaminant chemical form and mobility.
4. Characterize the contaminant mobility using tests that impose specific conditions, and collect temporal data for interpreting the mobility of the contaminant (e.g., by quantifying the rate of contaminant transfer to the aqueous phase).
5. Determine the oxygen and hydrogen isotopic signature of the pore water for use in comparing to existing data that may enable the source of the pore water within the sample to be evaluated.

3.2.1 Analysis Objective 1: Physical Characterization

Standard physical sediment analysis methods shown in Table 4 were applied as needed to meet analysis objective 1. Because of the long duration required for determining unsaturated hydraulic properties, results of the hydraulic property evaluation will be presented in a separate report.

Table 4. Physical sediment analysis methods.

Required Data	Method Basis
Moisture content	ASTM D2216-10
Intact-core dry bulk density, particle density and porosity	ASTM D7263-09, D854-14
Core particle size by sieve (4, 2, 1, 0.5 mm sieves)	ASTM D6913-04
Core particle size by laser diffraction (< 0.5 mm)	ASTM D4464-15
Lithology, texture, petrologic composition (sand, gravel, basalt, quartz) and photos	Geologist inspection of borehole samples
Mineralogy by X-ray diffraction (XRD) ^(a)	RGD106SOP

(a) XRD analysis was selected and conducted only for the two samples from borehole B-8 (C9488).

3.2.2 Analysis Objective 2: Contaminant Concentration, Distribution, and Oxidation-Reduction State

Contaminant data were interpreted based on the elements and compounds present in the sample pore water or on sediment surfaces. Contaminant information was obtained by the analyses listed in Table 9 (Section 3.2.6). Specific types of extractions along with the concentration information were applied to evaluate the contaminant conditions. Extractions applied to evaluate the contaminant conditions are listed in

Table 5.

Table 5. Extraction methods for contaminant analysis.

Required Data	Method Basis
Water extraction (1:1 sediment:H ₂ O)	Um et al. 2009 and Zachara et al. 2007
Acid extraction (1:3 sediment:H ₂ O, 8M HNO ₃)	Um et al. 2009 and Zachara et al. 2007
Sequential extractions: Artificial groundwater Ion exchangeable pH 5.0 acetate pH 2.3 acetic acid Oxalate, oxalic acid 8M HNO ₃ , 95°C	Gleyzes et al. 2002; Beckett 1989; Larner et al. 2006; Sutherland and Tack 2002; Section 3.2.2.1

3.2.2.1 Water and Acid Extraction of Contaminants from Sediments

The water extraction (at 1:1 sediment/water ratio) is the aqueous contaminant fraction extracted in deionized water with a 1.0-hour sediment-water contact time (from EPA 9045D, Rhoades 1996). The acid extraction is conducted at a 1:3 dry sediment/water ratio using 8M HNO₃ for 3 hours at 90°C to 95°C. This is a modified method based on EPA 3051a to not include the HCl, because the chloride ion interferes with U(VI) analysis.

3.2.2.2 Sequential Extractions

Six sequential liquid extractions were conducted on a sediment sample. Extraction 1 is the aqueous contaminant fraction, extraction 2 is the adsorbed contaminant fraction (ion exchangeable), extraction 3 is the “rind-carbonate” contaminant fraction, extraction 4 is the total carbonate extraction fraction, extraction 5 is the Fe-oxide contaminant fraction, and extraction 6 is defined as the hard-to-extract contaminant fraction. These sequential extractions were conducted at a 1:2 sediment:liquid ratio at room temperature (20°C to 25°C). The extraction used reagents 1 through 6 defined below.

- **Reagent 1 - Artificial groundwater:**

Constituent	Concentration (mM)
H ₂ SiO ₃ *nH ₂ O, silicic acid	0.2
KCl, potassium chloride	0.11
MgCO ₃ , magnesium carbonate	0.15
NaCl, sodium chloride	0.26
CaSO ₄ , calcium sulfate	0.49
CaCO ₃ , calcium carbonate	1.5

- **Reagent 2 - 0.5 mol/L Mg(NO₃)₂:** 128.2 g Mg(NO₃)₂*6H₂O + 30 μL 2 mol/L NaOH to pH 8.0, balance deionized (DI) H₂O to 1.0 liter
- **Reagent 3 - Acetate solution:** 136.1 g sodium acetate*3H₂O + 30 mL glacial acetic acid (17.4 mol/L), pH 5.0, balance DI H₂O to 2.0 liters
- **Reagent 4 - Acetic acid solution:** concentrated glacial acetic acid, pH 2.3; 50.66 mL glacial acetic acid (17.4 mol/L) + 47.2 g Ca(NO₃)₂*4H₂O, pH 2.3, balance DI H₂O to 2.0 liters
- **Reagent 5 - Oxalate solution:** 0.1 mol/L ammonium oxalate, 0.1 mol/L oxalic acid; 9.03 g anhydrous oxalic acid + 14.2 g ammonium oxalate*H₂O, balance DI H₂O to 1.0 liter
- **Reagent 6 - 8.0 mol/L HNO₃:** 502 mL conc. HNO₃ (15.9 mol/L) + 498 mL DI H₂O

In the first extraction, 6 mL of artificial groundwater (reagent 1) is mixed with 3.0 (±0.5) g of sediment for 50 minutes; the tube is then centrifuged at 3000 rpm for 10 minutes, and liquid is drawn off the top of the sediment and filtered (0.45-μm) for analysis. Extractions 2 and 3 are conducted with the same procedure except using reagents 2 and 3, respectively. The fourth extraction uses the same procedure except with a contact time of 5 days and with use of reagent 4. The fifth extraction is conducted the same as extraction 1 except using reagent 5. In the sixth extraction, 6 mL of nitric acid (reagent 6) is added and mixed for 2 hours at 95°C with the sediment; the tube is then centrifuged at 3000 rpm for 10 minutes, and liquid is drawn off the top of the sediment and filtered (0.45-μm) for analysis.

3.2.3 Analysis Objective 3: Geochemical Conditions

Geochemical conditions were interpreted based on the elements and compounds present in the sample pore water or on sediment surfaces. The geochemical information was obtained by the analyses listed in Table 9 (Section 3.2.6). However, specific types of extractions are applied to provide material for analysis. The type of extraction and the concentration of the element/compound were both needed to interpret the data in terms of the geochemical conditions. Extractions applied to evaluate the geochemical conditions are listed in Table 6.

Table 6. Extraction methods for geochemical analysis.

Required Data	Method Basis
Water extraction (1:1 sediment:H ₂ O)	Um et al. 2009 and Zachara et al. 2007; Section 3.2.2.1
Acid extraction (1:3 sediment:H ₂ O, 8M HNO ₃)	Um et al. 2009 and Zachara et al. 2007; Section 3.2.2.1
Sequential extractions: Artificial groundwater Ion exchangeable pH 5.0 acetate pH 2.3 acetic acid Oxalate, oxalic acid 8M HNO ₃ , 95°C	Gleyzes et al. 2002; Beckett 1989; Larner et al. 2006; Sutherland and Tack 2002; Section 3.2.2.2
Iron/Mn phase extractions: Ion exchangeable Fe(II), Mn, Oxide/sulfide, Total Fe(II), Fe(III), Mn, Amorphous- Fe(III), Mn-oxides,	Heron et al. 1994; Chao and Zhou 1983; and Hall et al. 1996; Section 3.2.3.1

3.2.3.1 Iron and Manganese Extractions

Iron extractions were conducted to quantify ferrous and ferric iron (Gibbs 1976) and manganese that are solubilized by different solutions. These extractions are conducted in an anoxic chamber.

- For the first extraction, sediment samples (2.0 ± 0.5 g) were mixed with 10.0 mL of ion exchange solution (1.0 mM CaCl₂) for 50 minutes at 6 rpm, centrifuged (3000 rpm, 10 minutes), liquid filtered (0.45- μ m), and the solution was analyzed for Fe(II) and Mn.
- For the second extraction, sediment samples (2.0 ± 0.5 g) were mixed with 10.0 mL of 0.5M HCl (reagent 10) for 24 hours at 6 rpm, centrifuged (3000 rpm, 10 minutes), liquid filtered (0.45- μ m), and the solution was analyzed for Fe(II) and Mn.
- For the third extraction, sediment samples (2.0 ± 0.5 g) were mixed with 10.0 mL of 5.0M HCl for 24 hours at 6 rpm, centrifuged (3000 rpm, 10 minutes), liquid filtered (0.45- μ m), and the solution was analyzed for Fe(II) and Mn.

3.2.4 Analysis Objective 4: Contaminant Release Rate from Sediment and Mobility

Contaminant mobility was evaluated for some selected sediment samples (see Table 1) in soil-column leaching tests that impose specific conditions and collect temporal data. These tests exposed contaminated sediment to an aqueous solution (simulated groundwater) and measured changes in contaminant concentration over time under flowing conditions (Table 7). For the column tests, sequential extractions for contaminants (Section 3.2.2) were conducted on a larger set of samples to select the samples for the soil-column leaching tests. Contaminant and other geochemical constituent information from samples collected during the tests was obtained by the analyses listed in Table 9 (Section 3.2.6).

Table 7. Contaminant mobility tests.

Required Data	Method Basis
1-D soil-column test	Qafoku et al. 2004; Szecsody et al. 2013; Section 3.2.4.1

3.2.4.1 Soil-Column Test

Sediment column experiments were conducted with 1-D, vertical, bottom-up flow of injected simulated groundwater solution through contaminated sediment. The concentration of contaminant in the effluent was measured. A non-sorbing, non-reactive tracer (bromide ion) was included in the injection solution and its breakthrough was measured to assess column flow dynamics. The flow rate was set to achieve a residence time of between 1 and 4 hours. Sampling frequency in the effluent was varied based on typical contaminant elution dynamics, with more dynamics present at earlier times (fewer pore volumes).

Stop-flow events ranging from 16 to 300 hours were conducted where the flow rate of solution through the column was stopped to provide time for contaminants present in one or more surface phases on the sediment surface to partition into pore water (i.e., from diffusion from intraparticle pore space or time-dependent dissolution of precipitate phases or slow desorption). Operationally, initiating a stop-flow event involves turning off the pump and plugging both ends of the column (to prevent water movement out of the sediment column). Ending a stop-flow event involves reconnecting the column to the pump, turning on the effluent sample collector, and then turning on the pump. The calculation of the contaminant release rate from sediment ($\mu\text{g contaminant/g of sediment/day}$) uses the contaminant effluent concentration before and after the stop-flow event, and the length of time of the stop-flow event.

3.2.5 Analysis Objective 5: Oxygen and Hydrogen Isotopic Signature of the Pore Water

Isotopic analysis for oxygen (^{18}O) and hydrogen (^2H) can be applied to either water samples or water extracted from sediment (Prudic et al. 1997). Within the vadose zone, the small amounts of available water is typically associated with either mineral surfaces or contained within pore spaces. An extraction procedure was used to quantitatively remove water from solid soil samples. It is important to note that isotope fractionation can occur when only a portion of the total water is extracted from the soil. Thus, it is essential that the methods applied have an extremely high extraction efficiency. Table 8 shows the methods used for isotopic analysis.

Table 8. Isotopic analysis tests.

Required Data	Method Basis
Water extraction	West et al. 2006 and Goebell and Lascano 2012
Water isotope analysis	Newman et al. 2009

A vacuum distillation apparatus (Figure 4) was used for extracting water from 31 grab samples taken from the vadose zone via four different cores (C9497, C9503, C9555, and C9513). This apparatus was constructed based on slightly modified versions of those discussed in West et al. (2006) and Goebel and Lascano (2012). For use, a soil sample was added to a glass tube on one end of the system and then temporarily frozen at liquid nitrogen temperatures to prevent water migration out of the material. A

vacuum was established to remove all air from the headspace, following which the sample was heated ($\sim 95^{\circ}\text{C}$) to drive off the native water. The resulting water vapor migrated through the glass transfer line and was then condensed/frozen into a cryogenic trap cooled with liquid nitrogen. Pressure can be monitored to help guide the overall duration of the extraction to ensure complete water transfer (typical extractions take up to 6 hours). The ^{18}O and ^2H content of the extracted water were analyzed using a high-precision, spectroscopy-based, water analyzer. Water was extracted using the methods outlined in a PNNL test instruction (TI-DVZ-CHPRC-0011) and isotopic analysis was performed using a PNNL operating procedure (OP-DVZ-AFRI-002) for the analytical instrument.

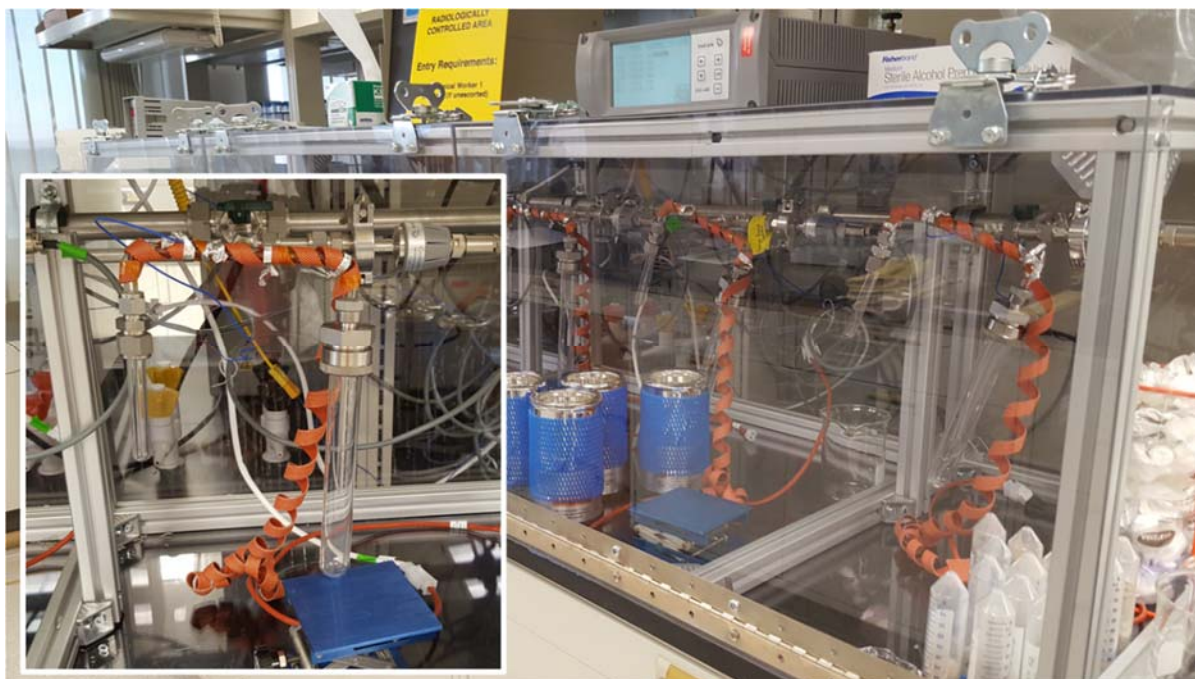


Figure 4. Water extraction line system used for quantitative collection of sorbed and pore waters from vadose zone samples. The insert shows a single cell on the line where a sample is placed in the large tube on the right and water is cryogenically trapped in the smaller tube on the left. The backdrop shows the larger system setup, whereby a series of these cells are connected and share access to a common vacuum manifold (the stainless steel line behind the extraction cells). The larger system contains a total of six extraction ports, which can be used in parallel to extract multiple samples simultaneously.

3.2.6 Chemical Analysis Methods

Standard chemical analytical methods were applied to quantify elements and compounds that are present in extraction solutions and temporal samples from the tests described in Section 3.2, as shown in Table 9.

Table 9. Chemical analyses.

Analysis ^(a)	Hold Time	Constituents Analyzed	Method Basis
Metals by ICP-OES	6 months	Al, Ba, Ca, Fe, K, Mg, Mn, Na, Si, Sr, Cr	EPA 6010D
U, Tc-99 by ICP-MS	6 months	U, Tc-99	EPA 6020B
Iodine species by ICP-MS	6 months	Iodide, iodate	PNNL-ESL-ICPMS-iodine
Kinetic phosphorescence analysis	6 months	U(VI)	Brina and Miller 1992
Cr(VI)	24 hr	Cr(VI)	Hach 8023
Fe(II)	24 hr	Fe(II)	Hach 8147
Br ⁻ by electrode	28 days	Br ⁻	EPA 9211
Anions by ion chromatography	Nitrate, nitrite: each 48 hr; PO ₄ : 48 hr	Cl ⁻ , F ⁻ , Br ⁻ , NO ₃ ⁻ , NO ₂ ⁻ , PO ₄ ³⁻ , SO ₄ ²⁻	EPA 9056A
pH by electrode	Immediate (12 hr)	pH	EPA 9040C
Specific conductance (SpC) by electrode	Immediate (12 hr)	SpC	EPA 9050A
Total carbon (TC) and total inorganic carbon (TIC) ^(b)	28 days	TC and TIC	EPA 9060A

ICP is inductively coupled plasma; MS is mass spectrometry; OES is optical emission spectrometry.

(a) Analyses were for aqueous samples except as noted footnote b.

(b) TC and TIC were also analyzed directly on sediment samples as an information-only analysis using manufacturer procedures (SHIMADZU SSM-5000A procedure).

4.0 Results

The laboratory analysis data are described below and interpreted in relation to the three main objectives of the work (Section 2.0). These objectives were developed to be consistent with EPA guidance for evaluating natural attenuation of contaminants, and to provide data and parameters that support contaminant fate and transport assessments. The sections below present the data for each of the three objectives. Quantification of hydraulic properties, as described in Section 3.2.1, for selected samples is also being conducted to support these objectives. However, because of the long-term nature of those tests, results of hydraulic property evaluation will be provided in a separate report.

In Section 4.1, contaminant distribution data are presented in the context of the hydrologic and biogeochemical setting from the following activities:

- Measurement of contaminant and geochemical constituents
- Iron and manganese characterization
- Evaluation of oxygen and hydrogen isotopes
- Sediment physical characterization

This information enables the data collected in this effort to be linked with the 200-DV-1 OU characterization data compiled by CHPRC. Collectively, this information is a foundation for interpreting contaminant distribution, correlations between contaminant data and other types of information, and the sediment conditions relevant for interpreting attenuation and transport parameters. For these analyses, an initial set of core samples were used (Table 1, Section 3.1). The data from these basic analyses allowed the development of a targeted approach for the selection of samples for further tests. The samples for further attenuation analyses (i.e., sequential extractions and 1-D soil-column leaching experiments) were selected from core samples with sufficient COC concentrations and from a set of grab samples collected and analyzed by CHPRC as part of developing a vertical COC concentration profile in the well.

Section 4.2 presents and interprets data in terms of identifying contaminant attenuation processes and the types of attenuation mechanisms that are suggested by these data resulting from sequential extractions. Some of these data quantify how contaminants are distributed in different phases within the vadose zone. This distribution provides input to interpretation of attenuation processes and contaminant mobility.

Section 4.3 presents data and interpretations that support quantification of attenuation and transport parameters. Soil-column experimental data provide information to estimate contaminant release rates from sediments. This report provides an initial interpretation of attenuation and transport parameters. The data will also be useful for additional interpretation by others through modeling of the results.

4.1 Contaminant Distribution

Contaminant and geochemical constituent concentration measurements provide data about their distributions at the selected sample locations. These data include measurements for sediments using water, and acid extractions. Characterization of iron and manganese was conducted to assess the potential for redox reactions and iron-oxide sorption. Oxygen and hydrogen isotopes were measured as a potential

means to distinguish different sources of pore water. Sediment physical properties were measured, photographs of the sediments were taken, and geologic material was classified. Collectively, this information defines the foundation for scaling and interpreting attenuation and transport parameters for field applications.

4.1.1 Contaminants and Geochemical Constituents

Different extractions were used for evaluating contaminant distribution and geochemical constituents to characterize specific fractions of ions and contaminants from the pore water and sediments (adsorbed on surfaces or as precipitates). The water extraction was used to evaluate pore water geochemistry (i.e., pH, specific conductance), including COCs, and cations and anions present in pore water. The water extraction may also remove some fraction of adsorbed ion/contaminants; however, due to short water/sediment contact time (1 hour) there is little dissolution of contaminants that are present in precipitates. Time-dependent water elution of contaminants in 1-D columns is described in Section 4.3. In addition, an 8M nitric acid extraction was used to dissolve most (but not all) surface precipitates that may contain contaminants. Consequently, this extraction yields a measure of the total contaminant present in pore water, adsorbed phases, and surface precipitates. The results of the water and acid sediment extractions are shown in Table 10. Note that for the purpose of evaluating iodine attenuation and transport behavior, this project used total iodine data in these extractions because its concentration is above the method detection limit. Although total iodine is not an identified contaminant of potential concern, its transport behavior is expected to be the same as I-129.

Geochemical characterization of the pore water and sediments was conducted through a series of extractions as shown in Table 11. These geochemical indicators, identified by the EPA MNA guidance, are those associated with formation of categories of precipitates that may affect contaminants, those associated with contaminant sorption (e.g., iron oxides), and those associated with redox processes. Therefore, these indicators support the evaluation of geochemical conditions and interpreting the COC behavior. Both water and acid extractions were applied to provide material for analysis. The type of extraction and the concentration of the element/compound were both needed to interpret the data in terms of the geochemical conditions.

As can be seen in Table 10, contaminant concentrations in all of the samples were low or non-detect, except for moderate uranium and total chromium concentrations in two S-13 (C9513) borehole samples (B39X10 and B39X55), and just the uranium concentration in one T-7 (C9503) borehole sample (B39VY1). This sample also showed a significant nitrate concentration in water extractions. The total chromium measurements from the acid extractions for boreholes B-42 (C9497), T-7 (C9503), and T-3 (C9555) showed relatively low concentrations, and are likely natural chromium present in the sediment.

Table 10. Water and acid extractable concentration of contaminants in sediments.

Water Extracts							
Sample Name	Sample Location	Technetium-99 pCi/g dry	Uranium µg/kg dry	Chromium µg/kg dry	Total Iodine µg/kg dry	Cr(VI) µg/kg dry	Nitrate µg/kg dry
C9497-B39M00	B-42 39C (CCUg)	ND	6.28E-02	ND	0.480	NR	3720
C9513-B39X10	S-13 18E (H2/CCUz)	NM	7.24E+02	301	NM	359 ^c	386
C9513-B39X55	S-13 25D (CCUc)	NM	5.79E+01	30.4	NM	53.3 ^c	439
C9513-B39XC3	S-13 39D (Rwie)	NM	3.62E-01	ND	NM	ND	495
C9555-B3DB67	T-3 57B (H2/CCUz)	NM	9.51E+00	ND	NM	ND	6070
C9555-B3BL58	T-3 31D (Rwie)	NM	7.14E-01	ND	NM	ND	1880
C9503-B39VR9	T-7 5C (H2/CCUz)	NM	2.47E+00	15.2	NM	15.8 ^b	58500
C9503-B39VT4	T-7 6B (CCUz/CCUc)	NM	4.23E+00	148	NM	153 ^c	370000
C9503-B39VY1	T-7 18C (Rwie)	NM	2.23E+01	258	NM	288 ^c	1850000

^b This value for Cr(VI) was not within 20% of the total Cr and it is for information only.
^c The duplicate associated with this samples set did not meet the acceptance criteria (35%) with a value of 37.8%. This is likely due to heterogeneity in the sample.
 NM indicates that this element was not measured.
 NR indicates not reported.

Acid Extracts							
Sample Name	Sample Location	Technetium-99 pCi/g dry	Uranium µg/kg dry	Chromium µg/kg dry	--	--	--
C9497-B39M00	B-42 39C (CCUg)	ND	241	2510	--	--	--
C9513-B39X10	S-13 18E (H2/CCUz)	NM	10400	26500	--	--	--
C9513-B39X55	S-13 25D (CCUc)	NM	4950	39000	--	--	--
C9513-B39XC3	S-13 39D (Rwie)	NM	125	3690	--	--	--
C9555-B3DB67	T-3 57B (H2/CCUz)	NM	16900	6250	--	--	--
C9555-B3BL58	T-3 31D (Rwie)	NM	288	7290	--	--	--
C9503-B39VR9	T-7 5C (H2/CCUz)	NM	400	10000	--	--	--
C9503-B39VT4	T-7 6B (CCUz/CCUc)	NM	425	12700	--	--	--
C9503-B39VY1	T-7 18C (Rwie)	NM	290	7650	--	--	--

Table 11. Geochemical characterization of sediment pore water by water/sediment (1:1) extraction.

		Water Extracts																	
Sample Name	Sample Location	pH	SpC mS/cm	Al µg/g dry	Ba µg/g dry	Ca µg/g dry	Fe µg/g dry	Mg µg/g dry	Mn µg/g dry	K µg/g dry	Si µg/g dry	Na µg/g dry	Sr µg/g dry	Cl µg/g dry	Fl µg/g dry	Nitrite µg/g dry	PO4 µg/g dry	SO4 µg/g dry	
C9497-B39M00	B-42 39C (CCUg)	8.27	0.102	0.102	ND	6.78	0.164	1.83	ND	2.59	3.67	5.04	ND	0.741	0.165	ND	ND	18.9	
C9513-B39X10	S-13 18E (H2/CCUz)	8.81	0.153	0.0872	ND	2.67	0.11 ^a	0.819	ND	2.5	5.09	29.5	ND	1.09	0.436	ND	ND	4.45	
C9513-B39X55	S-13 25D (CCUc)	8.58	0.425	ND	ND	7.72	ND	5.68	ND	3.65	25.6	72	0.052 3	1.95	1.91	ND	ND	19.8	
C9513-B39XC3	S-13 39D (Rwie)	8.4	0.018	0.0753	ND	0.163	0.139 ^a	0.0667	ND	0.47	3.11	2.17	ND	0.131	0.233	ND	0.174	0.538	
C9555-B3DB67	T-3 57B (H2/CCUz)	9.9	0.254	0.488	ND	0.554	0.658	0.285	ND	37.4	7.64	21.5	ND	1.31	10.3	ND	ND	2.67	
C9555-B3BL58	T-3 31D (Rwie)	10	0.442	1.56	ND	1.17	1.63	0.574	0.026 7	16.9	12.9	77.5	ND	1.87	11.3	ND	ND	2.62	
C9503-B39VR9	T-7 5C (H2/CCUz)	10.3	1.27	0.436	ND	0.677	0.434 ^a	0.199	ND	21.4	34.4	241	ND	3.95	39	ND	6.18	12.1	
C9503-B39VT4	T-7 6B (CCUz/CCUc)	9.76	4.53	2.35	ND	1.07	0.542 ^a	0.372	ND	99.3	3.93	957	ND	15.9	367	ND	59.5	44	
C9503-B39VY1	T-7 18C (Rwie)	9.84	4.64	0.216	ND	1.12	0.081 ^a	0.333	ND	9.57	4.94	958	ND	23.3	16.3	ND	ND	65.3	

^a The duplicate failed for iron associated with these samples. The relative percent difference for Fe associated with these samples was 50.9%, which is outside the acceptance criteria of 35%. This is likely due to heterogeneity of the sample.

		Acid Extracts																	
Sample Name	Sample Location	Al µg/g dry	Ba µg/g dry	Ca µg/g dry	Fe µg/g dry	Mg µg/g dry	Mn µg/g dry	K µg/g dry	Si µg/g dry	Na µg/g dry	Sr µg/g dry	--	--	--	--	--	--	--	
C9497-B39M00	B-42 39C (CCUg)	2700	37.8	3710	8390	1910	115	399	ND	173	14.4	--	--	--	--	--	--	--	
C9513-B39X10	S-13 18E (H2/CCUz)	3560	58.4	6830	6500	2560	205	986	ND	169	22.5	--	--	--	--	--	--	--	
C9513-B39X55	S-13 25D (CCUc)	9760	117	179000	9510	10000	269	1360	36.3	757	244	--	--	--	--	--	--	--	
C9513-B39XC3	S-13 39D (Rwie)	1770	15.8	966	3660	1310	79.9	402	ND	46.3	6.5	--	--	--	--	--	--	--	
C9555-B3DB67	T-3 57B (H2/CCUz)	4600	59.1	19900	8590	3910	162	2410	51.4	712	56.3	--	--	--	--	--	--	--	
C9555-B3BL58	T-3 31D (Rwie)	3360	21.5	6540	5950	2200	114	898	ND	566	20.6	--	--	--	--	--	--	--	
C9503-B39VR9	T-7 5C (H2/CCUz)	4880	46.9	11400	6850	3210	168	2150	28	1980	28.8	--	--	--	--	--	--	--	
C9503-B39VT4	T-7 6B (CCUz/CCUc)	13400	126	13600	14200	6090	344	5100	39.2	4240	33.9	--	--	--	--	--	--	--	
C9503-B39VY1	T-7 18C (Rwie)	3460	27.9	1680	6120	2310	137	753	ND	1780	10.5	--	--	--	--	--	--	--	

TOC Sediment and Water Extract																	
Sample Name	Sample Location	TC-sed µg/g dry	TIC-sed µg/g dry	TOC- sed µg/g dry	TOC- WE µg/g dry	TIC- WE µg/g dry	Moisture wt%	--	--	--	--	--	--	--	--	--	--
C9497-B39M00	B-42 39C (CCUg)	913	535	378	ND	ND	2.54	--	--	--	--	--	--	--	--	--	--
C9513-B39X10	S-13 18E (H2/CCUz)	3930	2870	1060	26	ND	6.27	--	--	--	--	--	--	--	--	--	--
C9513-B39X55	S-13 25D (CCUc)	59400	53800	5600	276	ND	14.8	--	--	--	--	--	--	--	--	--	--
C9513-B39XC3	S-13 39D (Rwie)	ND	ND	ND	ND	ND	3.97	--	--	--	--	--	--	--	--	--	--
C9555-B3DB67	T-3 57B (H2/CCUz)	1280	852	428	ND	ND	6.12	--	--	--	--	--	--	--	--	--	--
C9555-B3BL58	T-3 31D (Rwie)	4380	1670	2710	ND	ND	2.05	--	--	--	--	--	--	--	--	--	--
C9503-B39VR9	T-7 5C (H2/CCUz)	422	527	ND	ND	ND	7.08	--	--	--	--	--	--	--	--	--	--
C9503-B39VT4	T-7 6B (CCUz/CCUc)	988	424	564	ND	ND	20.1	--	--	--	--	--	--	--	--	--	--
C9503-B39VY1	T-7 18C (Rwie)	612	306	306	ND	ND	4.79	--	--	--	--	--	--	--	--	--	--
C9488-B355M0	B-8 37D (CCU Perched Interval)	3250	3030	220	--	--	--	--	--	--	--	--	--	--	--	--	--
C9488-B355M1	B-8 37E (CCU Perched Interval)	4080	4010	70	--	--	--	--	--	--	--	--	--	--	--	--	--

Geochemical data (Table 11) show similar conditions with relatively low levels throughout the range of indicators in general. Based on the nitrite and sulfate concentrations, no indications of reduced conditions were observed in any of the samples. Iron and manganese concentrations in the water extracted for all samples were low or non-detect. Similarly, organic carbon was present in some samples, though generally at low concentrations.

Based on both the water and acid extraction results for contaminants, no significant COC concentrations were observed in the sample analyzed for the B-42 (C9497) borehole (Table 10). Analysis of the sample from this borehole resulted in a non-detect for Tc-99, uranium was $6.28\text{E-}02$ $\mu\text{g/kg}$, and total iodine was 0.480 $\mu\text{g/kg}$ in water extractions. Similarly, very low levels of uranium and total chromium were observed in acid extractions. Because of the low contaminant levels observed in the B-42 (C9497) borehole sediment, a decision was made collectively by the CHPRC and PNNL technical team that the sequential extraction and soil-column leaching studies were not needed for this specific sample. However, based on some grab sample (i.e., samples other than those originally targeted for attenuation testing) results, two additional samples for this borehole were selected for sequential extractions. The grab samples were collected throughout the borehole at the vertical locations where COC analyses were conducted by CHPRC. Selected grab samples for the B-42 (C9497) borehole represent those locations with high Tc-99 and Cr(VI) concentrations, at levels of 11.1 pCi/g and 1100 $\mu\text{g/kg}$, respectively. Selected samples for sequential extractions are also shown in Table 12.

Three samples were analyzed for borehole S-13 (C9513). Relative to the other boreholes, slightly elevated uranium and Cr(VI) concentrations were observed in water extracts in two of the S-13 (C9513) borehole samples, B39X10 and B39X55, albeit still at very low levels. Also, these two samples from this borehole yielded some moderate levels of uranium and total chromium in acid extractions (Table 10). While sample B39X10 was from a transition zone from the Hanford unit to CCU silt material, sample B39X55 was from the CCU caliche unit with a high carbonate concentration. As a result of the geochemical analysis, a higher carbonate content in sample B39X55 (the highest content by a significant amount) was indeed observed, as indicated by high calcium and magnesium concentrations in the acid extractions, and by the high total inorganic carbon in the sediment analyses (Table 11). Therefore, slightly higher uranium concentrations observed in sample B39X55 may have been due to formation of uranium carbonate compounds. The results from the borehole S-13 (C9513) samples were compared to some grab samples (i.e., samples other than those originally targeted for attenuation testing). Four grab samples that represent those locations with high U and Cr(VI) levels for the S-13 borehole were selected for sequential extractions (Table 12).

Two samples from borehole T-3 (C9555) were analyzed for contaminant concentrations and geochemical indicators. Elevated uranium concentrations were observed in acid extractions from sample B3DB67 at a concentration of $16,900$ $\mu\text{g/kg}$. This sample was selected for sequential extractions to analyze uranium. Total chromium concentrations in all T-3 samples were relatively low, and are likely natural chromium present in the sediment.

Three samples from borehole T-7 (C9503) were analyzed. Uranium and chromium concentrations were very low for these samples for both the water and acid extractions. However, an increasing trend can be observed for total chromium (ranging from 15 to 258 $\mu\text{g/kg}$) with depth for this borehole. Also, an elevated nitrate concentration ($1,850,000$ $\mu\text{g/kg}$) was observed for one of the samples (B39VY1). This

sample was selected for sequential extraction upon a collective decision between CHPRC and PNNL. Also of note, a high moisture content of about 20% was also observed for B39VT4.

Two perched zone samples from borehole B-8 (C9488) were only analyzed for total carbon, total inorganic carbon, and total organic carbon. As can be seen in Table 11, both samples indicated moderate levels of total carbon, more than 90% of which was characterized as inorganic carbon.

Table 12 below lists the final set of samples (both core and grab) selected for sequential extractions based on the evaluation of the results discussed in this section.

Table 12. Samples selected for sequential extractions.

Borehole Designation	Borehole ID	Core	Sample ID	Nominal Geologic Unit	Depth Interval (ft bgs)	COCs Selected for Sequential Extractions
B-42	C9497	23 (Grab)	B3BMT1	H2	161-163.5	Tc-99
B-42	C9497	44 (Grab)	B3BMW9	CCUg	260-261.2	Cr(VI)
S-13	C9513	13 (Grab)	B3DCJ2	H2	90.5-92	U, Cr
S-13	C9513	21 (Grab)	B3DCJ7	CCUc	131.5-133.5	U, Cr
S-13	C9513	24 (Grab)	B3DCK2	CCUc	146.1-148.8	Cr
S-13	C9513	29 (Grab)	B3DCK7	Below CCUc	171-175	Cr
T-3	C9555	57B	B3DB67	H2/CCUz	106-107	U
T-7	C9503	18C	B39VY1	Rwei	152-153	U

4.1.2 Iron and Manganese Characterization

Iron and manganese exist in multiple redox states and chemical forms in the subsurface. The relative distribution of iron and manganese in different forms provides insight into the sorptive and reactive capacity of the sediments. A series of extractions with measurement of iron and manganese was conducted to characterize the sediments using extraction techniques identified in scientific literature (and referred to in EPA MNA guidance [EPA 2015]).

Table 13 and Table 14 show the results of the extractions and iron and manganese analyses, respectively. For context, the information is also plotted, showing the relative portions of different iron forms and the relative amount of redox-active iron and ferrous iron phases (Figure 5a) and Mn phases (Figure 5b).

Table 13. Ferrous and ferric iron phases in sediments based on liquid extractions.

location	formation	borehole	HEIS #	ads. Fe ^{II}	Fe ^{II} CO ₃ , FeS	total Fe ^{II} *	am. Fe ^{III}	total Fe ^{III}	fraction Fe ^{II} / Fe ^{II} +Fe ^{III}
				(mg/g)	(mg/g)	(mg/g)	(mg/g)	(mg/g)	
B-42	CCUg	C9497 39C	B39M00	ND	0.542	4.67	1.40	7.05	0.398
B-42	CCUg	C9497 39C	B39M00	ND	0.726	4.94	1.22	7.29	0.404
B-42	CCUg	C9497 39C	B39M00	ND	0.643	4.60	1.28	6.40	0.418
S-13	H2/CCUz	C9513 18E	B39X10	ND	0.442	1.43	0.941	8.56	0.143
S-13	CCUc	C9513 25D	B39X55	ND	ND	1.81	ND	8.51	0.175
S-13	Rwie	C9513 39D	B39XC3	ND	ND	0.723	0.566	5.91	0.109
T-3	Rwie	C9555 31D	B3BL58	ND	1.26	0.336	0.463	7.57	0.042
T-3	H2/CCUz	C9555 57B	B3DB67	ND	0.445	2.22	0.633	9.02	0.198
T-7	H2/CCUz	C9503 5C	B39VR9	ND	0.684	0.517	0.605	10.7	0.046
T-7	CCUz/CCUc	C9503 6B	B39VT4	ND	1.14	2.16	1.53	14.2	0.132
T-7	Rwie	C9503 18C	B39VY1	ND	0.699	0.472	0.548	8.18	0.055

*blank spike did not meet ±20% acceptance criteria

Table 14. Manganese phases in sediments based on liquid extractions.

location	formation	borehole	HEIS #	ads. Mn ^{II}	am. Mn ^{II+IV}	total Mn ^{II+IV}
				(mg/g)	(mg/g)	(mg/g)
B-42	CCUg	C9497 39C	B39M00	4.21E-04	0.0724	0.344
B-42	CCUg	C9497 39C	B39M00	5.04E-04	0.0860	0.397
B-42	CCUg	C9497 39C	B39M00	4.89E-04	0.0863	0.363
S-13	H2/CCUz	C9513 18E	B39X10	1.03E-02	0.220	0.381
S-13	CCUc	C9513 25D	B39X55	2.58E-03	0.0152	0.355
S-13	Rwie	C9513 39D	B39XC3	1.65E-04	0.0721	0.193
T-3	Rwie	C9555 31D	B3BL58	1.42E-03	0.0895	0.221
T-3	H2/CCUz	C9555 57B	B3DB67	5.45E-05	0.134	0.391
T-7	H2/CCUz	C9503 5C	B39VR9	7.99E-05	0.174	0.339
T-7	CCUz/CCUc	C9503 6B	B39VT4	1.10E-04	0.400	0.570
T-7	Rwie	C9503 18C	B39VY1	4.96E-04	0.140	0.293

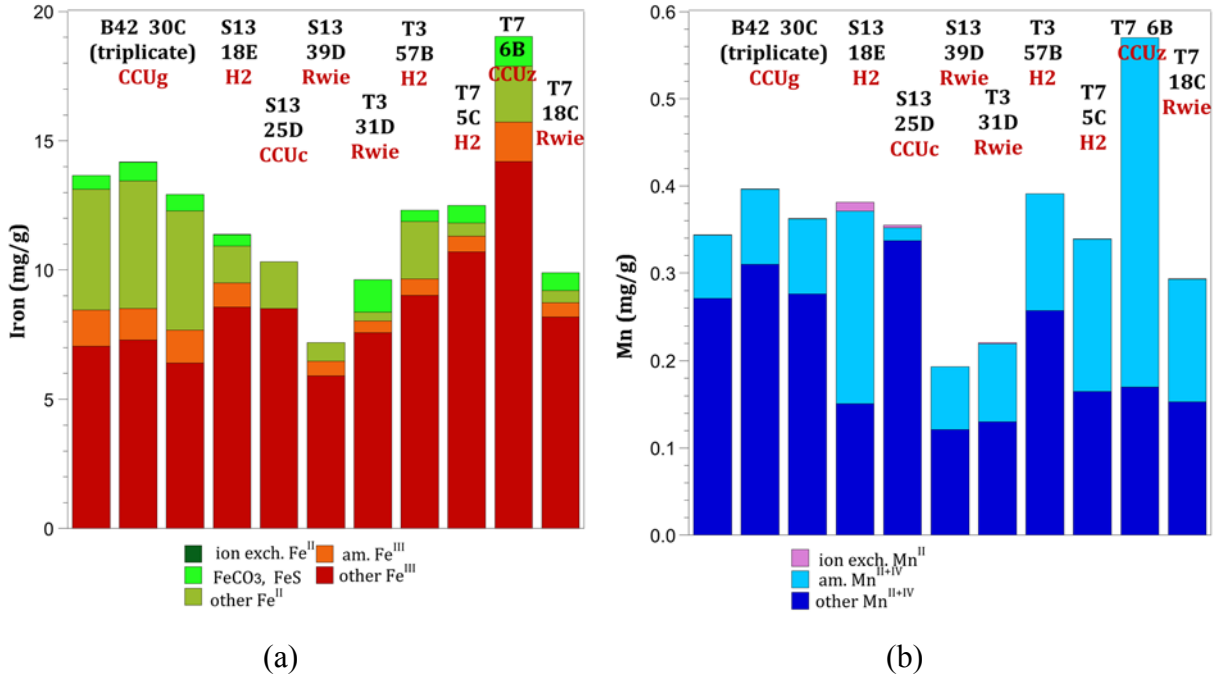


Figure 5. Iron (a) and manganese (b) surface phase distributions in sediments, based on liquid extractions.

The distribution of iron and manganese surface phases in different oxidation states provides insight into the sorption and redox reactive capacity of the sediments. Iron extractions indicated an average of 10.7 mg/g iron, which was mainly ferric iron (8.49 mg/g, average). Hanford, Ringold, and Cold Creek formation sediments contain a mixture of mafic (i.e., sediments derived from basalt) and granitic minerals, with mafic minerals (pyroxenes, amphiboles) and clay minerals containing significant Fe and Mn phases (Table 15). The ferrous iron phases were a small fraction (4% to 20%) in S- and T-Complex boreholes (in Hanford, Ringold, and Cold Creek units), but larger in the B-Complex core (Cold Creek gravel), which showed ~40% ferrous iron phases (Table 13, Figure 5a). The ferrous iron phases consisted of no measured adsorbed ferrous iron, a small fraction of iron sulfide/ferrous carbonate, and a larger fraction of unidentified ferrous iron (from magnetite or other minerals).

The manganese extractions indicated an average of 0.35 mg/g Mn, or 3.3% that of the total iron phases (Table 14, Figure 5b). However, there was some measured adsorbed Mn(II), in contrast to no measured adsorbed ferrous iron. The most redox reactive phases in the sediments are adsorbed Fe(II) and Mn(II), followed by iron sulfide/ferrous carbonate phases.

Table 15. Summary of Hanford mineralogy (after Xue et al. 2003).

Mineral	Formula	Both Fm (% wt)	Hanford Fm (% wt)	Ringold Fm (% wt)
Quartz	SiO ₂	37.7 ± 12.4	38.4 ± 12.8	37.03 ± 12.4
Microcline	KAlSi ₃ O ₈	17.0 ± 6.7	15.3 ± 4.4	18.7 ± 8.0
Plagioclase	NaAlSi ₃ O ₈ -CaAl ₂ Si ₂ O ₈	18.7 ± 7.7	22.2 ± 7.2	15.5 ± 6.8
Pyroxenes	(Ca, Mg, Fe)Si ₂ O ₆	3.03 ± 5.99	5.01 ± 7.83	1.14 ± 2.52
Calcite	CaCO ₃	4.97 ± 7.19	1.91 ± 1.71	0.68 ± 0.92
Magnetite	Fe ₃ O ₄	5.09 ± 4.37	4.46 ± 4.12	5.68 ± 4.63
Amphiboles	Ca ₂ (Mg, Fe, Al) ₅ (Al, Si) ₈ O ₂₂ (OH) ₂	5.55 ± 5.97	5.46 ± 5.67	5.64 ± 6.40
Apatite	Ca ₁₀ (PO ₄) ₆ (OH) ₂	0.60 ± 1.04	0.52 ± 0.92	0.67 ± 1.16
Mica ^(a)	(K, Na, Ca)(Al, Mg, Fe) ₂₋₃ (Si, Al) ₄ O ₁₀ (O, F, OH) ₂	2.07 ± 4.47	2.46 ± 3.74	1.71 ± 5.15
Ilmenite	FeTiO ₃	2.51 ± 2.66	1.28 ± 1.51	3.67 ± 3.00
Epidote	{Ca ₂ } {Al ₂ Fe ³⁺ } [O OH SiO ₄ Si ₂ O ₇]	1.65 ± 2.98	1.78 ± 3.75	1.52 ± 2.14

(a) muscovite, biotite, phlogopite, lepidolite, clintonite, illite, phengite

4.1.3 Oxygen and Hydrogen Isotopes

Isotopic analysis of water for its oxygen and hydrogen isotopic content is applied for multiple purposes (Prudic et al. 1997). For instance, the stable isotopes of water ($\delta^2\text{H}$ [deuterium] and $\delta^{18}\text{O}$ [18-oxygen]) can be used to assist with tracking of underground contaminant plumes or linking a water source to a measured water sample. For this study, the pore water in the vadose zone is a mixture of water from previous natural recharge and the anthropogenic water discharges of waste streams. Isotopic data was collected to assess whether the signatures from different areas can be correlated to mixtures of different types of water sources. In this report, data for sediment samples collected from the B-, T-, and S-Complex boreholes are discussed. The selected samples and the isotope data values are also shown in Table 16. Isotopic ratios for ^2H and ^{18}O are reported in delta (δ) notation, defined as

$$\delta = \left(\frac{R_{sa}}{R_{std}} - 1 \right) \times 1000$$

where R is the ratio of the abundance of the heavy to light isotope (i.e., $^2\text{H}/^1\text{H}$, $^{18}\text{O}/^{16}\text{O}$), *sa* denotes the sample, and *std* indicates the standard (McKinney et al. 1950). Delta values are reported in per mil (‰), with $\delta^2\text{H}$ and $\delta^{18}\text{O}$ values relative to Vienna Standard Mean Ocean Water (which has, by convention, $\delta^2\text{H} = 0\text{‰}$, $\delta^{18}\text{O} = 0\text{‰}$).

Table 16. Sediment samples selected for isotope analyses and data values.

Borehole Designation	Core	Borehole ID	Sample ID	Depth Interval (ft bgs)	Geologic Unit	$\delta^{18}\text{O}$ (‰)	$\delta^2\text{H}$ (‰)
B-42	11	C9497	B3BMP8	65.3-68.8	H1	-13.27 (0.34)	-120.87 (2.09)
B-42	4	C9497	B3BMN2	102.0-104.0	H2	-14.60 (0.43)	-127.08 (2.01)
B-42	23	C9497	B3BMT0	161.0-163.5	H2	-16.30 (0.32)	-139.31 (2.08)
B-42	37	C9497	B3BMW2	231.0-233.0	CCUg	-14.82 (0.38)	-132.49 (2.80)
B-42	39	C9497	B3BM02	235.0-236.0	CCUg	-18.10 (0.47)	-147.57 (2.61)
B-42	44	C9497	B3BMW8	260.0-261.2	CCUg	-12.65 (0.47)	-97.84 (2.60)
T-7	6	C9503	B39VT5	90.0-91.0	CCUz	-16.88 (1.59)	-129.00 (5.43)
T-7	41	C9503	B3D1D9	98.0-99.0	CCUc	-15.73 (0.21)	-123.30 (1.51)
T-7	13	C9503	B3D1H2	126.0-128.0	Rwie	-16.72 (0.50)	-136.95 (2.92)
T-7	16	C9503	B3D1H8	140.0-145.0	Rwie	-16.58 (0.60)	-135.33 (2.21)
T-7	22	C9503	B3D1K0	171.3-174.1	Rwie	-16.26 (0.90)	-135.46 (3.95)
T-7	25	C9503	B3D1K7	186.2-189.2	Rwie	-14.56 (0.43)	-129.26 (0.95)
T-7	29	C9503	B3D1L4	206.1-209.1	Rwie	-15.98 (0.16)	-133.11 (0.66)
T-7	32	C9503	B3D1M0	220.5-221.5	Rwie	-16.38 (0.48)	-134.88 (1.10)
T-3	17-18	C9555	B3FCL5	110.4-111.2	CCUz	-21.63 (0.98)	-157.00 (9.44)
T-3	24	C9555	B3FCM1	135.0-136.4	CCUc	-21.31 (0.46)	-155.20 (2.97)
T-3	28	C9555	B3FCM8	156.7-158.2	Rtf	-18.66 (1.52)	-139.86 (6.25)
T-3	50	C9555	B3FLP9	170.3-171.8	Rwie	-18.64 (1.00)	-132.05 (8.19)
T-3	35	C9555	B3FLR3	200.3-202.8	Rwie	-19.63 (0.82)	-141.88 (3.86)
T-3	37	C9555	B3FLR7	210.4-212.4	Rwie	-18.20 (0.74)	-135.81 (5.83)
T-3	41	C9555	B3FLT1	230.2-232.2	Rwie	-17.41 (0.55)	-131.46 (3.38)
T-3	44	C9555	B3FLT5	245.0-247.6	Rwie	-18.78 (0.86)	-135.20 (6.25)
S-13	10	C9513	B3DCH7	76.0-79.0	H2	-15.71 (0.29)	-128.84 (2.28)
S-13	13	C9513	C3DCJ2	90.5-92.0	H2	-17.58 (0.30)	-136.06 (1.88)
S-13	18	C9513	B3F940	115.6-116.6	H2	-17.16 (0.32)	-139.86 (4.35)
S-13	21	C9513	B3DCJ7	131.5-133.5	H2	-18.21 (0.81)	-138.98 (3.65)
S-13	24	C9513	B3DCK2	146.1-148.8	CCUz	-20.13 (1.95)	-150.12 (10.37)
S-13	29	C9513	B3DCK7	171.5-174.3	Rtf	-18.68 (1.36)	-147.63 (10.80)
S-13	33	C9513	B3DCL2	191.7-194.1	Rtf	-15.84 (0.75)	-134.89 (2.97)
S-13	40	C9513	B3DCL7	225.0-227.0	Rwie	-15.94 (0.74)	-128.61 (7.84)
S-13	41	C9513	B3DCM2	231.4-234.0	Rwie	-16.18 (0.52)	-125.53 (2.28)

The ^2H and ^{18}O isotopic ratio within water are impacted in similar ways by evaporation, condensation/precipitation, and transport. As a result, Craig (1961) quantified this relationship using measurements of water taken from around the globe, and thus described the global meteoric water line. Graham (1983) performed a similar analysis focused on the regional precipitation within the Hanford/Rattlesnake areas to define a local meteoric water line. The deviation between the local and global meteoric water lines is attributed to evaporative processes coupled to the typically short precipitation durations and semi-arid nature of the local region. Finally, Spane and Webber (1995) described typical ranges for isotopic values of water within the Columbia River, which largely originates from outside the Hanford region and carries the isotopic signature of its region of origin.

The results of the isotopic analysis of the 31 samples are given in Table 16 and analyzed in the context of these previous descriptions of the isotopic content of relevant waters (Figure 6). A cursory analysis of the data shows that the overall isotopic trend, in all of the samples analyzed, was roughly parallel to the local meteoric water line. However, closer inspection of the data shows trends in this relationship between samples. For instance, the data from borehole T-3 (C9555) fall largely above/to the left of the regional meteoric water line while samples from, most notably, borehole B-42 (C9497) fall to the right/below this line. In general, data falling below the meteoric water line indicate isotopic enriched by evaporation of portion of the water. The kinetics of water evaporation slightly favor the light isotopes, which have slightly higher vapor pressures than water with a heavy isotope substitution. As a result, evaporation preferentially removes water with light isotopes, resulting in increases of ^2H and ^{18}O within the residual, non-evaporated pool. Thus, while the residual water is isotopically enriched, the water removed by evaporation is isotopically depleted in the heavier isotope. Samples analyzed from borehole T-3 (C9555) are consistent with inclusion of recondensate of the isotopically depleted evaporate water and likely indicate that such recondensate was collected and either pumped or allowed to percolate into the subsurface. Note, this may have been performed in an industrial process to reduce waste volume within a tank. In addition to borehole B-42 (C9497), samples from boreholes T-7 (C9503) and S-13 (C9513) show possible signs of an evaporitic history; namely, they contain sample points trending below the regional meteoric water line. It is important to note that the meteoric water line captures the isotopic trends within regional precipitation. However, evaporation of soil moisture following precipitation events can also induce isotopic enrichment (Singleton et al. 2004), making it challenging to discern natural isotopic enrichment from that linked to industrial processes associated with Hanford site activities.

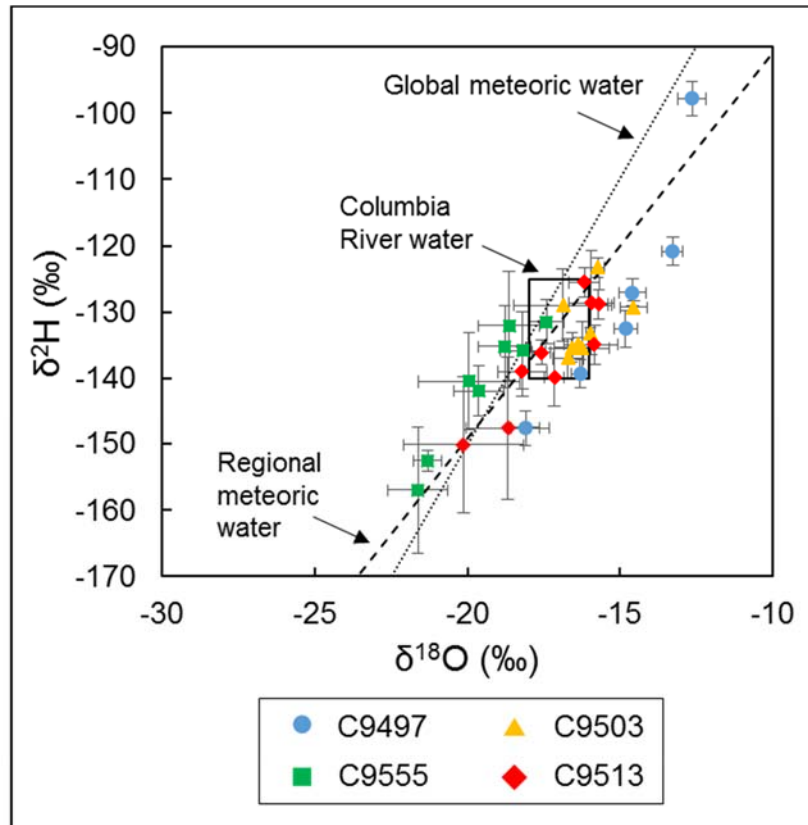


Figure 6. Isotopic results from the analysis of vadose zone waters extracted.

To help clarify the water dynamics within these systems and better connect surface activities with the isotopic content of vadose zone water samples, isotopic analysis of grab samples (collected over a depth profile within the sample cores) was performed (Figure 7). DePaolo et al. (2004) previously reported the isotopic depth profile of samples collected from within the 200 West area at Hanford. They observed a shallow zone (1 to 2 m) near the surface of the core associated with evaporitic (isotopic) enrichment. Following this, the isotopic content of the water remained relatively stable throughout the depth profile, demonstrating migration of surface-derived water as a coherent plug as it migrated down the depth profile once depth exceeded the zone of surface evaporation. This behavior is similar to that described by Barnes and Allison (1988), who used a series of laboratory tests to show the relative limitation of evaporitic enrichment (even in unsaturated soils) to relatively shallow levels. Further, the isotopic stability of water down the depth profile measured by DePaolo et al. (2004) allowed them to identify one depth horizon with an anomalous isotopic value, which they were able to link to a leaking pipe containing service water derived from the nearby Columbia River. Similarly, this study used a depth profile isotopic analysis to identify anthropogenic influence on the vadose water depth profile, although it is anticipated that any likely influence would be through more diffuse, surface-derived inputs versus the point source (i.e., leaking pipe) identified by DePaolo et al. (2004).

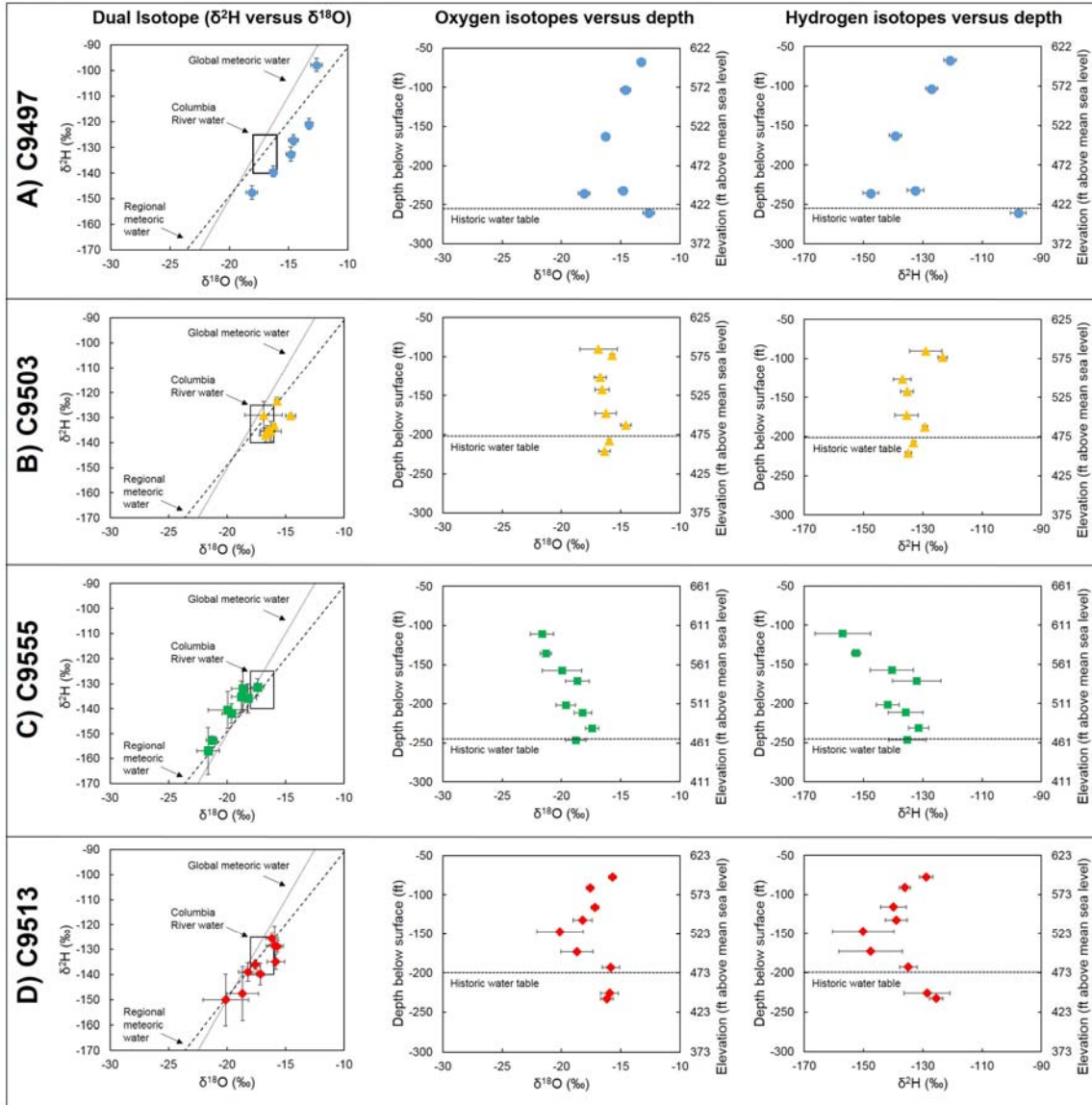


Figure 7. Results for each set of samples showing dual isotope plots and isotopic variability of water isotopes ($\delta^{18}\text{O}$ and $\delta^2\text{H}$) over core depth.

Samples collected from borehole T-7 (C9503) (Figure 7B) showed a pattern consistent with that observed by DePaolo et al. (2004). There is little variability in the isotopic data from samples collected between 90.5 and 207.6 feet below surface; standard deviation from the eight samples is 0.74‰ and 4.61‰ for $\delta^{18}\text{O}$ and $\delta^2\text{H}$ respectively. The historical (1970) water table level for this location is 202 feet below surface and there is no observable shift in $\delta^{18}\text{O}$ and $\delta^2\text{H}$ of extracted water above or below this level, suggesting little anthropogenic influence on the water isotopics in this area.

Samples collected from borehole B-42 (C9497) (Figure 7A) show isotopic variability over the vertical profile. For instance, the data collected from the upper three data points (67.1, 103.0, 162.3 feet below surface) show a linear correlation with depth (R^2 of 0.996 and 0.998 for $\delta^{18}\text{O}$ and $\delta^2\text{H}$ respectively), while inclusion of the deepest three data points erases any linear correlation (R^2 of 0.0493 and 0.0042 for $\delta^{18}\text{O}$ and $\delta^2\text{H}$ respectively). The historical water table depth for this location is 256 feet below surface and,

while the data density is somewhat sparse, this general depth appears to demarcate isotopic behavior between shallower and deeper waters. The shallower water shows an isotopic trend with depth, while below 256 feet a return to isotopic values more similar to both what was observed in borehole T-7 (C9503) and to values previously reported for the Hanford region was observed (Hearn et al. 1989; DOE/RL 82-3). Taken together, the depth profile data strongly suggest mixing of a shallow water with a deeper water body near the location of the historical water table (roughly 256 feet below surface).

The isotope depth profile further suggests more processes are occurring beyond a simple mixing of two waters with different isotopic compositions. The upper water body does not have a constant isotope value, but rather shows an isotopic shift with depth (until reaching near the historical water table level). This pattern could be consistent with a variable flux of industrial process water near the surface that is propagating downward. The higher this flux of water, the larger the isotopic shift we would expect since it would be mixing with a small amount of natural vadose zone water. DePaolo et al. (2004) demonstrated the downward migration of water as a plug that does not shift its isotopic signature once depth exceeds roughly 2 meters. Therefore, the isotopic variability of the “shallow” water (depth < ~235 feet below surface) is expected to reflect variable input of industrial water to produce the observed shift in value with depth. Confounding a more thorough interpretation is that the industrial process water is expected to be derived from the Columbia River, which has an overall more negative/depleted isotopic signature than native Hanford vadose water or groundwater. Thus, the isotopic trend seen in the shallow three data points could conceivably be attributed to two explanations. First, the swing in isotope values could be capturing the tailing front of Columbia River water (with low $\delta^{18}\text{O}$ and $\delta^2\text{H}$ content) undergoing mixing as it migrates into the deeper groundwater pool. However, the historical isotope measurements of water from the Columbia River (Spane and Weber 1995) do not overlap with the more enriched values observed in this borehole, suggesting that addition of Columbia River water alone cannot account for the observed trends. Alternatively, the data could show the leading front of a more evaporitically enriched pool of water as it migrates downward; possibly reflecting an industrial process shift from release of Columbia River water to release of evaporitically enriched water originating in a storage pond or crib. Age dating of representative waters, interpretation of the isotopic trends against other geochemical signatures, and/or inclusion of additional depth points in future studies may help further elucidate the water history in this case. It should also be noted that a restricted depth profile (four samples) of vadose water was performed by Truex et al. (2017) on core C9552, also within the 200-DV-1 OU, and produced similar isotopic trends.

Samples from C9513 (Figure 7D) exhibited an isotopic depth profile very similar to that observed with C9497. In short, the historical water table depth (200 feet below surface) appeared to demarcate a shallow from a deeper water. However, the overall $\delta^{18}\text{O}$ and $\delta^2\text{H}$ data of this sample indicates less isotopic enrichment of the waters due to evaporation than in C9497 (Figure 6). Thus, there is a stronger possibility in this case that the depleted isotopic signatures we see in depth profiles result from a high flux of Columbia River water into the system. If this were true, the isotopic trends would be consistent with the isotopic shift indicating the tailing front of a pulse of river water moving through the system. The isotopic values from the shallow depth in this core (77.5 feet below surface) are fairly consistent with expected native vadose zone water, suggesting water at this depth correlates with a time period when the addition of river water was minimized or concluded.

Similar to boreholes B-42 (C9497) and T-7 (C9503), the depth profile associated with borehole T-3 (C9555) (Figure 7C) also shows an isotopic trend with depth and a possible demarcation into shallow and deeper waters by the historical water table (245 feet below surface). In contrast to the above examples,

however, is that borehole T-3 (C9555) shows a reverse isotopic trend with depth; namely, both $\delta^{18}\text{O}$ and $\delta^2\text{H}$ progressively enrich with depth. Further, the depleted isotope data from this location (as depleted as $\delta^{18}\text{O} = -21.63\text{‰}$ and $\delta^2\text{H} = -157.0\text{‰}$) are more depleted than those expected from either Columbia River water or typical winter precipitation. Of the precipitation samples examined by Graham (1983), only two snow samples (out of a total of 68 precipitation samples) showed isotopic signatures close to those observed in borehole T-3 (C9555), which helps exclude a natural source for the measured isotopic signatures. Instead, the extreme isotopic depletion observed in this borehole likely results from industrial processing of water and injection into this reverse well. Evaporitic recondensate would be expected to have depleted isotopic signatures that could be consistent with those observed in this sample. Interestingly, borehole T-3 (C9555) correlates with a reverse well and all reported data points correlate to collection within or below the screened depth of the well (105 to 204 feet below surface; Williams and Rohay 2015). Analysis of additional samples collected from above the screen depth would be expected to reveal a more enriched isotopic signature consistent with anticipated natural isotopic patterns.

Taken together, the isotopic evaluation of vadose zone waters provided interesting insights on the four sets of samples analyzed. First, samples from boreholes B-42 (C9497), T-7 (C9503), and S-13 (C9513) all showed signs of isotopic enrichment in ^2H and ^{18}O when compared to regional precipitation. Based only on the measured values, it is difficult to determine whether the observed isotopic shifts resulted from natural, anthropogenic, or a mixture of the influences. Combining depth profile measurements provided additional clarity and showed borehole T-7 (C9503) to be largely consistent with expected natural patterns while boreholes B-42 (C9497) and S-13 (C9513) showed likely anthropogenic influence in producing the isotopic trends. Further, borehole T-3 (C9555) showed strong signs of being influenced by industrial processes with the strong isotopic depletion signature being a hallmark indication of release of recondensate.

4.1.4 Sediment Physical Characterization

Physical characterization of the sediments is conducted to define the hydrogeologic context for the observed contaminant and geochemical data. Data presented here include the information about the geologic logs and associated core pictures of the sediment core samples selected for contaminant concentration and geochemical analyses. Detailed hydraulic characterization, including saturated and unsaturated hydraulic properties as well as particle size distribution, particle and bulk density, and porosity measurement, is currently being conducted for a set of selected samples (Table 3), and will be described in a separate report. Full interpretation of data is best conducted by considering the information from other samples in the vadose zone as well as the data from the detailed hydraulic characterization. That broader interpretation will be conducted by CHPRC as part of their overall CSM efforts for the 200-DV-1 OU.

Core photographs are shown in Figure 8 through Figure 16. The geologist logs for these samples are included in Appendix A.



Figure 8. Core images of borehole B-42 (C9497) for sample B39M00 (Liner 39C, CCUg sample).

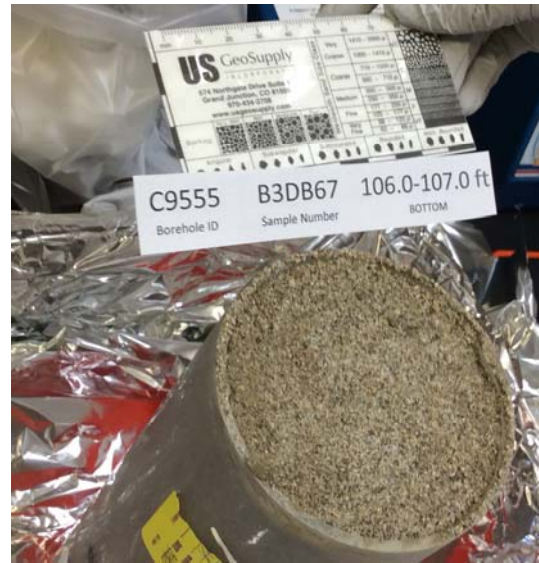
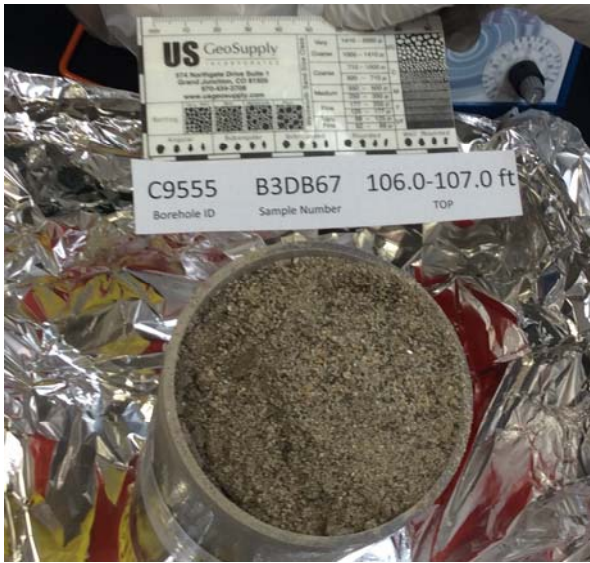


Figure 9. Core images of borehole T-3 (C9555) for sample B3DB67 (Liner 57B, H2/CCUz sample).



Figure 10. Core images of borehole T-3 (C9555) for sample B3BL58 (Liner 31D, Rwie sample).



Figure 11. Core images of borehole T-7 (C9503) for sample B39VR9 (Liner 5C, H2/CCUz sample).

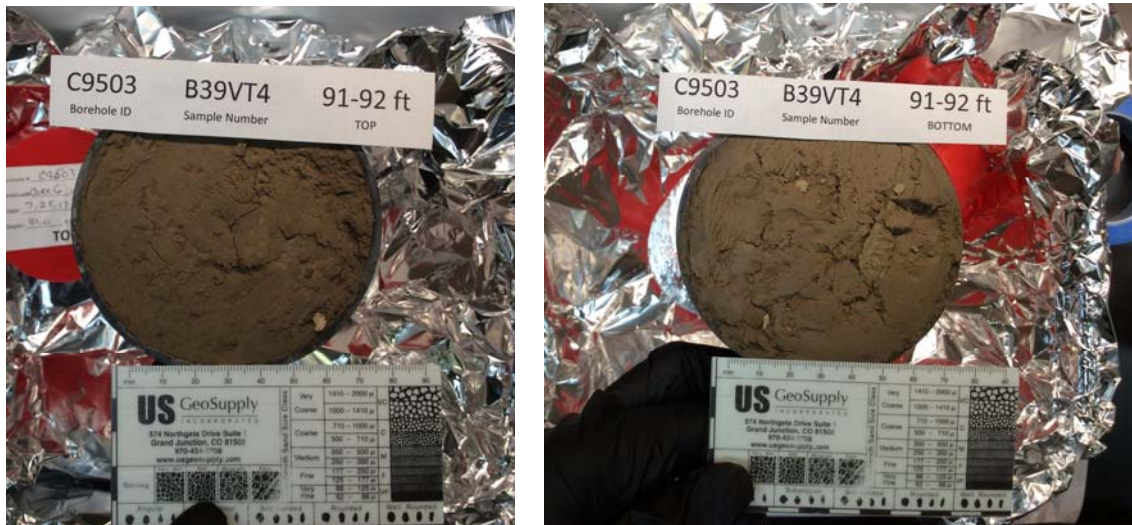


Figure 12. Core images of borehole T-7 (C9503) for sample B39VT4 (Liner 6B, CCUz/CCUc sample).



Figure 13. Core images of borehole T-7 (C9503) for sample B39VY1 (Liner 18C, Rwie sample).



Figure 14. Core images of borehole S-13 (C9513) for sample B39X10 (Liner 18E, H2/CCUz sample).



Figure 15. Core images of borehole S-13 (C9513) for sample B39X55 (Liner 25D, CCUc sample).



Figure 16. Core images of borehole S-13 (C9513) for sample B39XC3 (Liner 39D, Rwie sample).

The physical data characterize the basic hydrogeologic setting for each sample. The set of samples analyzed for this report represents a diverse set of hydrogeologic settings relevant to contaminant attenuation and transport in the Hanford Central Plateau vadose zone and important lithologic features for each targeted borehole (waste site). Additional information on hydraulic properties and physical properties for the selected samples will be reported separately.

4.1.5 B-Complex Perched Zone XRD Analysis

A quantitative analysis of mineralogy was conducted for two perched zone samples from borehole B-8 (C9488) using the XRD technique. Table 17 and Figure 17 present the results of this analysis for the two samples. While the fractions of the minerals that are observed in the XRD patterns are listed in the table, Figure 17 compares the observed XRD patterns to the reference patterns (represented by colored bars).

As can be seen in these results, the perched zone samples mostly consist of quartz and feldspar with smaller amounts of other minerals. However, a background signal of 20-30% of the response may indicate the presence of some quantity of amorphous material in these samples. The amorphous materials cannot be specifically identified with this technique.

Table 17. XRD analysis results of the perched zone samples from borehole B-8 (C9488).^(a)

Sample Name	Sample Location	Sample Depth Interval (ft bgs)	Quartz (%)	Feldspar (%)	Mica (%)	Chlorite (%)	Calcite (%)	Amphibole (%)
C9488-B355M0	B-8 37D (CCU Perched Zone)	223.5-224.5	40	37	14	6	2	2
C9488-B355M1	B-8 37E (CCU Perched Zone)	224.5-225.5	44	34	12	6	2	2

(a) For QA purposes, data presented in this table are for information only.

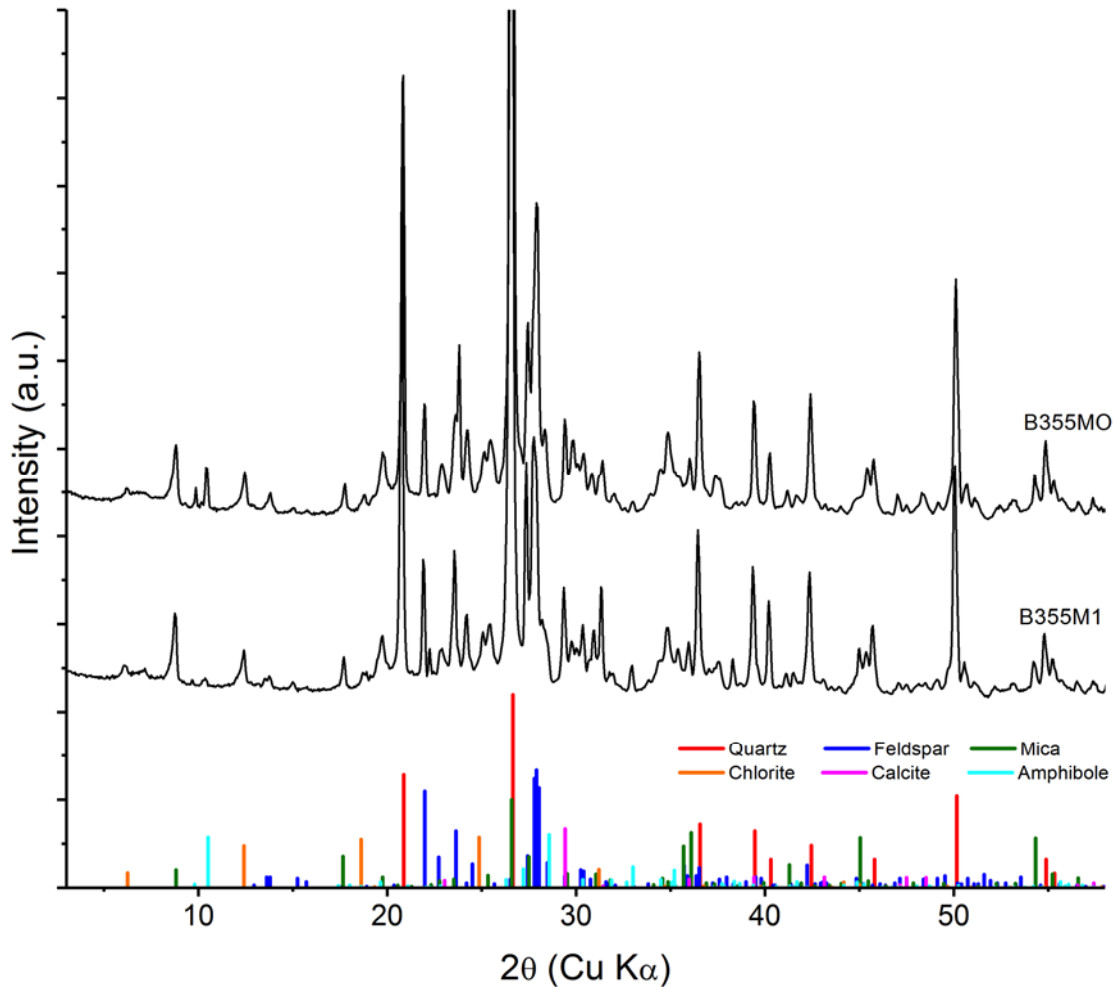


Figure 17. Comparison of the XRD results from the perched zone sample analysis to the reference patterns. (For QA purposes, data presented in this figure are for information only.)

4.2 Contaminant Attenuation Processes

Identifying attenuation processes involves collecting data that can be used to demonstrate whether contaminants have interacted with sediments in a way that changes their mobility. One type of data is from sequential extractions (Table 18). In this process, a sediment sample is sequentially exposed to more harsh extraction solutions and the contaminant concentration in each solution is measured. These data show how the contaminant mass in a sediment sample is distributed among different water- and sediment-associated phases.

A set of eight sediment samples were selected for sequential extractions for this study to quantify contaminants present in aqueous, adsorbed, and specific precipitate phases. As shown in Table 1 in Section 3.1, the set included four samples from borehole S-13 (C9513), two samples from borehole B-42 (C9497), one sample from borehole T-3 (C9555), and one samples from borehole T-7 (C9503). These

samples were mainly analyzed for uranium and chromium, except one of the samples from borehole B-42 (C9497) that was analyzed for Tc-99.

Table 18. Sequential extraction of contaminants from sediment samples.







Extraction Solution	Hypothesized Targeted Sediment Components	Interpreted Contaminant Mobility of Extracted Fraction	Color Code
1. Aqueous: uncontaminated Hanford groundwater	Contaminants in pore water and a portion of sorbed uranium	Mobile phase	
2. Ion exchange: 1M Mg-nitrate	Readily desorbed contaminants	Readily mobile through equilibrium partitioning	
3. Acetate pH 5: 1 hour in pH 5 sodium acetate solution	Contaminants associated with surface-exposed carbonate precipitates and other readily dissolved precipitates	Moderately mobile through rapid dissolution processes	
4. Acetate pH 2.3: 1 week in pH 2.3 acetic acid	Dissolution of most carbonate compounds, and sodium boltwoodite (a hydrous uranium silicate)	Slow dissolution processes for contaminant release from this fraction; mobility is low with respect to impacting groundwater	
5. Oxalic acid: 1 hour	Dissolution of some aluminosilicates and oxides	Slow dissolution processes are associated with contaminant release; mobility is very low with respect to impacting groundwater	
6. 8M HNO ₃ : 2 hours in 8M nitric acid at 95°C	Considered to represent total contaminant extraction for this study (though not completely dissolving the sediment particles)	Very slow dissolution processes are associated with contaminant release; functionally immobile; some or all of the contaminants in this phase may be naturally occurring	

Table 19, and associated Figure 18 and Figure 19 show the sequential extraction contaminant results for each selected sample for uranium, chromium, and technetium. As can be seen in Table 19, there was a very small amount of total extractable Tc-99 in sample B3BMT1 (borehole B-42, C9497) compared to the adjacent grab sample which indicated 11.1 pCi/g Tc-99. This indicates some heterogeneity in technetium distribution at this location. Due to the very low level of Tc-99, no further analyses were conducted for this sample and no additional discussion was included in this section. Uranium and chromium results are discussed in detail below.

Table 19. Contaminant distribution in sequential liquid extracted sediments for U-238, Cr, and Tc-99.

----- U-238 (all µg/g) -----													
Borehole Designation	Borehole ID	Sample ID	Core	Depth Interval (ft bgs)	Geologic Unit	extr. 1	extr. 2	extr. 3	extr. 4	extr. 5	extr. 6	Total	K _d (mL/g)
S-13	C9513	B3DCJ2	13 (Grab)	90.5-92	H2	4.30	2.80	2.68	3.27	2.71	5.13	20.89	2.29
S-13	C9513	B3DCJ7	21 (Grab)	131.5-133.5	CCUc	3.28	1.40	5.37	4.74	1.06	1.36	17.20	1.51
S-13	C9513	B3DCJ7	21 (Grab)	131.5-133.5	CCUc	3.09	1.42	5.09	5.13	1.15	1.29	17.17	1.58
T-3	C9555	B3DB67	57B	106-107	H2/CCUz	0.04	0.18	3.23	2.21	4.85	18.94	29.44	14.23
T-7	C9503	B39VY1	18C	152-153	Rwei	0.0153	0.0154	0.0393	0.0299	0.0359	0.163	0.299	3.17
----- Cr (all µg/g) -----													
Borehole Designation	Borehole ID	Sample ID	Core	Depth Interval (ft bgs)	Geologic Unit	extr. 1	extr. 2	extr. 3	extr. 4	extr. 5	extr. 6	Total	K _d (mL/g)
S-13	C9513	B3DCJ2	13 (Grab)	90.5-92	H2	0.083	0.0090 ^(a)	0.860 ^(a)	7.51	6.73	52.41	67.60	0.382
S-13	C9513	B3DCJ7	21 (Grab)	131.5-133.5	CCUc	0.24	0.509	0.845 ^(a)	5.41	4.38	31.73	43.11	3.49
S-13	C9513	B3DCJ7	21 (Grab)	131.5-133.5	CCUc	0.23	0.506	0.750 ^(a)	5.23	4.20	29.62	40.53	7.64
S-13	C9513	B3DCK2	24 (Grab)	146.1-148.8	CCUc	0.23	0.249	1.21	8.68	6.87	34.56	50.80	2.66
S-13	C9513	B3DCK7	29 (Grab)	171-172	Below CCUc	0.025	0.019 ^(a)	0.978 ^(a)	3.37	5.32	20.57	30.28	
B-42	C9497	B3BMW9	44 (Grab)	260-261.2	CCUg	ND	0.000	0.166	1.91	1.61	5.23	8.91	
----- Tc-99 (all µg/g) -----													
Borehole Designation	Borehole ID	Sample ID	Core	Depth Interval (ft bgs)	Geologic Unit	extr. 1	extr. 2	extr. 3	extr. 4	extr. 5	extr. 6	Total	K _d (mL/g)
B-42	C9497	B3BMT1	23 (Grab)	161-163.5	H2	2.11E-4 ^(b)	ND	ND	ND	ND	ND	2.11E-4	--

(a) Quality control associated with these values were not within acceptable limits. Values are for information only.

(b) Equivalent to 3.58 pCi/g.

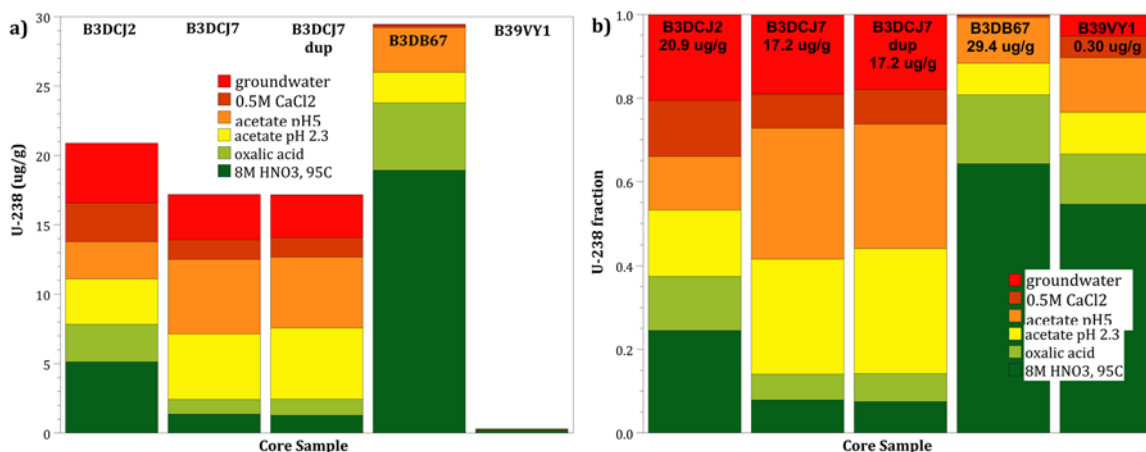


Figure 18. Sequential liquid extractions with analysis of uranium shown as: a) total uranium concentration in each phases, and b) fraction of uranium in each phases.

Sequential extraction data for uranium (Table 19, Figure 18) show a moderate amount of uranium contamination (i.e., 18 to 27 $\mu\text{g/g}$ total U) compared to natural uranium in Hanford sediments ($< 1.5 \mu\text{g/g}$). The T-3 borehole (C9555) sediment sample indicated the highest amount of U-contamination with 29.44 $\mu\text{g/g}$ total U. S-Complex samples also showed significant U-238 levels that ranged from about 17.2 to 20.9 $\mu\text{g/g}$.

The distribution of uranium in different cores indicated significant differences in uranium surface phases. The most mobile uranium (aqueous and adsorbed, shown in red in Figure 18) ranged from 0.5% to 20%. Sample B3DCJ2 from borehole S-13 (C9513) showed the highest fraction of mobile uranium in the H2 geologic unit, indicating some uranium mass that might transport under equilibrium-partitioning conditions. The minimum mobile fraction was observed in the sample B3DB67 from borehole T-3 (C9555), which showed the highest total U-contamination, indicating limited or no uranium transport under equilibrium conditions.

The acetate-extractable uranium (shown in orange and yellow in Figure 18), uranium that typically is associated with carbonates, varied from 15% to 70% among all the selected samples. The highest fraction of uranium mass for this extraction was observed in sample B3DCJ7 of CCU high-carbonate sediment from borehole S-13 (C9513). The “mobile” uranium fraction is considered the aqueous, adsorbed, and about half of the acetate-extractable fractions, so it ranged from 10% to 55% of the uranium in the sediment, or 0.1 to 9 $\mu\text{g/g}$. The highest mobile fraction was observed in the samples from borehole S-13 (C9513).

The oxalate-extractable uranium (i.e., oxides) ranged from 5% to 12%, and the 8M nitric acid extractable uranium ranged from 8% to 62% of the total uranium (Table 19, Figure 18). The sample B3DB67 from borehole T-3 (C9555) showed a significant level of uranium during these two extraction phases with a total concentration of 23.79 $\mu\text{g/g}$ (about 80% of the total U for this sample).

The distribution coefficient (K_d) values for uranium calculated based on the aqueous and adsorbed concentrations ranged from 1.51 to 14.2 mL/g (Table 19). In Section 4.3, this mobile uranium extractable fraction is compared to the leached uranium in 1-D column studies. In typical uranium leaching behavior,

aqueous and adsorbed fractions leach first (with some adsorption and within 10 pore volumes), followed by the slow release of uranium from carbonates over tens of pore volumes.

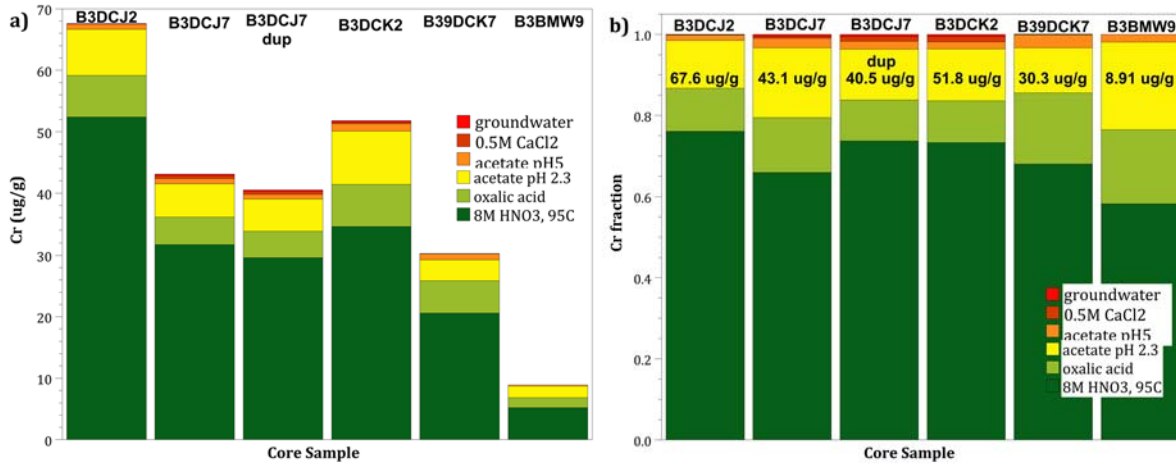


Figure 19. Sequential liquid extractions with analysis of chromium shown as a) total Cr concentration in each phases, and b) fraction of Cr in each phases.

Sequential extraction results for chromium require a different interpretation from that of uranium. Anthropogenic chromium as chromate generally is aqueous with little adsorption. Only a small fraction of chromium (as chromate) may precipitate in carbonates. Therefore, anthropogenic chromium is typically identified by the aqueous, adsorbed, and pH 5 acetate extractions, and the remaining extractions dissolve natural minerals containing chromium, indicating a low mobility for this fraction.

Table 19 and Figure 19 show the sequential extraction results for chromium for the selected sediment samples. While the results from these samples ranged considerably from 8.9 to 68 $\mu\text{g/g}$ total Cr, the “mobile” chromium ranged from 0.95 to 1.6 $\mu\text{g/g}$ Cr, with samples B3DCK2 and B3DCJ7 containing aqueous Cr. The highest total Cr amounts were observed in samples from borehole S-13 (C9513). Borehole B-42 (C9497) had the least amount of chromium in the sediment.

The distribution coefficient (K_d) values for Cr calculated based on the aqueous and adsorbed concentrations ranged from 0.38 to 7.64 mL/g. While chromate sorption is typically expected to be very limited, some of the elevated K_d values may indicate more sorption than expected. In contrast to uranium, chromium leaching behavior is generally at a high concentration within the first few pore volumes from the aqueous phase (because of little adsorbed chromium), followed by a small (or sometimes below detection limits) release from carbonates over tens of pore volumes.

4.3 Contaminant Mobility

To evaluate the rates of release of contaminants that are needed for fate and transport assessments, soil-column leaching experiments were conducted for three selected sediment samples. As shown in Table 1, these included two samples from borehole S-13 (C9513), and one sample from borehole T-3 (C9555) analyzed for both uranium and chromium, also shown in Table 20.

Table 20. Selected sediment samples for 1-D soil-column leaching experiments.

Borehole Designation	Borehole ID	Sample ID	Core	Depth Interval (ft bgs)	Geologic Unit
S-13	C9513	B3DCJ2	13 (Grab)	90.5-92	H2
S-13	C9513	B3DCJ7	21 (Grab)	131.5-133.5	CCUc
T-3	C9555	B3DB67	57B	106-107	H2/CCUz

Soil-column leaching tests allow sediments to contact with a clean flowing artificial groundwater under saturated conditions. Contaminant concentrations in the effluent of the column are controlled by the magnitude of equilibrium partitioning and kinetically controlled contaminant release processes (e.g., dissolution of precipitates or small-pore diffusion). Soil-column tests provide data that can be interpreted in terms of modeling contaminant release and partitioning under 1-D transport conditions. Slower release of contaminant mass from the column (i.e., continued release over many pore volumes of water flow through the column) indicates that the partitioning and/or kinetically controlled processes are attenuating the mobility of the contaminant. In addition, stop-flow events, where the water flow in the column is stopped for tens to hundreds of hours, can indicate the presence of kinetically controlled contaminant release if the contaminant concentration increases during the stop-flow event.

During the experiments conducted and reported here, the three sediment samples were subject to long-term leaching with artificial groundwater in 1-D column studies to evaluate the rate at which contaminants were released from the sediment. These experiments consisted of leaching a total of 109 to 125 pore volumes of artificial groundwater through the sediment at a constant flow rate. Effluent samples were collected during the leaching, and were analyzed for U-238, Cr, and a tracer (bromide). In addition, three stop-flow events were used to further evaluate the presence of kinetically controlled contaminant release rate from the sediments at 3, 16, and 100 pore volumes. The stop-flow intervals ranged from 71 hours (at 2 pore volumes), to 78 hours (at 16 pore volumes), and 509 hours (at 100 pore volumes).

For some of the data interpretation, data from S-Complex and T-Complex boreholes (Truex et al. 2016) and B-Complex boreholes (Szecsody et al. 2017) are included on figures. It was not possible to interpret breakthrough of the bromide tracer in the injecting water, as it appeared that sediment pore water contained low, but variable, bromide.

4.3.1 S-13 Waste Site (C9513) Samples

Two sediment samples were analyzed from the S-Complex borehole at varying depths. Sample B3DCJ2 was contaminated with 20.89 $\mu\text{g/g}$ uranium, of which a significant fraction was present in highly mobile aqueous and adsorbed phases (Table 19). Calculated K_d for uranium for this sample was 2.29 mL/g.

For this sample, flowing artificial groundwater through the sediment resulted in a high initial uranium concentration leaching (33,000 $\mu\text{g/L}$, Figure 20), which decreased to about 100 $\mu\text{g/L}$ by 30 pore volumes and continued to leach at that concentration to 110 pore volumes. By 10 pore volumes, 70% of the uranium was released (compared to the total leached uranium by 110 pore volumes). The continued uranium leaching over the 110 pore volumes and the increased uranium concentration at each stop-flow event, indicated by red arrows in Figure 20(b) and (c), indicate slow uranium release from the sediment. This may be due to slow carbonate dissolution, which contains uranium co-precipitate. The uranium

sequential extraction for this sample showed high aqueous and adsorbed uranium (7.1 $\mu\text{g/g}$) and a total of about 10 $\mu\text{g/g}$ mobile uranium (i.e., aqueous, adsorbed, and half of the acetate-extractable uranium). Leaching at 110 pore volumes consistently resulted in about 11 $\mu\text{g/g}$ of uranium cumulatively.

This sample also contained a small concentration of aqueous and adsorbed Cr (likely anthropogenically sourced); however, most of the total extracted Cr was from mineral precipitates (about 65.9 $\mu\text{g/g}$), which were most likely naturally occurring. The calculated K_d for Cr was 0.382 mL/g (Table 19). In contrast to uranium, as can be seen in Figure 20, chromium leaching behavior showed aqueous Cr in the first three samples (< 0.4 pore volumes), followed by nearly no detectable Cr in the effluent. This is consistent with the sequential extraction data, which indicated small aqueous and adsorbed Cr in the sediment. Although there was no detectable chromium over most of the 110 pore volumes, the 509-hour stop-flow event at 110 pore volumes did result in a low Cr concentration (0.52 $\mu\text{g/L}$), indicating a very slow dissolution process likely from a Cr-containing precipitate.

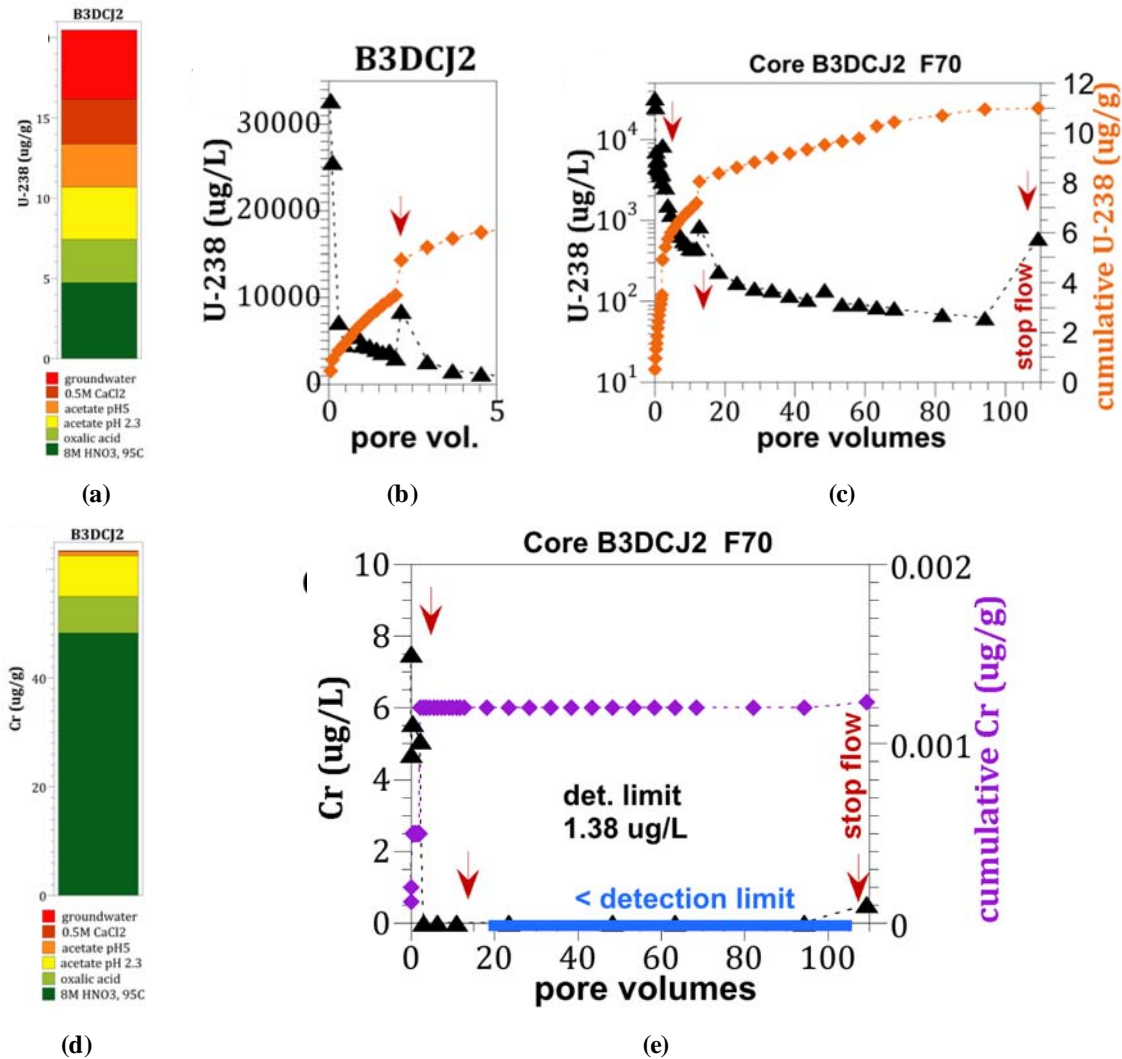


Figure 20. Contaminant leaching behavior in sample B3DCJ2 (S-13, C9513) as shown by a) U sequential extraction, b) U leaching (0 to 10 pore volumes), c) U leaching (to 110 pore volumes), d) Cr sequential extraction, and e) Cr leaching (to 110 pore volumes).

For sample B3DCJ7, the total uranium contamination was 17.2 $\mu\text{g/g}$, of which a significant fraction (about 14 $\mu\text{g/g}$) was present in highly mobile aqueous, adsorbed, and acetate-extractable U (Table 19). The calculated K_d for uranium for this sample was 1.54 mL/g, based on duplicate extractions. Artificial groundwater flow through the sediment resulted in a high initial uranium concentration in the effluent (22,000 $\mu\text{g/L}$, Figure 21), which ultimately decreased to about 200 $\mu\text{g/L}$ by 30 pore volumes and continued to leach at that concentration to 120 pore volumes. By 10 pore volumes, 60% of the uranium was released (compared to the total leached uranium by 120 pore volumes). The continued uranium leaching over the 120 pore volumes and the increased uranium concentration at each stop-flow event, as shown by red arrows in Figure 21(b), indicate slow uranium release from the sediment. This may be from slow carbonate dissolution as this sample was taken from a CCU unit with higher carbonate content, and carbonate minerals contain some uranium co-precipitate. Uranium sequential extraction for this sample showed high aqueous and adsorbed uranium, with a total of about 10 $\mu\text{g/g}$ of mobile U (i.e., aqueous,

adsorbed, and half of the acetate-extractable U). Leaching the sediment for 120 pore volumes yielded about 21 $\mu\text{g/g}$ of uranium cumulatively, which was higher than the ~ 10 $\mu\text{g/g}$ predicted amount from the sequential extractions.

The sample also contained low concentrations of aqueous and adsorbed Cr, which is likely due to anthropogenic sources. However, most of the total extracted Cr was from mineral precipitates (about 42 $\mu\text{g/g}$), which were most likely naturally occurring. The calculated K_d for Cr was 3.49 mL/g (Table 19). The chromium leach behavior showed high initial aqueous Cr (2440 $\mu\text{g/L}$), followed by a lower Cr concentration leached for 8 pore volumes (Figure 21(d)), after which no detectable Cr was observed. The total Cr leached from the sediment by 125 pore volumes was 1.2 $\mu\text{g/g}$, compared with 0.8 $\mu\text{g/g}$ mobile Cr indicated by sequential extractions. Leaching showed that 97% of the Cr mass was leached by 10 pore volumes. The sequential extraction data (Table 19) did indicate small aqueous and adsorbed Cr in this sediment sample.

All three stop-flow events for this sample resulted in a higher Cr concentration, indicating a very slow kinetic dissolution of a Cr-containing precipitate. Cumulative Cr leached from the sediment continued until 10 pore volumes and then ceased. This is opposite of the cumulative U leaching behavior since U continued to leach after 10 pore volumes.

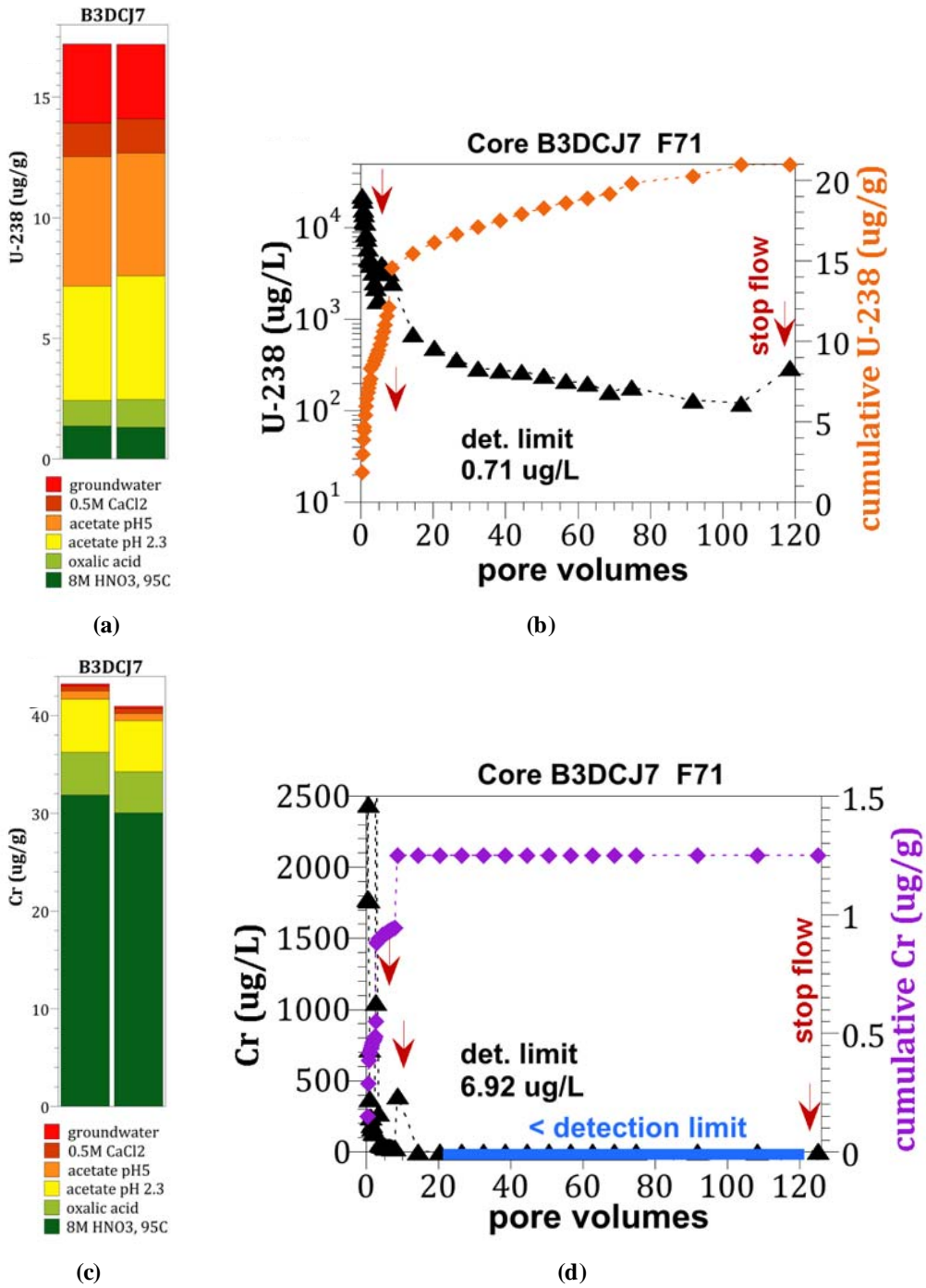


Figure 21. Contaminant leaching behavior in sample B3DCJ7 (S-13, C9513) as shown by a) U sequential extraction, b) U leaching (to 125 pore volumes), c) Cr sequential extraction, and d) Cr leaching (to 125 pore volumes).

4.3.2 T-3 Reverse Well Waste Site (C9555) Sample

Sample B3DB67 from borehole T-3 (C9555) was contaminated with 29.44 $\mu\text{g/g}$ uranium, of which a small mass (0.22 $\mu\text{g/g}$) was present as aqueous and adsorbed uranium. The acetate-extractable U accounted for most of the mobile uranium (2.7 $\mu\text{g/g}$, Table 19). The calculated K_d for uranium was 14.2 mL/g. Duplicate soil-column leach experiments were conducted. Artificial groundwater flowing through the sediment resulted in a moderate initial uranium concentration (70 $\mu\text{g/L}$ in Figure 22(b), 417 $\mu\text{g/L}$ in Figure 22(c)), which decreased to less than 20 $\mu\text{g/g}$ by 20 pore volumes in both experiments and continued to leach at that concentration to 120 pore volumes. The total uranium leached from the sediment (0.7 $\mu\text{g/g}$) was smaller than ~ 2.9 $\mu\text{g/g}$ predicted from the sequential extractions. The leaching behavior was unusual, with slowly increasing uranium concentrations between 30 and 80 pore volumes in both leach experiments (Figure 22(b) and (c)). In addition, at stop-flow events at 2.5 and 12 pore volumes, the uranium concentration increased slightly, indicating some U release from the sediment. However, the uranium concentration decreased slightly at 107 pore volumes, indicating uranium precipitation or slow adsorption. The slow uranium release from the sediment is typically attributed to slow carbonate dissolution (which contains some uranium), in contrast to the behavior observed in these duplicate experiments. Since the injected artificial groundwater was the same for these experiments, this observed leaching behavior may indicate the presence of a slowly released uranium-complex that is unidentified.

The duplicate leach experiments were also analyzed for aqueous Cr, although the sediment was not considered to have Cr contamination. Although the sequential extractions were not analyzed for Cr, leach experiments showed low concentrations (12 to 73 $\mu\text{g/L}$ Cr) in the first few leach samples (Figure 22(d) and (e)). In addition, the stop-flow event at 122 pore volumes showed an increasing Cr concentration, indicating a very slow dissolution of a Cr-containing precipitate.

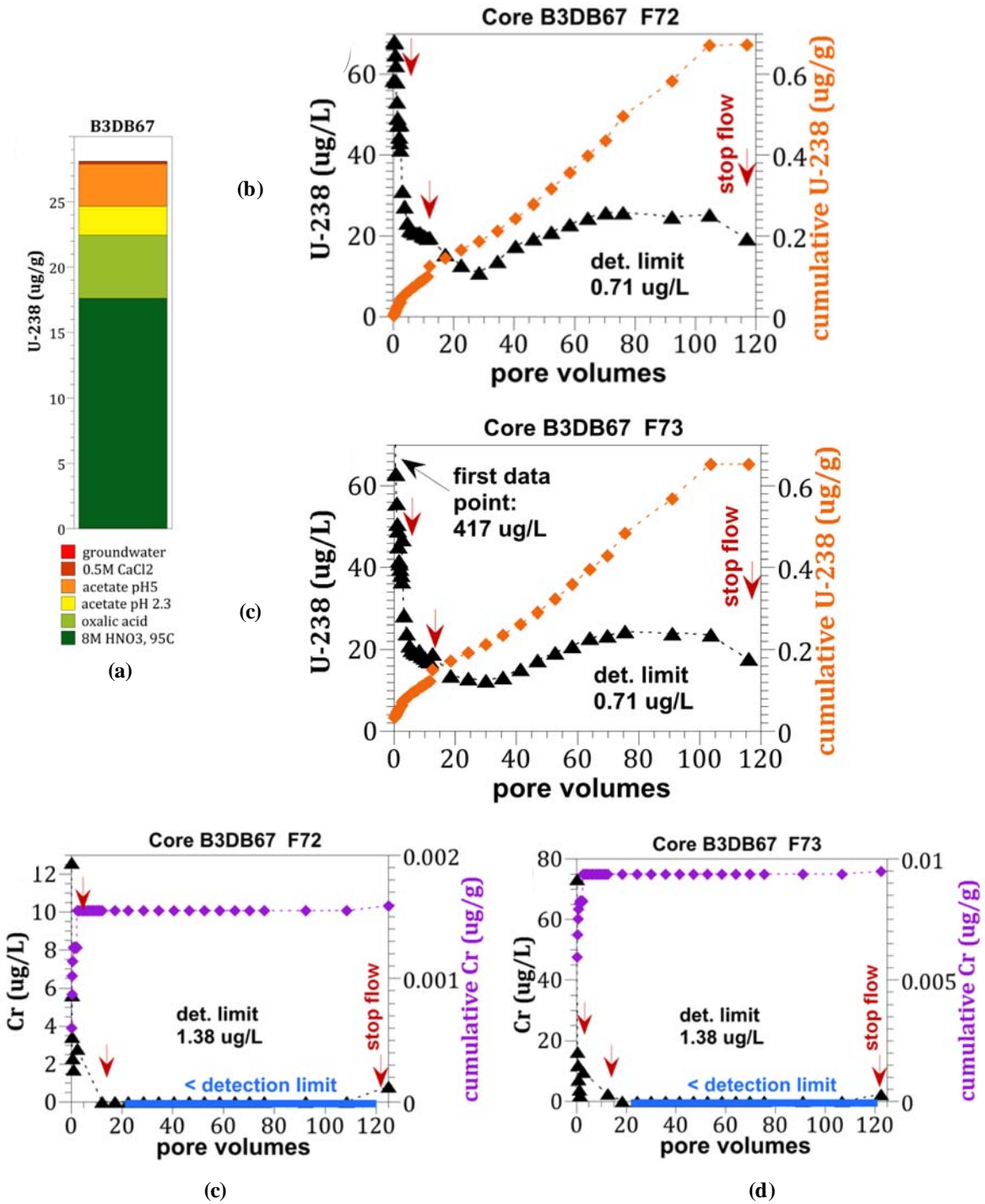


Figure 22. Contaminant leaching behavior in sample B3DB67 (T-3, C9555) as shown by a) U sequential extraction, b) U leaching (to 120 pore volumes), c) U leaching (to 120 pore volumes) in a duplicate experiment, d) Cr leaching (to 125 pore volumes), and e) Cr leaching (to 125 pore volumes) in a duplicate experiment.

4.3.3 Uranium and Chromium Release Rate from Sediments

The three stop-flow events (at approximately 2, 15, and 100 pore volumes) in leach experiments were used to evaluate the uranium and chromium release rates from sediments. For uranium, the release rate in the first few pore volumes is typically high due to uranium partitioning from the adsorbed phase into the aqueous (leached) phase. At a higher number of pore volumes, the release rate is typically one to two orders of magnitude lower as a result of uranium being released due to dissolution of a solid phase (such as carbonate dissolution) or diffusion from microfractures in sediment grains.

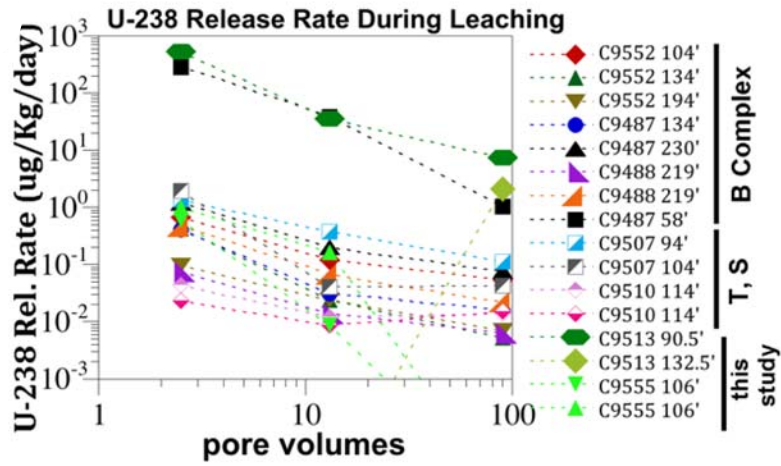
For the three sediments analyzed in the 1-D soil-column leaching tests in this study, the typical uranium release behavior of decreasing release rate was observed for two of the samples (B3DCJ2, B3DCJ7, Table 21, Figure 23) with high release rates from U-contaminated sediment. The sample B3DB67, which showed unusual release behavior in the 30 to 80 pore volume range (Figure 22) had lower release rates, similar to that found in natural sediments. There was a regular trend of the uranium leached mass and the leach rate, as shown in Figure 23(a) for this study and previous studies, for DV-1 and UP-1 sediments (Figure 23(b)). This regular trend indicates that, in general, high uranium contamination is not held strongly on sediment, and it leaches at a faster rate. In contrast, natural uranium in the sediment is close to equilibrium, so it leaches at a slower rate and a lesser cumulative amount. This general trend can be used to estimate the uranium release rate from the sediments given the leached mass, as the leached mass can be estimated from sequential extractions.

For chromium, the calculated release rates show a high rate for the Cr-contaminated sample (B3DCJ7, Table 21) at 2 pore volumes, then a decrease by one order of magnitude by 12 pore volumes, and an additional decrease by three orders of magnitude by 100 pore volumes (Figure 24). In this Cr-contaminated sample, the total amount of Cr leached was also high (Figure 24(b)). Therefore, there was a similar trend of mass release and release rate as observed with uranium data. The other two sediment samples had small amounts of leached Cr, and rates were low.

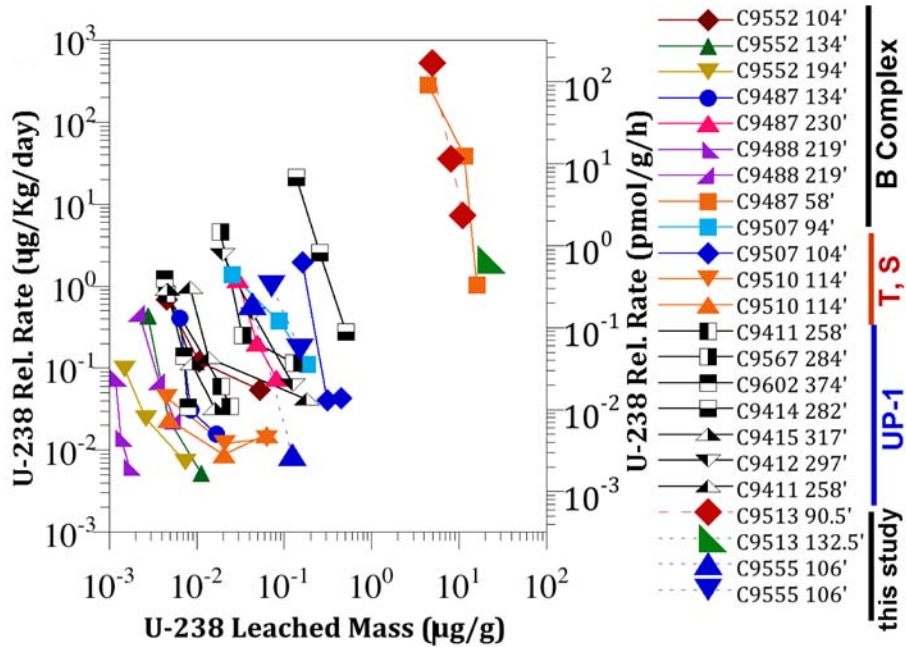
Finally, while multiple previous studies have concluded that uranium incorporates into calcite (Zachara et al. 2007a,b; Qafoku and Icenhower 2008; Catalano et al. 2008), only one recent study indicates that Cr can incorporate into calcite (Truex et al. 2015b). For these sediments, if U and Cr were initially being leached from aqueous and adsorbed phases, but at later pore volumes if both were being released from the sediment as a result of calcite dissolution, then release rates should correlate between U and Cr. While a correlation appears to exist (Figure 25), there is only a small amount of Cr leach data available.

Table 21. Contaminant release rates calculated for stop-flow events during soil-column leaching experiments.

Borehole Designation	Sample ID	Core	Depth Interval (ft bgs)	Geologic Unit	Stop Flow (pv)	U-238 Rel. Rate (µg/kg/day)	Cr Rel. Rate (µg/kg/day)	Stop Flow (pv)	U-238 Rel. Rate (µg/kg/day)	Cr Rel. Rate (µg/kg/day)	Stop Flow (pv)	U-238 Rel. Rate (µg/kg/day)	Cr Rel. Rate (µg/kg/day)
S-13 (C9513)	B3DCJ2	13 (Grab)	90.5-92	H2	2.00	5.33E+02	5.03E-01	11.82	3.58E+01	0.0000	95.70	7.40E+00	7.22E-03
S-13 (C9513)	B3DCJ7	21 (Grab)	131.5-133.5	CCUc	2.67	-3.74E+01	1.78E+02	7.81	-5.65E+01	28.705	108.3	2.13E+00	5.56E-02
T-3 (C9555)	B3DB67	57B	106-107	H2 /CCUz	2.32	6.12E-01	2.68E-01	11.30	8.74E-03	0.0000	108.6	-7.77E-02	1.06E-02
T-3 (C9555)	B3DB67	57B	106-107	H2 /CCUz	2.50	9.93E-01	9.25E-01	11.70	1.66E-01	0.210	106.7	-7.90E-02	3.10E-02

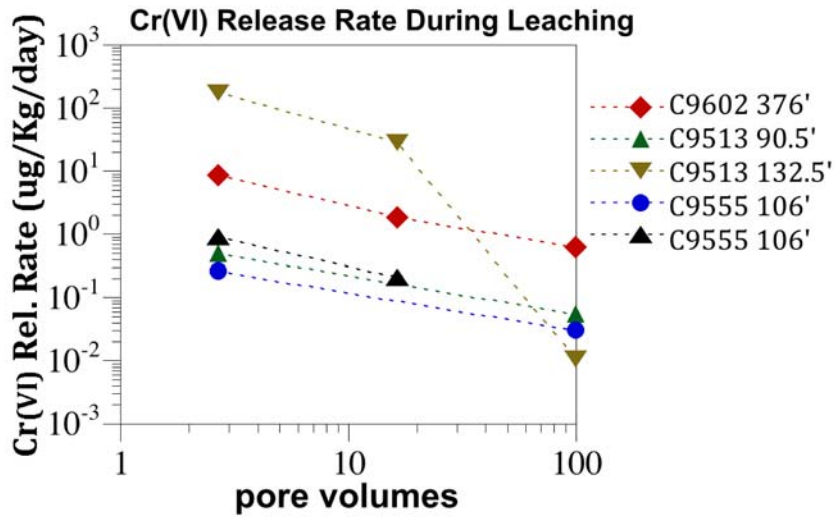


(a)

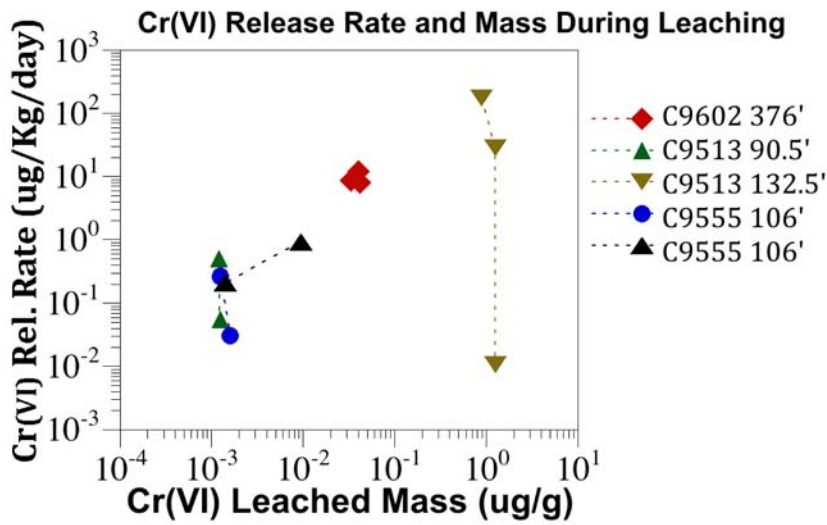


(b)

Figure 23. Uranium release rate calculated from sediment leach studies at stop-flow events showing release rate as a function of: a) pore volume, b) uranium leached mass.



(a)



(b)

Figure 24. Chromium release rate calculated from sediment leach studies at stop-flow events showing release rate as a function of a) pore volume, b) chromium leached mass.

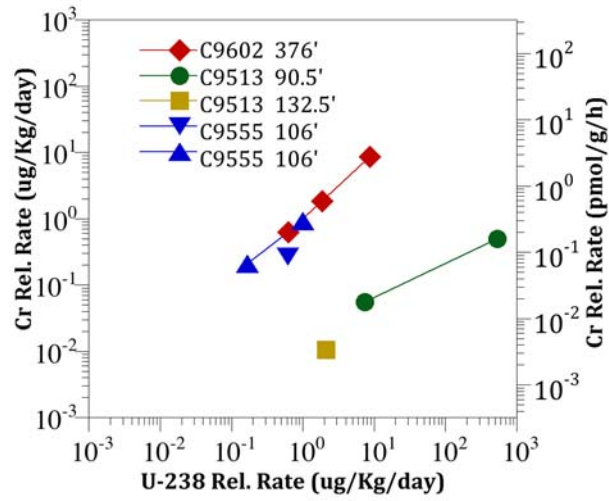


Figure 25. Correlation between the uranium and chromium release from sediments during stop-flow events in leach studies.

5.0 Quality Assurance

The PNNL QA Program is based upon the requirements as defined in DOE Order 414.1D, *Quality Assurance*, and 10 CFR 830, “Energy/Nuclear Safety Management,” Subpart A, Quality Assurance Requirements. PNNL has chosen to implement the following consensus standards in a graded approach:

- ASME NQA-1-2000, *Quality Assurance Requirements for Nuclear Facility Applications*, Part 1, Requirements for Quality Assurance Programs for Nuclear Facilities.
- ASME NQA-1-2000, Part II, Subpart 2.7, Quality Assurance Requirements for Computer Software for Nuclear Facility Applications, including problem reporting and corrective action.
- ASME NQA-1-2000, Part IV, Subpart 4.2, Guidance on Graded Application of Quality Assurance (QA) for Nuclear-Related Research and Development.

The procedures necessary to implement the requirements are documented through PNNL’s “How Do I...? (HDI), a system for managing the delivery of laboratory-level policies, requirements, and procedures.

The *DVZ-AFRI Quality Assurance Plan* (QA-DVZ-AFRI-001) was applied as the applicable QA document for this work under the NQA-1 QA program. This QA plan conforms to the QA requirements of DOE Order 414.1D and 10 CFR 830, Subpart A. This effort is subject to the *Price Anderson Amendments Act*.

The implementation of the Deep Vadose Zone – Applied Field Research Initiative QA program is graded in accordance with NQA-1-2000, Part IV, Subpart 4.2, Guidance on Graded Application of Quality Assurance (QA) for Nuclear-Related Research and Development. The technology level defined for this effort is Development Research, which consists of developing information that will be used directly by the Hanford Site to support remediation decisions.

This work was conducted under the Development Research level to ensure the reproducibility and defensibility of these experimental results. As such, reviewed calculation packages are available upon request except where experimental information is denoted as a scoping or preliminary study.

This work used PNNL’s Environmental Sciences Laboratory (ESL) for chemical analyses. The ESL operates under a dedicated QA plan that complies with the *Hanford Analytical Services Quality Assurance Requirements Document* (HASQARD; DOE 2007), Rev. 3. ESL implements HASQARD through *Conducting Analytical Work in Support of Regulatory Programs* (CAWSRP). Data quality objectives established in CAWSRP were generated in accordance with HASQARD requirements. Chemical analyses of testing samples and materials were conducted under the ESL QA Plan.

QA reviews of data and analyses were conducted for this work in accordance with the QA plan. There were no reportable QA issues with the data included in this report.

6.0 Conclusions

The data collected in this laboratory study addressed the following three objectives:

- Define the contaminant distribution and the hydrologic and biogeochemical setting.
- Identify attenuation processes and describe the associated attenuation mechanisms.
- Quantify attenuation and transport parameters for use in evaluating remedies.

These objectives are elements of the framework identified in EPA guidance (EPA 2015) for evaluating MNA of inorganic contaminants, and they directly support updating the CSM for these waste sites (and generally for the Hanford Central Plateau). Importantly, the information supports defining suitable contaminant transport parameters that are needed to evaluate migration of contaminants through the vadose zone and to the groundwater. This type of transport assessment supports a coupled analysis of groundwater and vadose zone contamination. The laboratory study information, in conjunction with transport analyses, can be used as input to evaluate the feasibility of remedies for the 200-DV-1 OU. This remedy evaluation will be enhanced by considering these study results that improve the understanding of controlling features and processes for transport of contaminants through the vadose zone to the groundwater.

Interpretation of this laboratory study can be considered from several perspectives relevant to supporting 200-DV-1 OU activities. Results for each contaminant were evaluated across all of the samples to identify contaminant-specific conclusions and to enable consideration of how results from this study may be relevant to other waste sites. Results are also evaluated with respect to conclusions relevant to the specific waste sites included in the study. Lastly, study results were evaluated with respect to updating CSMs and future evaluation of remedies, including the associated fate and transport assessment needed as a basis for remedy evaluation.

The data and information from these attenuation and transport studies were interpreted to support the following conclusions about contaminant behavior observed across the waste sites sampled in this study.

- Uranium
 - Uranium concentrations were low in most samples analyzed for this study, which indicates that a significant fraction of uranium may be associated with natural background. However, moderate levels of uranium were observed in two of the core samples (B39X10 and B39X55) from borehole S-13 (C9513) and one of the core samples (B39VY1) from borehole T-7 (C9503). However, the total uranium found in B39VY1 was still significantly lower than the S-13 (C9513) samples, and mostly in mineral precipitate forms. Sample B39X55 was from the CCU caliche unit with a high carbonate concentration. Consistently, the results for this sample indicated high total inorganic carbon which suggests formation of uranium carbonate compounds potentially attenuating uranium in this formation. Sequential extraction results for the same unit as discussed below confirmed this behavior. Sample B39X10 was from a transition zone between H2 and CCUz formations. Sequential extractions conducted for a grab sample in H2 formation for this borehole also indicated moderate levels of uranium with about 20% being in the aqueous and adsorbed phases. Thus, some portion of uranium in this borehole (S-13, C9513) may be migrating from H2 sediments into CCUc and where it may then complex with carbonate. Uranium-

carbonate precipitation was identified as an important attenuation mechanism that reduce uranium mobility. This attenuation mechanism will have to be accounted for in transport assessments.

- Uranium surface phases showed significant differences for different boreholes. Aqueous and adsorbed uranium, that would be transported under equilibrium conditions, ranged from 0.5% to 20% among the samples from the S-13 (C9513), T-3 (C9555), and T-7 (C9503) boreholes, with the highest fraction observed in sample B3DCJ2 (grab sample, S-13, C9513). The mobile fraction of uranium that also includes part of the acetate-extractable uranium in addition to the aqueous and adsorbed phases ranged from 10% to 55%, with the highest mobility observed in the samples from borehole S-13 (C9513). While the T-3 (C9555) sample yielded the highest amount of total contamination (29.44 $\mu\text{g/g}$), most of the uranium in borehole T-3 (C9555) was associated with precipitates where transport of uranium would be controlled by slow dissolution processes.
 - Slow-release transport behavior that is potentially due to slow carbonate dissolution was observed in soil-column leaching experiments for the samples from borehole S-13 (C9513). However, core sample B3DB67 (T-3, C9555) showed an unusual transport behavior with initially decreasing concentrations followed by slight increase, indicating a slowly released uranium-complex that is unidentified.
 - Uranium K_d values were varied across the different samples tested. The highest K_d value was associated with the sample (B3DB67) from borehole T-3 (C9555), which also had the highest amount of uranium contamination. Thus, in transport assessments, selection of a K_d value for uranium should consider spatial variation of the K_d value.
- Iodine
 - Total iodine concentrations in the vadose zone were only measured for the sample from borehole B-42 (C9497), which showed a very low level.
 - Tc-99
 - Tc-99 was only measured for the sample from borehole B-42 (C9497) and was a non-detect.
 - A grab sample (i.e., samples other than those originally targeted for attenuation testing) from borehole B-42 (C9497) with a Tc-99 concentration of 11.1 pCi/g was selected collectively by PNNL and CHPRC for sequential extractions. A sample adjacent to this grab sample was analyzed for Tc-99. The result indicated a very small amount of total extractable Tc-99 in this sediment. (about four orders of magnitude lower than the grab sample targeted), indicating heterogeneity in Tc-99 distribution. No further soil-column leaching tests were conducted for this sample due to the low value observed for this sample. However, sequential extraction results indicate that Tc-99 is in the mobile phase in this sediment.
 - Chromium
 - Cr(VI) was not detected in most core samples and, when detected, was present at a low concentration. Total chromium measured in acid extractions was likely from natural background.
 - Sequential extraction results (conducted with a set of grab samples) showed a wide range of total Cr concentrations (8.9 to 68 $\mu\text{g/g}$) among the selected samples. However, the mobile chromium ranged only from 0.95 to 1.6 $\mu\text{g/g}$. Some of the elevated K_d values determined in sequential extractions for Cr indicated more sorption than expected for the sediment from borehole S-13 (C9513), attenuating its mobility in this borehole.

- Nitrate
 - Nitrate concentrations were low in all of the samples, except the samples from borehole T-7 (C9503), which indicated an increasing trend with depth, indicating very little attenuation potential.

The following conclusions were developed for the specific boreholes/waste sites analyzed in this study.

- B-42
 - One core sample selected for the laboratory study from the B-42 waste site (borehole C9497) was of CCU gravel material. This sample did not show any signs of altered geochemistry induced by the waste discharge. Contaminant levels were also observed to be very low or non-detect.
 - Six samples analyzed for isotopic signature, with varying depths from this borehole, showed two distinct patterns over the depth profile correlated to the historic water table depth for this location (256 ft below surface). Results suggested mixing of a distinct upper water (above 256 ft) with a distinct lower water near the location of the historical water table. Furthermore, upper data (above 256 ft) also showed isotopic shifts that are consistent with a flux of industrial process water near the surface that is propagating downward.
- S-13
 - Core samples for the contaminant concentration and geochemical evaluation from the S-13 waste site (borehole C9513) were materials from the transition of Hanford formation to CCU silt, CCU caliche (CCUc), and Ringold (silty, sandy gravel). The samples from the transition zone and CCUc showed moderate levels of uranium and total chromium with very small amounts of Cr(VI). The sample from the Ringold formation only had very small amounts of contaminants present. None of these samples showed any significant nitrate levels. The sediment from the CCUc formation also showed high levels of total carbon and total inorganic carbon, as well as higher calcium and magnesium, indicating the presence of carbonate in this sample. Slightly elevated levels of uranium found in this sample are likely due to formation of uranium carbonate compounds.
 - A total of four grab samples were selected for sequential extractions for this borehole for uranium and chromium analyses. For the two samples analyzed for uranium, it was observed that some uranium was in mobile phase (aqueous, adsorbed, and acetate extractable), which may transport in aqueous phase under equilibrium-partitioning conditions. The sample from the CCUc formation showed uranium associated with the acetate-extractable portion, indicating complexation with carbonate. All four samples were analyzed for chromium and showed total chromium concentrations ranging from 30.28 to 67.60 $\mu\text{g/g}$ with a very small fraction of mobile chromium. Slightly elevated K_d values for Cr (0.382-7.64 mL/g) indicated more sorption behavior than expected. Soil-column leaching experiments confirmed a decreasing release rate over time for uranium consistent with dissolution of a solid phase. For chromium, these experiments indicated a small release during the early stages of the experiment and a very slow kinetic dissolution of a Cr-containing precipitate.
 - Isotope analysis for this borehole showed an anthropogenic influence similar to borehole B-42. It is likely that the isotopic signature indicates a high flux of Columbia River water (e.g., as process water) into the system.

- Based on the data collected in this laboratory study, the following attenuation processes are important at this waste site. Sorption processes are important for uranium. Formation of uranium-carbonate precipitates also appears to be an attenuation mechanism in S-13 borehole samples. The potential for reduction through abiotic (e.g., ferrous iron) mechanisms is very limited, and would not affect the future contaminant migration.
- T-7
 - Core samples from the T-7 waste site (borehole C9503), analyzed for contaminant distribution and geochemistry, were materials from the transition of Hanford formation to CCU silt, transition of CCU silt to caliche, and Ringold (silty, sandy gravel). Only one sample (B39VY1) showed a slightly elevated uranium concentration where the other two samples yielded very low concentrations. All sampled showed low levels of chromium. However, nitrate levels were noticeably elevated, showing an increasing trend with depth.
 - Sequential extractions yielded very small amount of total uranium, with a large fraction in functionally immobile form associated with solid phases in the sediment. The K_d value was calculated as 3.17 ml/g.
 - Isotope analysis for this borehole yielded patterns largely consistent with expected natural patterns, indicating very little anthropogenic influence in this area.
 - Based on the data collected in this laboratory study, the following attenuation processes are important at this waste site. Sorption processes are important for uranium. No indications of reduction were observed in these samples and the potential for reduction through abiotic (e.g., ferrous iron) processes is limited.
- T-3
 - Core samples from the T-3 reverse well waste site (borehole C9555), analyzed for contaminant distribution and geochemistry, were from the transition of Hanford formation to CCU silt and Ringold (silty, sandy gravel). The sample from the transition zone showed slightly elevated nitrate levels accompanied by a high uranium concentration in acid extractions. No Cr(VI) was detected in water extractions and acid extractions yielded a very small amount of total chromium for this sample. The sample from the Ringold unit didn't show any significant contaminant levels.
 - The sample from the transition unit was further evaluated through sequential extractions. The total uranium contamination was observed to be the highest among the selected samples from all boreholes. However, the majority of this uranium was found to be associated with functionally immobile solid phases, requiring dissolution processes for contaminant release. The total uranium leached from this sediment was less than predicted from the sequential extractions, with an unusual leaching behavior of initially decreasing, but later slowly increasing, concentrations. This behavior may indicate the presence of a slowly released uranium-complex that is unidentified. The K_d value for uranium was calculated to be 14.23 mL/g. A very small concentration of Cr was also observed in the leaching experiments with the initial few leach samples. Stop-flow events indicated a very slow dissolution of a Cr-containing precipitate.
 - Isotope analysis for this borehole indicates a strong influence of an industrial process that correlates with a reverse well and its screen depth.

- Based on the data collected in this laboratory study, the following attenuation processes are important at this waste site. Sorption processes are important for uranium and chromium. No indications of reduction were observed in these samples and the potential for reduction through abiotic (e.g., ferrous iron) processes is limited.

The study provided a set of data that addressed the study objectives and can support future evaluation of remedies, including MNA and the associated fate and transport assessment that is needed as a basis for remedy evaluations. The first objective was to jointly evaluate contaminant concentrations and the biogeochemical and hydrologic setting for these data. This information provides a baseline for interpreting attenuation and transport studies. As noted, there were significant variations in transport parameter values and some attenuation mechanisms linked to specific sediment characteristics (e.g., carbonate content). For scaling and use of this information in fate and transport assessments, these variations should be considered in light of the sample properties. For this study, the sample properties were linked to the sediment units sampled. However, geochemical indicators did not show any significant difference or effect of contamination. Scaling and use in future efforts can translate the attenuation and transport information from this laboratory study to other waste sites based on the distribution of similar sediment units (e.g., the CCU silt and CCU caliche).

Another objective of the study was to identify attenuation processes that appear to be active in these samples and that will affect contaminant transport through the vadose zone. Sorption processes were found important for uranium, and to a lesser extent for chromate. Carbonate content appeared to be important for uranium and its release behavior. Accumulation in carbonate precipitates was identified as an attenuation mechanism for uranium. Slow release of uranium was evident in leaching experiments. Geochemical signatures of reducing conditions were minimal or non-existent in the samples. Attenuation mechanisms relevant to Tc-99 (other than sorption) could not be fully assessed because of the low/non-detect concentration of this contaminant. Chromium release from the sediment occurred only during the initial phases of the leaching experiments and chromium was found to be strongly associated with mineral precipitates, which were most likely naturally occurring.

A key objective of the study was to quantify attenuation and transport parameters to support parameterization of fate and transport assessments. This type of assessment will be needed to evaluate transport of contaminants through the vadose zone, to evaluate the coupled vadose zone-groundwater system, and to assess the need for, magnitude of, and/or design of remediation. The contaminant- and sample-specific values from stop-flow portions of soil-column experiments and sequential extractions provide a set of information that can be directly used to develop transport parameters. Soil-column effluent concentration data can also be compared to 1-D simulations to assess fate and transport model configurations for K_d or for surface complexation models.

Collectively, the information from this laboratory study can be considered in terms of updating the CSM for contaminants in the vadose zone. It can also provide input to describing the coupled vadose zone-groundwater system that needs to be considered for remedy determinations. CSM elements from this laboratory study are listed below. These elements will need to be incorporated with other data collected during the 200-DV-1 OU remedial investigation as part of updating the CSMs for the 200-DV-1 OU component waste sites.

- Sequential extraction experiments (and more coarsely indicated by comparison of water- and acid-extraction contaminant data) show that only a small fraction of the uranium mass in samples is in a

mobile form that would transport under equilibrium-partitioning conditions. Leaching experiment results confirmed that slow-release processes affect the transport behavior of uranium. The relative amount of uranium mass in the mobile versus functionally immobile phases affects the potential for future mass discharge from the vadose zone to the groundwater.

- Laboratory data suggest that formation and dissolution of uranium-carbonate precipitates is a potential attenuation mechanism affecting the relative mobile and immobile mass fractions and the transport characteristics of uranium.
- Attenuation and sorption are not uniform in the vadose zone, especially for uranium. Lithology (e.g., the presence and extent of layers such as the CCU) and carbonate content affected the transport parameter values for these contaminants.
- For the waste sites included in this study, the effects of waste chemistry, other than contaminant concentrations, did not penetrate deep into the vadose zone. The geochemical signature of samples shows that a transport evaluation at these waste sites will not need to include properties modified by waste chemistry for the deep portion of the vadose zone.
- While the CSM should acknowledge the potential for transformation processes (e.g., abiotic reduction), minimal evidence was observed that these processes are active. However, such transformations may have occurred in the past and contributed to the currently observed contaminant distribution within the sediment and pore water.
- Oxygen and hydrogen isotope data were collected and primarily show correlation to regional precipitation with some variations from evaporative and condensation processes. They also provide an indication of anthropogenic effects (e.g., industrial processes) for some of the waste sites.
- It will be important to incorporate variations in physical property data into the CSM to augment existing data and correlate to indirect measures of lithology (e.g., geophysical logging). Additional detailed hydraulic property data were collected for this laboratory study and will be documented in a separate report.

This laboratory study extended the characterization of the 200-DV-1 OU to include identification and quantification of contaminant attenuation processes and parameters that will be needed to evaluate transport of contaminants through the vadose zone into the groundwater. This type of site-specific information enhances the technical basis to support remedy evaluation. Quantifying transport of contaminants in the vadose zone in terms of a source to groundwater under existing and future conditions without additional intervention is a basic element of remedy evaluation for the vadose zone. This type of evaluation and the supporting laboratory data describing the factors that affect transport (i.e., attenuation processes) are used in the process of considering MNA as all or part of a remedy. For cases where future contaminant discharge from the vadose zone will create or continue plumes of concern in the groundwater, the transport behavior and magnitude of the source discharge are used to define the target for vadose remediation (i.e., the extent of an engineered remedy needed in addition to natural attenuation) and assess potential remedy options. Thus, the information in this laboratory study was included in the 200-DV-1 OU characterization efforts to support the upcoming remedy evaluation in the feasibility study.

7.0 References

10 CFR 830, "Energy/Nuclear Safety Management," Subpart A, Quality Assurance Requirements. *Code of Federal Regulations*, as amended.

ASME NQA-1-2000, *Quality Assurance Requirements for Nuclear Facility Applications*. American Society of Mechanical Engineers, New York, New York.

Barnes, C.J. and G.B. Allison (1988) Tracing of water movement in the unsaturated zone using stable isotopes of hydrogen and oxygen. *Journal of Hydrology*, **100**, 143-176.

Beckett P. 1989. "The use of extractants in studies on trace metals in soils, sewage sludges, and sludge-treated soils." In *Advances in Soil Science*, Volume 9, Springer-Verlag, New York, New York, pp. 144-176.

Brina R and AG Miller. 1992. "Direct detection of trace levels of uranium by laser induced kinetic phosphorimetry." *Analytical Chemistry* 64(13):1413-1418.

Catalano J, J McKinley, J Zachara, S Heald, S Smith, and G Brown. 2008. "Changes in Uranium Speciation Through a Depth Sequence of Contaminated Hanford Sediments." *Environmental Science and Technology* 40(8):2517-2524.

Chao T and L Zhou. 1983. "Extraction techniques for selective dissolution of amorphous iron oxides from soils and sediments." *Soil Science Society of America Journal* 47(2):225-232.

CHPRC. 2015a. *Conceptual Site Models for the 200-DV-1 Operable Unit Waste Sites in the T Complex Area, Central Plateau, Hanford, Washington*. SGW-49924, Rev. 0, CH2M Hill Plateau Remediation Company, Richland, Washington.

CHPRC. 2015b. *Conceptual Site Models for the 200-DV-1 Operable Unit Waste Sites in the S Complex Area, Central Plateau, Hanford, Washington*. SGW-50280, Rev. 1, CH2M Hill Plateau Remediation Company, Richland, Washington.

Craig H. 1961. "Isotopic variations in meteoric waters." *Science* 133:1702-1703.

DePaolo DJ, ME Conrad, K Maher, and GW Gee. 2004. "Evaporation effects on oxygen and hydrogen isotopes in deep vadose zone pore fluids at Hanford, Washington." *Vadose Zone Journal* 3:220-232.

DOE. 2007. *Hanford Analytical Services Quality Assurance Requirements Document*. DOE/RL-96-68, Rev. 3, U.S. Department of Energy, Richland, Washington.

DOE. 2012. *Characterization Sampling and Analysis Plan for the 200-DV-1 Operable Unit*. DOE/RL-2011-104, U.S. Department of Energy, Richland Operations Office, Richland, Washington.

DOE. 2016. *Remedial Investigation/Feasibility Study and RCRA Facility Investigation/Corrective Measures Study Work Plan for the 200-DV-1 Operable Unit*. DOE/RL-2011-102, U.S. Department of Energy, Richland Operations Office, Richland, Washington.

DOE Order 414.1D, *Quality Assurance*. U.S. Department of Energy, Washington, D.C.

EPA. 2007a. *Monitored Natural Attenuation of Inorganic Contaminants in Ground Water- Volume 1, Technical Basis for Assessment*. EPA/600/R-07/139, U.S. Environmental Protection Agency, Washington, D.C.

EPA. 2007b. *Monitored Natural Attenuation of Inorganic Contaminants in Ground Water- Volume 2, Assessment for Non-Radionuclides Including Arsenic, Cadmium, Chromium, Copper, Lead, Nickel, Nitrate, Perchlorate, and Selenium*. EPA/600/R-07/140, U.S. Environmental Protection Agency, Washington, D.C.

EPA. 2010. *Monitored Natural Attenuation of Inorganic Contaminants in Ground Water- Volume 3, Assessment for Radionuclides Including Tritium, Radon, Strontium, Technetium, Uranium, Iodine, Radium, Thorium, Cesium, and Plutonium-Americium*. EPA/600/R-101093, U.S. Environmental Protection Agency, Washington, D.C.

EPA. 2015. *Use of Monitored Natural Attenuation for Inorganic Contaminants in Groundwater at Superfund Sites*. OSWER Directive 9283.1-36, U.S. Environmental Protection Agency, Office of Solid Waste and Emergency Response, Washington, D.C.

Gibbs C. 1976. "Characterization and Application of Ferrozine Iron Reagent as a Ferrous Iron Indicator." *Analytical Chemistry* 48(8):1197-1200.

Graham DL. 1983. *Stable isotopic composition of precipitation from the Rattlesnake Hills area of south-central Washington State*. RHO-BW-ST-44 P, Rockwell Hanford Operations, Richland, Washington.

Gleyzes C, S Tellier, and M Astruc. 2002. "Fractionation studies of trace elements in contaminated soils and sediments: a review of sequential extraction procedures." *Trends in Analytical Chemistry* 21:(6 & 7):451-467.

Goebel TS and RJ Lascano. 2012. "System for high throughput water extraction from soil material for stable isotope analysis of water." *Journal of Analytical Sciences, Methods and Instrumentation* 2:203-207.

Hall G, J Vaive, R Beer, and N Hoashi. 1996. "Selective leaches revisited, with emphasis on the amorphous Fe oxyhydroxides phase extraction." *Journal of Geochemical Exploration* 56:59-78.

Hearn PP Jr., WC Steinkampf, DG Horton, GC Solomon, LD White, and JR Evans. 1989. "Oxygen-isotope composition of ground water and secondary minerals in Columbia Plateau basalts: Implications for the paleohydrology of the Pasco Basin." *Geology* 17:606-610.

Heron G, C Crozet, AC Bourg, and TH Christensen. 1994. "Speciation of Fe(II) and Fe(III) in contaminated aquifer sediments using chemical extraction techniques." *Environmental Science and Technology* 28:1698-1705.

Larner B, A Seen, and A Townsend. 2006. "Comparative study of optimized BCR sequential extraction scheme and acid leaching of elements in certified reference material NIST 2711." *Analytica Chimica Acta* 556:444-449.

McKinney CR, JM McCrea, S Epstein, HA Allen, and HA Urey. 1950. "Improvements in mass spectrometers for the measurement of small differences in isotope abundance ratios." *Review of Scientific Instruments* 21:724-730.

Newman B, A Tanweer, and T Kurttas. 2009. *IAEA Standard Operating Procedure for Liquid-Water Stable Isotope Analyser*. International Atomic Energy Agency, Vienna. http://www-naweb.iaea.org/napc/ih/documents/other/laser_procedure_rev12.pdf.

Prudic D, D Stonestrom, and R Streigl. 1997. *Tritium, Deuterium, and Oxygen-18 in Water Collected from Unsaturated Sediments near a Low-Level Radioactive-Waste Burial Site South of Beatty, Nevada*. Water Resources Investigations Report 97-4062, U.S. Geological Survey, Reston, Virginia.

Qafoku NP, CC Ainsworth, JE Szecsody, and OS Qafoku. 2004. "Transport-controlled kinetics of dissolution and precipitation in the sediments under alkaline and saline conditions." *Geochimica et Cosmochimica Acta* 68(14):2981-2995.

Qafoku NP and JP Icenhower. 2008. Interactions of aqueous U(VI) with soil minerals in slightly alkaline natural systems. *Reviews in Environmental Science and Biotechnology* 7:355-380.

Rhoades, JD. 1996. *Methods of Soil Analysis Part 3. Chemical Methods*. Soil Science Society of America, Madison, WI.

Serne RJ, BN Bjornstad, JM Keller, PD Thorne, DC Lanigan, JN Christensen, and GS Thomas. 2010. *Conceptual Models for Migration of Key Groundwater Contaminants Through the Vadose Zone and Into the Upper Unconfined Aquifer Below the B-Complex*. PNNL-19277, Pacific Northwest National Laboratory, Richland, Washington.

Singleton MJ, EL Sonnenthal, ME Conrad, DJ DePaolo, and GW Gee. 2004. "Multiphase reactive transport modeling of seasonal infiltration events and stable isotope fractionation in unsaturated zone pore water and vapor at the Hanford site." *Vadose Zone Journal* 3:775-785.

Spane FA Jr. and WD Webber. 1995. *Hydrochemistry and Hydrogeologic Conditions within the Hanford Site Upper Basalt Confined Aquifer System*. PNL-10817, Pacific Northwest National Laboratory, Richland, Washington.

Sutherland R and F Tack. 2002. "Determination of Al, Cu, Fe, Mn, Pb, and Zn in certified reference materials using the optimized BCR sequential extraction procedure." *Analytica Chimica Acta* 454:249-257.

Szecsody JE, BD Lee, MJ Truex, CE Strickland, JJ Moran, MMV Snyder, CT Resch, AR Lawter, L Zhong, BN Gartman, DL Saunders, SR Baum, II Leavy, JA Horner, B Williams, BB Christiansen, EM McElroy, MK Nims, RE Clayton, and D Appriou. 2017. *Geochemical, Microbial, and Physical Characterization of 200-DV-1 Operable Unit Cores from Boreholes C9552, C9487, and C9488, Hanford Site Central Plateau*. PNNL-26266, Pacific Northwest National Laboratory, Richland, Washington.

Szecsody J, M Truex, N Qafoku, D Wellman, T Resch, and L Zhong. 2013. "Influence of acidic and alkaline co-contaminants on uranium migration in vadose zone sediments." *Journal of Contaminant Hydrology* 151:155-175.

- Truex MJ and KC Carroll. 2013. *Remedy Evaluation Framework for Inorganic, Non-Volatile Contaminants in the Deep Vadose Zone*. PNNL-21815, Pacific Northwest National Laboratory, Richland, Washington.
- Truex MJ, JE Szecsody, N Qafoku, and JR Serne. 2014. *Conceptual Model of Uranium in the Vadose Zone for Acidic and Alkaline Wastes Discharged at the Hanford Site Central Plateau*. PNNL-23666, Pacific Northwest National Laboratory, Richland, Washington.
- Truex MJ, M Ostrom, and GD Tartakovsky. 2015a. *Evaluating Transport and Attenuation of Inorganic Contaminants in the Vadose Zone for Aqueous Waste Disposal Sites*. PNNL-24731, Pacific Northwest National Laboratory, Richland, Washington.
- Truex MJ, JE Szecsody, N Qafoku, R Sahajpal, L Zhong, AR Lawter, and BD Lee. 2015b. Assessment of Hexavalent Chromium Natural Attenuation for the Hanford Site 100 Area. PNNL-24705, Pacific Northwest National Laboratory, Richland, WA.
- Truex MJ, BD Lee, CD Johnson, NP Qafoku, GV Last, MH Lee, and DI Kaplan. 2016. *Conceptual Model of Iodine Behavior in the Subsurface at the Hanford Site*. PNNL-24709, Rev. 1., Pacific Northwest National Laboratory, Richland, Washington.
- Truex MJ, JE Szecsody, NP Qafoku, CE Strickland, et al. 2017. *Contaminant attenuation and transport characterization of 200-DV-1 operable unit sediment*. PNNL-26208, Pacific Northwest National Laboratory, Richland, Washington.
- Um W, J Serne, M Truex, A Ward, M Valenta, C Brown, C Iovin, K Geiszler, I Kutnyakov, E Clayton, H Chang, S Baum, R Clayton, and D Smith. 2009. *Characterization of Sediments from the Soil Desiccation Pilot Test (SDPT) Site in the BC Cribs and Trenches Area*. PNNL-18800, Pacific Northwest National Laboratory, Richland, Washington.
- West AG, SJ Patrickson, and JR Ehleringer. 2006. "Water extraction times for plant and soil materials used in stable isotope analysis." *Rapid Communication in Mass Spectrometry* 20:1317-1321.
- Williams BA and VJ Rohay. 2015. *Conceptual site models for the 200-DV-1 operable unit waste sites in the T Complex area, central plateau, Hanford, Washington*. SGW-49924, CH2M Hill Plateau Remediation Company, Richland, Washington.
- Xue Y, C Murray, G Last, and R Mackley. 2003. Mineralogical and Bulk-Rock Geochemical Signatures of Ringold and Hanford Formation Sediments. PNNL-14202, Pacific Northwest National Laboratory, Richland, Washington.
- Zachara J, C Liu, C Brown, S Kelly, J Christensen, J McKinley, J Davis, J Serne, E Dresel, and W Um. 2007. *A Site-Wide Perspective on Uranium Geochemistry at the Hanford Site*. PNNL-17031, Pacific Northwest National Laboratory, Richland, Washington.

Appendix A

Geologist Descriptions of Samples

The following files show the geologist description of the samples used in this study.

Pacific Northwest National Laboratory		BOREHOLE SAMPLE LOG		Boring/Well No	Depth	Date	Sheet	
				7N-1 C9555	106 - 182.3'	10/14/17	1 of 1	
Location				Project				
C9555 (F-2)								
Logged by <u>Nichelle Snyder</u> <u>M. William Snyder</u>				Drilling Contractor				
Reviewed by _____				Driller				
Date _____				Drill Method				
Lithologic Class. Scheme <u>Folk - Wentworth</u>				Procedure		Rev _____		
DEPTH (ft)	SAMPLES		MOISTURE	GRAPHIC LOG			LITHOLOGIC DESCRIPTION (particle size distribution, sorting, mineralogy, roundness, color, reaction to HCl, maximum grain size, consolidation, structure, etc.)	COMMENTS
	TYPE	ID NUMBER		C	Z	S		
106	G	B3D867	GM				Open end caps
107							
				S- Sand. 40% fine, 4% medium, 2% coarse sand. Moderately sorted. No compaction. 254 u/3 (lt. yellowish brown). gap = 3mm, 6mm				
				bottom - same				
				Note: Sieving sample - there is some (<5%) G.				
				20 max 10/14/17				
181.3	C	B3B658	D				20 max 10/14/17
182.3							
				MS G - 70% Z, 20% v. fine sand, fine sand, 10% G. Max G = 60mm (large gravel in middle of top core - sneaking out ~ 85mm) Poorly sorted. G - rounded. 254 u/2 (lt. brownish gray)				
				bottom - underfilled - same as above - 4 in. center ~ 30mm				

C = Core, G = Grab

D = Dry, M = Moist, W = Wet

2015/EVI/GeosciencesGroup/Procedures/SampleLog/001 (02/06)

Pacific Northwest National Laboratory		BOREHOLE SAMPLE LOG		Boring/Well No	Depth	Date	Sheet
				CA503	87-90'	9/20/17	3 of 8
Location				Project			
DV-1 (5-7)				DV-1			
Logged by						Drilling Contractor	
Michelle Snyder Michelle Snyder							
Reviewed by						Driller	
Lithologic Class. Scheme				Procedure		Rev	
Fall - Winterborn							
DEPTH (ft)	SAMPLES		MOISTURE	GRAPHIC LOG	LITHOLOGIC DESCRIPTION <small>(particle size distribution, sorting, mineralogy, roundness, color, reaction to HCl, maximum grain size, consolidation, structure, etc.)</small>	COMMENTS	
	TYPE	ID NUMBER					C
87	C	B39V29	U		LM) S - 10% Z, 90% fine to medium sand. Well-sorted 2.5V 5/3 (lt. olive brown). bottom - same (slightly over-filled on bottom - < 5mm)	rad - opened top + bottom	
88	C	B39V28				top = 150 counts (1500 dpm)	
89	C	B39V27	SU		likely due to heat B39V27 bottom - U - appears dark in color; all fines Well-sorted. 2.5V 4/4 (light yellowish brown)	bottom 500 counts (5000 dpm) direct 9/21/17	
90					V28 top MS - 30% Z, 70% v. fine to fine sand. Well-sorted. 2.5V 7/3 (pale yellow)	V27 bottom RPT Scan = 700-800 counts 1000- 8 UVV 9/21/17 600-700 counts 600-1000 dpm V28 top same	

C = Core, G = Grab

D = Dry, M = Moist, W = Wet

2015/CVL/GeosciencesGroup/Procedures/SampleLog/001 [02/06]

Pacific Northwest National Laboratory		BOREHOLE SAMPLE LOG		Boring/Well No <u>C4503</u>	Depth <u>90-153</u>	Date <u>9/12/17</u>	Sheet <u>4</u> of <u>8</u>
Location <u>DV-1 (T-1)</u>				Project _____		Logged by <u>Michelle Snyder Michelle Snyder</u>	
Reviewed by _____				Date _____		Drilling Contractor _____	
Lithologic Class. Scheme <u>Folk-Wentworth</u>				Procedure <u>PNNL-ESU-Geology</u>		Rev <u>1</u>	
Drill Method _____		Driller _____					

DEPTH (ft)	SAMPLES		MOIS- TURE	GRAPHIC LOG				LITHOLOGIC DESCRIPTION <small>(particle size distribution, sorting, mineralogy, roundness, color, reaction to HCl, maximum grain size, consolidation, structure, etc.)</small>	COMMENTS
	TYPE	ID NUMBER		C	Z	S	G		
90	C	B39V15	M	[Hand-drawn lithologic log]				ms - 20% Z, 80% fine sand. Well sorted. 2.54 5/ft. Moderate consolidation. bottom: same	opening top & bottom of core
91	C	B39V14	M	[Hand-drawn lithologic log]				V14 - top - same as above	
92									
				X					
152	C	B39V11	SM	[Hand-drawn lithologic log]				Top: ms G, 59% Z, 41% G, 35% sand. Max (ms) 40 mm. 2.54 V13. Poorly sorted, G - rounded. Some gravel broken - primarily basalt visible. Moderately consolidated. bottom - some gravel sticking over end cap (8mm) same as top.	
153									

C = Core, G = Grab D = Dry, M = Moist, W = Wet 2015/CVI/GeosciencesGroup/Procedures/SampleLog/001 (02/06)

Pacific Northwest National Laboratory		BOREHOLE SAMPLE LOG		Boring/Well No. <u>CA513</u>		Depth <u>114.2-118.6</u>		Date <u>10/31/17</u>		Sheet <u>4</u> of <u>3</u>	
Logged by <u>Michelle Snyder</u>				Reviewed by <u>Michelle Snyder</u>				Date _____		Drilling Contractor _____	
Lithologic Class. Scheme <u>Folk-Wentworth</u>				Procedure _____				Rev _____		Drill Method _____	
DEPTH (ft)	SAMPLES		MOISTURE	GRAPHIC LOG				LITHOLOGIC DESCRIPTION (particle size distribution, sorting, mineralogy, roundness, color, reaction to HCl, maximum grain size, consolidation, structure, etc.)	COMMENTS		
	TYPE	ID NUMBER		C	Z	S	G				
114.2	C	B39X00	M	[Hand-drawn lithologic log showing sand with some clay]				MS - slightly muddy sand 80% Z, 20% fine to v. fine sand. Well sorted. Muddy (MS) at the bottom of core.	Sawed core open - in half horizontally		
115.2				[Hand-drawn lithologic log showing sand with some clay]							
116.6	C	B39X10	M	[Hand-drawn lithologic log showing sand with some clay]				MS - muddy sand, 30% Z, 70% v. fine to medium sand. Moderately sorted. Center of core has more sand, ends have more Z visible. 2.5V 513 (lt. olive brown)			
118.0	D	B39X08	M	[Hand-drawn lithologic log showing sand with some clay]				X09 - Same as above - w/ sandier portion in middle, & Z on ends.			
118.6				[Hand-drawn lithologic log showing sand with some clay]				X08 MS - 30% Z, 70% v. fine to fine sand. Well-sorted. interbeds of Z + sandy layers. 2.5V 513.			

C = Core, G = Grab

D = Dry, M = Moist, W = Wet

2015/GVL/GeosciencesGroup/Procedures/SampleLog/001 (07/06)

Pacific Northwest National Laboratory		BOREHOLE SAMPLE LOG		Boring/Well No. <u>09513</u>	Depth <u>151.7 - 152.7'</u>	Date <u>10/6/17</u>	Sheet <u>2</u> of <u>3</u>	
Location <u>DV.1 (S-13)</u>				Project _____				
Logged by <u>Michelle Snyder, M. Michelle Snyder</u>				Drilling Contractor _____				
Reviewed by _____ Date _____				Driller _____				
Lithologic Class. Scheme <u>Folk Wentworth</u>				Procedure _____ Rev _____		Drill Method _____		
DEPTH (ft)	SAMPLES		MOIS- TURE	GRAPHIC LOG			LITHOLOGIC DESCRIPTION <small>(particle size distribution, sorting, mineralogy, roundness, color, reaction to HCl, maximum grain size, consolidation, structure, etc.)</small>	COMMENTS
	TYPE	ID NUMBER		C	Z	S		
151.7	C	B39255	M				u 80% 2-20µ Fine sand. Well sorted. Compacted. 2.5% 6/16 (olive yellow)	opened end caps 1 foot core
152.7							bottom - same as above (slightly underfilled in center, N < 10mm)	

C = Core, G = Grab

D = Dry, M = Moist, W = Wet

2015/GN/GeosciencesGroup/Procedures/SampleLog/001 (02/06)

Pacific Northwest National Laboratory		GEOLOGIC LOG			Boring/Well No. <u>CA497</u>	Depth <u>287-288</u>	Date <u>8/1/17</u>	Sheet <u>1</u> of <u>1</u>	
Logged by <u>Michelle Snyder Michelle Snyder</u>					Drilling Contractor _____				
Reviewed by _____					Driller _____				
Lithologic Class. Scheme <u>Folk - Wentworth</u>					Procedure <u>PNNL-ES-Geology</u> Rev <u>1</u>				
Drill Method <u>Spir Spoon</u>									
DEPTH (ft)	SAMPLES		MOIS- TURE	GRAPHIC LOG C Z S G	LITHOLOGIC DESCRIPTION	sediment class, range in particle size, maximum particle size, mat% reaction to 10% HCl, structure, fabric, and any other characteristics			COMMENTS
	TYPE	ID NUMBER							
287	C	B391M00	SM		MSCL - Muddy sandy gravel. 60% cl, 30% sand, 5% g. Max gravel = 3mm. Angular to sub-round. sand 40% mat%, 60% fusc. Poorly sorted. no rxn to HCl. 2.5Y 5/2				1 foot core
288									

W - Wet, M - Moist, SM - Slightly Moist, D - Dry

2008/DCI/FORMS/Geolog/001 (03/18)

Pacific Northwest National Laboratory		BOREHOLE SAMPLE LOG		Boring/Well No <u>C9497</u>	Depth <u>1121-261</u>	Date <u>11/24/17</u>	Sheet <u>1</u> of <u>1</u>
Logged by <u>Michelle Snyder</u> <u>Michelle Snyder</u>				Location _____		Project <u>DV1</u>	
Reviewed by _____				Date _____		Drilling Contractor _____	
Lithologic Class. Scheme <u>Folk - Wentworth</u>				Procedure _____		Rev _____	
Driller _____		Drill Method _____					

DEPTH (ft)	SAMPLES		MOIS- TURE	GRAPHIC LOG	LITHOLOGIC DESCRIPTION <small>(particle size distribution, sorting, mineralogy, roundness, color, reaction to HCl, maximum grain size, consolidation, structure, etc.)</small>	COMMENTS
	TYPE	ID NUMBER				
141	G	B38MT1	D		S sand, 30% coarse, 60% medium, 20% fine sand. 30% matric, 70% fusilic. Moderately sorted. 2.5% w/f (gray).	500 mL grab samples
144						
260	G	B38MV9	W		m.G. - muddy gravel 5% sand, 10% s, 85% G. clay G = or 15mm (couldn't pour out of grab container) G sub-round to round. 2.5% 4/2 (dark grayish brown).	

C = Core, G = Grab

D = Dry, M = Moist, W = Wet

2015/GVL/GeosciencesGroup/Procedures/SampleLog/001 (02/06)

Pacific Northwest National Laboratory		BOREHOLE SAMPLE LOG		Boring/Well No	Depth	Date	Sheet
				09513	905-48.8	11/29/17	1 of 2
Logged by				Drilling Contractor			
Reviewed by				Driller			
Lithologic Class. Scheme				Procedure		Drill Method	
Fine-Weathered							
DEPTH (ft)	SAMPLES		MOISTURE	GRAPHIC LOG	LITHOLOGIC DESCRIPTION (particle size distribution, sorting, mineralogy, roundness, color, reaction to HCl, maximum grain size, consolidation, structure, etc.)	COMMENTS	
	TYPE	ID NUMBER					
90.9	G	B3DCJ2	M		SM - 30% sand, 10% silt, well-sorted. 2.5Y 5/2 (grayish brown)	500 ml grab samples	
121.5	G	B3DCJ7	M		SM - sandy mud. 50% fine sand, 50% silt, well-sorted. 2.5Y 6/3 (light yellowish brown)		
144.1	G	B3DCJ2	M		SM - sandy mud. 60% silt, 40% fine sand, well-sorted. 2.5Y 5/3 (light olive brown)		

(C - Core, G - Grab) D - Dry, M - Moist, W - Wet

2015/G1/GeosciencesGroup/Procedures/SampleLog/001 (02/06)

Pacific Northwest National Laboratory		BOREHOLE SAMPLE LOG		Boring/Well No <u>09513</u>	Depth <u>M1-172</u>	Date <u>11/29/17</u>	Sheet <u>2 of 2</u>
Logged by <u>Michelle Snyder</u> <u>Michelle Snyder</u>				Location _____		Project <u>TN-1</u>	
Reviewed by _____				Date _____		Drilling Contractor _____	
Lithologic Class. Scheme <u>Folk - Wentworth</u>				Procedure _____		Rev _____	
				Driller _____		Drill Method _____	

DEPTH (ft)	SAMPLES		MOIS- TURE	GRAPHIC LOG			LITHOLOGIC DESCRIPTION (particle size distribution, sorting, mineralogy, roundness, color, reaction to HCl, maximum grain size, consolidation, structure, etc.)	COMMENTS
	TYPE	ID-NUMBER		C	Z	S		
171 172	G	B 20627	M				ms. muddy sand. bot. fine sand. foz. z. Well-sorted. 2.64 s/s (light olive brown)	

C = Core, G = Grab

D = Dry, M = Moist, W = Wet

2015/GPR/GeosciencesGroup/Procedures/SampleLog/001 (02/06)

Pacific Northwest National Laboratory		BOREHOLE SAMPLE LOG		Boring/Well No	Depth	Date	Sheet	
				09488	223.5-225.5'	3/23/18	1 of 1	
Location				Project				
09488, DV-1				DV-1				
Logged by				Drilling Contractor				
Michelle Snyder Michelle Snyder								
Reviewed by				Driller				
Lithologic Class. Scheme				Procedure		Drill Method		
Folk - Wentworth								
DEPTH (ft)	SAMPLES		MOISTURE	GRAPHIC LOG			LITHOLOGIC DESCRIPTION (particle size distribution, sorting, mineralogy, roundness, color, reaction to HCl, maximum grain size, consolidation, structure, etc.)	COMMENTS
	TYPE	ID NUMBER		C	Z	S		
223.5	C	B395M0	M	▬			M0 - Mud, 10% sand, 90% F. Well-sorted. Mica visible in sand. 2.5 Y 5/2 (grayish brown).	1 foot core. Core were cut in half.
225	C	B395M1	M	▬			M1 - Mud, 20% sand, 80% F. Well-sorted. Similar to sample above, but slightly more sand. 2.5 Y 5/2	

C = Core, G = Grab

D = Dry, M = Moist, W = Wet

2015/GNL/Geosciences/Group/Procedures/SampleLog/001 (02/06)

Distribution

**No. of
Copies**

**No. of
Copies**

1 External Distribution

CH2M Hill Plateau Remediation
Mark Byrns (PDF)

13 Local Distribution

Pacific Northwest National Laboratory
DI Demirkanli (PDF)
MJ Truex (PDF)
JE Szecsody (PDF)
MM Snyder (PDF)
JJ Moran (PDF)
MK Nims (PDF)
NP Qafoku (PDF)
AR Lawter (PDF)
CTResch (PDF)
DL Saunders (PDF)
BD Williams (PDF)
SR Baum (PDF)
Information Release (PDF)



Pacific Northwest
NATIONAL LABORATORY

*Proudly Operated by **Battelle** Since 1965*

902 Battelle Boulevard
P.O. Box 999
Richland, WA 99352
1-888-375-PNNL (7665)

U.S. DEPARTMENT OF
ENERGY

www.pnnl.gov